การบำบัดพร้อมกันของสารอินทรีย์ระเหยง่ายในก๊าซและฟีนอลในน้ำโดยใช้เครื่องปฏิกรณ์ปล่อยโคโรนา

นายขจรศักดิ์ เฟื่องนวกิจ

วิทยานิพนธ์นี้เป็นส่วนหนึ่งของการศึกษาตามหลักสูตรปริญญาวิศวกรรมศาสตรดุษฎีบัณฑิต
สาขาวิชาวิศวกรรมเคมี ภาควิชาวิศวกรรมเคมี
คณะวิศวกรรมศาสตร์ จุฬาลงกรณ์มหาวิทยาลัย
ปีการศึกษา 2547

ISBN 974-17-6462-6

SIMULTANEOUS TREATMENT OF GASEOUS VOLATILE ORGANIC COMPOUNDS AND AQUEOUS PHENOL USING A CORONA DISCHARGE REACTOR

Mr. Kajornsak Faungnawakij

A Dissertation Submitted in Partial Fulfillment of the Requirements
for the Degree of Doctor of Engineering in Chemical Engineering
Department of Chemical Engineering
Faculty of Engineering
Chulalongkorn University
Academic year 2004

ISBN 974-17-6462-6

Thesis Title	SIMULTANEOUS TREATMENT OF GASEOUS VOLATILE ORGANIC COMPOUNDS AND AQUEOUS PHENOL USING A CORONA DISCHARGE REACTOR
By	Mr. Kajornsak Faungnawakij
Filed of study	Chemical Engineering
Thesis Advisor	Professor Wiwut Tanthapanichakoon, Ph.D.
Thesis Co-advisor	Associate Professor Noriaki Sano, D.Eng.

Accepted by the Faculty of Engineering, Chulalongkorn University in Partial Fulfillment of the Requirements for the Doctor's Degree

…….. Dean of the Faculty of Engineering
(Professor Direk Lavansiri, Ph.D.)

THESIS COMMITTEE

…….. Chairman
(Associate Professor Tawatchai Charinpanitkul, D.Eng.)

……. Thesis Advisor
(Professor Wiwut Tanthapanichakoon, Ph.D.)

…….. Thesis Co-advisor
(Associate Professor Noriaki Sano, D.Eng.)

……. Member
(Associate Professor Wongpun Limpaseni, M.Sc.)

…… Member
(Associate Professor Prasert Pavasant, Ph.D.)

……. Member
(Woraporn Theerachaisupakij, D.Eng)

ขจรศักดิ์ เฟื่องนวกิจ : การบำบัดพร้อมกันของสารอินทรีย์ระเหยง่ายในก๊าซและฟีนอลในน้ำโดยใช้เครื่องปฏิกรณ์ปล่อยโคโรนา (SIMULTANEOUS TREATMENT OF GASEOUS VOLATILE ORGANIC COMPOUNDS AND AQUEOUS PHENOL USING A CORONA DISCHARGE REACTOR) อ. ที่ปรึกษา : ศ.ดร.วิวัฒน์ ตัณฑะพานิชกุล, อาจารย์ที่ปรึกษาร่วม: รศ.ดร.โนริอากิ ซาโน จำนวนหน้า 132 หน้า. ISBN 974-17-6462-6.

การบำบัดพร้อมกันของก๊าซและน้ำเสียโดยใช้เครื่องปฏิกรณ์ปล่อยโคโรนาแบบผนังเปียกถูกนำเสนอในงานวิจัยนี้ โดยอะเซทัลดีไฮด์ในอากาศและฟีนอลในน้ำถูกใช้เป็นกรณีศึกษา การศึกษาเริ่มจากการบำบัดอะเซทัลดีไฮด์ในก๊าซ, การบำบัดฟีนอลในน้ำ และการบำบัดพร้อมกันของอะเซทัลดีไฮด์ในก๊าซและฟีนอลในน้ำ หลังจากนั้นจึงทำการพัฒนาแบบจำลองทางคณิตศาสตร์ของระบบ โดยปัจจัยหลักที่ทำการศึกษาได้แก่ ความเข้มข้นขาเข้าของอะเซทัลดีไฮด์ ความเข้มข้นเริ่มต้นของฟีนอลในน้ำ ค่าความเป็นกรด-ด่างของน้ำ ทิศทางการไหลของก๊าซ และค่ากระแสโคโรนา ต่อกลไกและประสิทธิภาพการบำบัด ผลการทดลองชี้ให้เห็นว่าการบำบัดแบบพร้อมกันและแบบแยกของอะเซทัลดีไฮด์ในก๊าซและฟีนอลในน้ำสามารถทำได้จริงอย่างมีประสิทธิภาพ ในการบำบัดแบบพร้อมกันนั้นก๊าซอะเซทัลดีไฮด์สามารถถูกกำจัดจากกระแสก๊าซได้อย่างสมบูรณ์โดยการดูดซึมก๊าซผ่านกระบวนการบับบลิ้ง เมื่อความเข้มข้นขาเข้าต่ำกว่า 200 พีพีเอ็ม ในขณะเดียวกันฟีนอลและอะเซทัลดีไฮด์ที่ถูกดูดซึมในน้ำสามารถถูกย่อยสลายได้อย่างมีประสิทธิภาพโดย ไฮดรอกซิลแรดิคอล (OH) ในน้ำซึ่งผลิตจากการสัมผัสโดยตรงของก๊าซโคโรนากับน้ำ นอกจากนี้โอโซนยังสามารถย่อยสลายฟีนอลและผลผลิตข้างเคียงบางส่วน อะเซทัลดีไฮด์ในช่วงความเข้มข้นที่ต่ำกว่า 200 พีพีเอ็ม นั้น ไม่มีผลกระทบต่อการย่อยสลายของฟีนอลเข้มข้นต่ำกว่า 100 มิลลิกรัมต่อลิตร อย่างไรก็ตาม การย่อยสลายของออร์แกนิกคาร์บอนทั้งหมดจะถูกยับยั้งอย่างมากเมื่อความเข้มข้นขาเข้าของอะเซทัลดีไฮด์ สูงกว่า 100 พีพีเอ็ม ทั้งนี้เนื่องจากเกิดการสะสมในน้ำของกรดอะซิติกซึ่งเป็นผลผลิตระหว่างทางตัวสุดท้ายของระบบที่เกิดจากการย่อยสลายของอะเซทัลดีไฮด์ นอกจากนั้นยังพบว่า การเพิ่มค่าความเป็นกรด-ด่าง ถึง 11 สามารถเร่งอัตราการย่อยสลายกรดอะซิติกอย่างเห็นได้ชัด

แบบจำลองทางคณิตศาสตร์สำหรับระบบการบำบัดพร้อมกันที่พัฒนาขึ้นสามารถใช้ทำนายอัตราการย่อยสลายของอะเซทัลดีไฮด์ ฟีนอล และ ผลผลิตระหว่างทางได้อย่างค่อนข้างดีและสอดคล้องกับผลการทดลอง ซึ่งสามารถใช้เป็นพื้นฐานในการคำนวณขยายขนาดระบบบำบัดจริงได้ด้วย กระบวนการบำบัดพร้อมกันนี้ นอกจากจะสามารถประหยัดค่าใช้จ่ายในการดำเนินการ เวลา และพลังงานที่ใช้แล้ว ยังสามารถประหยัดเงินลงทุนด้านอุปกรณ์โดยการบำบัดก๊าซและน้ำเสียในกระบวนการเดียวกัน

ภาควิชา.....วิศวกรรมเคมี.....ลายมือชื่อนิสิต.....

สาขาวิชา.....วิศวกรรมเคมี.....ลายมือชื่ออาจารย์ที่ปรึกษา.....

ปีการศึกษา.....2547.....ลายมือชื่ออาจารย์ที่ปรึกษาร่วม.....

4471801521 : MAJOR CHEMICAL ENGINEERING

KEY WORD: CORONA DISCHARGE / RADICALS / OZONE / VOC / PHENOL / SIMULTANEOUS GAS-WATER PURIFAICATION

KAJORNSAK FAUNGNAWAKIJ : SIMULTANEOUS TREATMENT OF GASEOUS VOLATILE ORGANIC COMPOUNDS AND AQUEOUS PHENOL USING A CORONA DISCHARGE REACTOR. THESIS ADVISOR : PROF. WIWUT TANTHAPANICHAKOON, Ph.D., THESIS CO-ADVISOR : ASSOC. PROF. NORIAKI SANO, D.Eng., 132 pp. ISBN 974-17-6462-6.

Simultaneous treatment of gas and wastewater using a wetted-wall corona discharge reactor was proposed in this research work. Acetaldehyde-laden air and phenol-containing water were chosen as target compounds. Simultaneous treatment of gaseous acetaldehyde and aqueous phenol, and separate treatment of both compounds were thoroughly investigated by experiments. After that, modeling and simulation of the simultaneous system was carried out. Influences of key parameters, namely, inlet acetaldehyde concentration, initial phenol concentration, pH of water, gas flow direction and corona current on removal mechanism and efficiency were investigated. The experimental results show that the simultaneous and separate gas–water treatment could efficiently be achieved. In the simultaneous treatment, when inlet acetaldehyde concentration was lower than 200 mol-ppm, the acetaldehyde was completely removed from the gas stream by absorption via bubbling. Simultaneously, phenol and the acetaldehyde absorbed in water were effectively decomposed by OH radical which was produced by direct contact of the gaseous corona with the interfacial water. In addition, ozone contributed to the partial decomposition of phenol and its byproducts. The above concentration limit of acetaldehyde scarcely affects the decomposition of phenol when the initial phenol concentration was lower than 100 mg L^{-1}. However, decomposition of total organic carbon (TOC) in water was strongly attenuated when acetaldehyde concentration was higher than 100 mol-ppm. This was because acetic acid, the last intermediate mainly obtained from acetaldehyde decomposition, was accumulated in water. In addition, it was found that the decomposition of acetic acid was remarkably increased when the pH was raised up to 11.

The developed model and its simulation result for the decomposition of acetaldehyde, phenol and their intermediates were found to be in good agreement with experimental results. The model proposed will be useful for scale-up of the system for practical application. With simultaneous purification, not only can the operating cost, the operation time and the energy consumption be minimized, but the total investment costs for the equipment can also be reduced.

Department…….Chemical Engineering...Student’s signature.....

Field of study…..Chemical Engineering...Advisor’s signature.....

Academic year…2004.....Co-advisor’s signature.....

ACKNOWLEDGEMENTS

The author would like to thank Prof. Wiwut Tanthapanichakoon for his introducing this interesting subject with the greatest advice, deep discussion and constant encouragement throughout this project. The author is very grateful to the late Prof. Tatsuo Kanki and Assoc. Prof. Noriaki Sano, thesis co-advisors, for their indispensable guidance and supervision, especially, a meaningful contribution to the build-up of strong fruitful cooperation between our two universities.

The author received the full–expense scholarship under the Royal Golden Jubilee (RGJ) Ph.D. program from Thailand Research Fund (TRF), and earned a Student Exchange Scholarship from Association of International Education Japan (AIEJ) to do research at Himeji Institute of Technology (HIT)-University of Hyogo for one year (April 2003–April 2004). This work was also partially supported by Thailand-Japan Technology Transfer Project (TJTTP–JBIC) and TRF–RTA Project of Prof. Wiwut Tanthapanichakoon.

The author would like to acknowledge Assoc. Prof. Tawatchai Charinpanitkul, Assoc. Prof. Wongpun Limpaseni, Assoc. Prof. Prasert Pavasant, and Dr. Woraporn Theerachaisupakij for their useful comments and participation as the thesis committee.

Further, the author is indeed grateful to Mr. Jintawat Chaichanawong and Mr. Apiluck Iad-uea for their useful suggestions and encouragement. As well, the author thanks the teachers, research assistants, friends, brothers and sisters in Particle Technology and Material Processing Laboratory, Chulalongkorn University. Next, the author appreciates Mr. Daisuke Yamamoto, Ms. Yumi Hasegawa as well as all members of Transport Phenomena Laboratory, HIT, for their research collaboration, hospitality, and wonderful experience during the author's stay in Japan.

Last but not least, the author would like to thank his parents, brother, sisters and Ms. Saranya Jantasila for their love and total support.

CONTENTS

Page

ABSTRACT IN THAI…….. iv

ABSTRACT IN ENGLISH…….. v

ACKNOWLEDGEMENTS……. vi

CONTENTS……. vii

LIST OF TABLES……..... x

LIST OF FIGURES……..……. xi

NOMENCLATURE……..……... xix

CHAPTER

1. INTRODUCTION

1.1 Background…… 1

1.2 Objectives of Research Work……..... 6

1.3 Scope of Research Work…….…. 6

1.4 Expected Benefits from This Work……..… 7

2. LITERATURE REVIEW

2.1 Gas Purification Using High – Voltage Electrical Discharge…. 10

2.2 Water Purification Using High – Voltage Electrical Discharge… 19

2.3 Modeling and Simulation of Above Systems..……. 25

3. FUNDAMENTAL KNOWLEDGE

3.1 Corona Discharge …….…… 28

3.1 Corona Discharge Reactions…… 28

3.2 Simultaneous Gas-Water Treatment Concept…….. 29

3.3 Type of Corona Discharge Reactors……. 32

CONTENTS (Continued)

Page

4. EXPERIMENTAL

4.1 Test Materials and Chemicals ……..... 38

4.2 Experimental Setup ……. 39

4.3 Analytical Methods……..……..... 44

4.4 Experimental Procedure …….. 49

5. RESULTS AND DISCUSSION

5.1 Voltage-Current Characteristic …….……... 50

5.2 Treatment of Gaseous Acetaldehyde…… 51

5.2.1 Effect of Corona Current……..... 51

5.2.2 Effect of Influent Acetaldehyde Concentration……..……. 60

5.2.3 Effect of Gas Flow Direction…….. 62

5.2.4 Effect of Oxygen Gas…….……..…..... 64

5.2.5 Effect of pH: Type of Inorganic Additives……. 71

5.2.6 Comparison of Removal Extent and Byproduct……. 75
Formation between Wetted-Wall Reactor and
Dry-Deposition Reactor

5.2.7 Energy and Electron Efficiencies.....…….. 78

5.3 Treatment of Aqueous Phenol…….……. 81

5.3.1 Effect of Corona Current…….…… 81

5.3.2 Effect of Initial Phenol Concentration…… 85

5.3.3 Effect of Ozonation…….……. 87

5.3.4 Byproduct Formation.....…….…… 88

CONTENTS (Continued)

Page

5.4 Simultaneous Treatment of Gaseous Acetaldehyde ……...… 90
and Aqueous Phenol

5.4.1 Effect of Influent Acetaldehyde Concentration..... 90

5.4.2 Effect of Initial Phenol Concentration…….…… 92

5.4.3 Effect of pH…….……..….. 94

5.4.4 Effect of Ozonation…….……..….. 94

5.4.5 Byproduct Formation…….…….……...…. 98

6. DYNAMIC MODEL AND SIMULATION OF…….…. 100
SIMULTANEOUS TREATMENT

6.1 Concept of Mass Transfer Phenomena and Reaction Pathway…. 100

6.2 Modeling and Simulation……..… 104

6.3 Comparison of Simulation and Experimental Results……. 106

7. CONCLUSIONS AND RECOMMENDATIONS

7.1 Conclusions…….. 110

7.2 Recommendations for Future Work…….…..…….. 114

REFERENCES…….…….. 115

APPENDICES…….….... 123

APPENDIX A Publications Resulting from This Research Work….. 124

APPENDIX B Experimental Results…….…….……. 127

VITA……..….... 132

LIST OF TABLES

Page

Table 1.1 The typical waste compounds produced by commercial……..... 2
industries and agricultural activities including their sources
and effects

Table 1.2 Control methods of VOCs in gas phase. (Chaiyo, 2001)…….……. 4

Table 1.3 Control methods of VOCs in aqueous phase. (Kawamura, 1991)…… 5

Table 4.1 The specifications of test materials and chemicals…….. 38

Table 4.2 Operating conditions of FID gas chromatograph……..…… 45

Table 4.3 Retention time of aqueous species analyzed by HPLC…… 45

Table 5.1 Kinetic rate constants of decomposition of aqueous acetaldehyde 56
and aqueous acetic acid toward ozone (k_{O3}) (Bruno et al., 1991)
and OH radical (k_{OH}) (Buxton et al., 1988)

Table 5.2 The electron efficiency η_e and energetic efficiency J ……..…… 80
of removal of acetaldehyde in air at steady state

Table 6.1 Decomposition of organic species in aqueous phase ……..… 105

Table 6.2 Molar species material balance in aqueous phase……..... 105

LIST OF FIGURES

Page

Figure 3.1 The regions of corona discharge reactor…….. 29

Figure 3.2 Simultaneous treatment concept of gaseous acetaldehyde and…… 34
aqueous phenol using a wetted – wall corona discharge reactor

Figure 3.3 Types of corona-discharge reactor…… 37

Figure 4.1 (a) Photograph of present wetted – wall reactor……. 39

Figure 4.1 (b) Photograph of the experimental apparatus…..……. 39

Figure 4.2 (a) Schematic diagram of the experimental set-up for separate……. 40
treatment of gaseous acetaldehyde or aqueous phenol

Figure 4.2 (b) Schematic diagram of the experimental set-up for……. 40
simultaneous treatment

Figure 4.3 High - voltage DC generator……..…….. 43

Figure 4.4 Gas chromatograph GC-9A……. 46

Figure 4.5 Gas chromatograph GC-14B…… 46

Figure 4.6 High performance liquid chromatograph (HPLC)…… 47

Figure 4.7 TOC analyzer TOC-5000……..… 47

Figure 4.8 UV/VIS spectrophotometer UV-1600PC……. 48

Figure 5.1 V–I characteristic of wetted-wall corona discharge reactor……. 51
at various oxygen concentrations.

LIST OF FIGURES

Page

Figure 5.2 The concentration of acetaldehyde in treated gas during…….. 57
corona discharge operation. $C_{a\text{-}g\ inl}$=200 mol-ppm,
Gas flow direction:Upflow

Figure 5.3 Change of pH of water against discharge time……. 57
$C_{a\text{-}g\ inl}$=200 mol-ppm, Gas flow direction:Upflow.

Figure 5.4 Influence of pH on absorptivity of acetaldehyde…….. 58
$C_{a\text{-}g\ inl}$ =200 mol-ppm, Gas flow direction:Upflow.

Figure 5.5 The concentration of acetaldehyde in circulating water during…… 58
corona discharge operation. $C_{a\text{-}g\ inl}$=200 mol-ppm,
Gas flow direction:Upflow.

Figure 5.6 Influences of gas flow directions on a) TOC and aqueous…… 58
acetaldehyde and on b) gaseous acetaldehyde removals.
$C_{a\text{-}g\ inl}$=200 mol-ppm.

Figure 5.7 TOC concentration in water against discharge time at various……. 60
inlet concentrations of gaseous acetaldehyde. I=0.5 mA,
$C_{a\text{-}g\ inl}$=200 mol-ppm, Gas flow direction:Upflow.

Figure 5.8 The effluent concentration of gaseous acetaldehyde against…… 61
discharge time at various inlet concentrations of gaseous
acetaldehyde. I=0.5 mA, Gas flow direction:Upflow.

LIST OF FIGURES

Page

Figure 5.9 The concentration of aqueous acetaldehyde against discharge…… 61
time at various inlet concentrations of gaseous acetaldehyde.
I=0.5 mA, Gas flow direction:Upflow.

Figure 5.10 Acetaldehyde concentration profile in gas stream along…….. 63
the reactor. *I*=0 mA, $C_{a\text{-}g\ inl}$=200 mol-ppm, Time=4 hrs.

Figure 5.11 The concentration of acetaldehyde in treated gas during……. 68
corona discharge operation at various oxygen concentrations.
$C_{a\text{-}g\ inl}$=200 mol-ppm, Gas flow direction=Downward.

Figure 5.12 Removal extent of gaseous acetaldehyde against corona……. 69
discharge current at various oxygen concentrations.
$C_{a\text{-}g\ inl}$=200 mol-ppm, Gas flow direction=Downward.

Figure 5.13 Effect of oxygen on corona wind velocity. Q_g=100 $cm^3\ min^{-1}$…… 69

Figure 5.14 The concentration of acetaldehyde in circulating water during…... 70
corona discharge operation at various oxygen concentrations.
$C_{a\text{-}g\ inl}$=200 mol-ppm, Gas flow direction=Downward.

Figure 5.15 TOC concentration in water against discharge time at……. 70
various oxygen concentrations. $C_{a\text{-}g\ inl}$=200 mol-ppm,
Gas flow direction=Downward.

Figure 5.16 Effect of accumulating acetic acid on gaseous and aqueous…… 71
acetaldehyde removals. *I*=0.5 mA, $C_{a\text{-}g\ inl}$=200 mol-ppm,
Oxygen=21%, Gas flow direction=Downward.

LIST OF FIGURES

Page

Figure 5.17 Influence of dissolved inorganic additives on absorptivity……. 74
of acetaldehyde. $C_{a\text{-}g\ inl}$=200 mol-ppm,
Gas flow direction=Upward.

Figure 5.18 Effect of additives on the concentration of acetaldehyde in…… 74
treated gas during discharge time. I=0.1 mA,
$C_{a\text{-}g\ inl}$=200 mol-ppm, Gas flow direction=Upward.

Figure 5.19 Influence of additives on the accumulation of acetaldehyde…… 75
in circulating water. I=0.1 mA, $C_{a\text{-}g\ inl}$=200 mol-ppm,
Gas flow direction=Upward.

Figure 5.20 Removal extent of gaseous acetaldehyde against…… 77
corona discharge current. W=Wetted-wall type,
D=Deposition type, $C_{a\text{-}g\ inl}$=200 mole-ppm,
Q_g=100 $cm^3\ min^{-1}$

Figure 5.21 GC chromatograms of gas analysis. a) influent gas stream,…… 77
b) effluent gas stream of the deposition-type reactor in
the absence of water vapor, c) the effluent stream of
the deposition-type reactor in the presence of 2.3% water vapor,
and d) the effluent stream of the wetted-wall reactor.
I=0.1 mA, $C_{a\text{-}g\ inl}$=200 mol-ppm.

LIST OF FIGURES

Page

Figure 5.22 Decomposition of aqueous phenol using direct contact of ……. 82
corona discharge: $C_{p\text{-}l\ ini}$ = 30 mg L^{-1}, I=0.3 mA.

Figure 5.23 The concentration of aqueous phenol at various initial phenol…… 83
concentrations during discharge operation. I=0.3 mA.

Figure 5.24 The concentration of TOC at various initial phenol……... 83
concentrations during discharge operation. I=0.3 mA.

Figure 5.25 Removal ratio of phenol and TOC at various corona……..…… 84
currents during discharge operation. I=0.3 mA.

Figure 5.26 Phenol normalized concentration during corona discharge ……..... 86
operation at various initial concentrations of phenol: I=0.3 mA.

Figure 5.27 TOC normalized concentration during corona discharge …… 86
operation at various initial concentrations of phenol: I=0.3 mA.

Figure 5.28 Changes of phenol and TOC concentrations during…… 87
treatment operation compared between corona
discharge system and ozonation system.

Figure 5.29 Concentrations of phenol, TOC and intermediate byproducts…… 88
detected during simultaneous system against corona discharge
time. I=0.3 mA, $C_{p\text{-}l\ ini}$=30 mg L^{-1}, $C_{a\text{-}g\ inl}$=100 mol-ppm.

LIST OF FIGURES

Page

Figure 5.30 Concentrations of intermediate byproducts detected during…… 89
simultaneous system against corona discharge time
(extent of Figure 5.32 in large scale). I=0.3 mA,
$C_{p\text{-}l\ ini}$=30 mg L^{-1}, $C_{a\text{-}g\ inl}$=100 mol-ppm.

Figure 5.31 The concentration of a) aqueous phenol, b) aqueous acetaldehyde.. 91
and c) TOC, during corona discharge operation at various inlet
concentrations of gaseous acetaldehyde for fixed initial
concentration of phenol. I=0.3 mA.

Figure 5.32 Phenol normalized concentration during corona discharge……. 93
operation at various initial concentrations of phenol for
fixed inlet concentration of gaseous acetaldehyde.
$C_{a\text{-}g\ inl}$=30 mol-ppm, I=0.3 mA.

Figure 5.33 The concentrations of TOC during corona discharge operation….. 93
at various initial concentrations of phenol for fixed inlet
concentration of gaseous acetaldehyde.
$C_{a\text{-}g\ inl}$=30 mol-ppm, I=0.3 mA.

Figure 5.34 Influence of pH of solution on the simultaneous purification: ….. 96
a) aqueous acetic acid concentration at 480 min,
b) aqueous phenol concentration at 60 min, and
c) aqueous phenol concentration at 240 min.
$C_{p\text{-}l\ ini}$=30 mg L^{-1}, $C_{a\text{-}g\ inl}$=100 mol-ppm, I=0.3 mA.

LIST OF FIGURES

Page

Figure 5.35 Influence of ozonation on the simultaneous purification during…. 97
operation: a) removal extent of gaseous acetaldehyde,
b) aqueous acetaldehyde concentration, and c) TOC and phenol
concentrations in water. $C_{p\text{-}l\ ini}$=30 mg L^{-1}, $C_{a\text{-}g\ inl}$=100 mol-ppm,
I=0.3 mA.

Figure 5.36 Concentrations of intermediate byproducts detected during …….. 99
simultaneous system against corona discharge time.
I=0.3 mA, $C_{p\text{-}l\ ini}$=30 mg L^{-1}, $C_{a\text{-}g\ inl}$=100 mol-ppm.

Figure 5.37 The concentrations of acetic acid during corona discharge …… 99
operation. I=0.3 mA.

Figure 6.1 Concept of mass transfer phenomena and formation of ……. 103
OH radical in water

Figure 6.2 Reaction pathways of phenol and acetaldehyde……. 103

Figure 6.4 Concentration of a) aqueous phenol and b) aqueous acetaldehyde 108
during simultaneous treatment at various inlet concentrations
of gaseous acetaldehyde against fixed initial concentration
of phenol. I=0.3 mA.

Figure 6.5 Concentration of aqueous phenol during simultaneous treatment… 109
at various initial concentrations of phenol against fixed inlet
concentration of gaseous acetaldehyde. I=0.3 mA.

LIST OF FIGURES

Page

Figure 6.6 Intermediate aqueous products and TOC analysis during…… 109
simultaneous treatment: $C_{a\text{-}g\ inl}$ = 30 mol-ppm,
$C_{p\text{-}l\ ini}$=15 mg L^{-1}, I=0.3 mA.

NOMENCLATURE

$C_{a\text{-}g\ inl}$	=	Influent concentration of gaseous acetaldehyde (mol-ppm)
$C_{a\text{-}g}$	=	Effluent concentration of gaseous acetaldehyde (mol-ppm)
$C_{a\text{-}l}$	=	Concentration of aqueous acetaldehyde (mg L^{-1})
$C_{p\text{-}l}$	=	Concentrations of aqueous phenol (mg L^{-1})
$C_{p\text{-}l\ ini}$	=	Initial concentrations of aqueous phenol (mg L^{-1})
D.C.	=	Direct current
[AA]	=	Concentration of aqueous acetic acid (mg L^{-1})
[AD]	=	Concentration of aqueous acetaldehyde (mg L^{-1})
[BQ]	=	Concentration of aqueous 1, 4-benzoquinone (mg L^{-1})
[CC]	=	Concentration of aqueous catechol (mg L^{-1})
[HQ]	=	Concentration of aqueous hydroquinone (mg L^{-1})
[OH]	=	Concentration of aqueous hydroxyl radical (mg L^{-1})
[PH]	=	Concentration of aqueous phenol (mg L^{-1})
[RC]	=	Concentration of aqueous resorcinol (mg L^{-1})
$[O_2]$	=	Concentration of gaseous oxygen [mol-ppm]
$[O_3]$	=	Concentration of gaseous ozone [mol-ppm]
e	=	Elemental charge (1.602×10^{-19} coulomb)
I	=	Corona discharge current (mA)
J	=	Energetic efficiency (mol J^{-1})
k_i	=	Rate constant of reaction i^{th} (M^{-1} L^{-1})
N	=	Avogadro's number (6.02×10^{23} molecules $mole^{-1}$)
N_e	=	The number of electrons produced by the corona discharge per unit time (mol sec^{-1})

Q_g	=	Gas flow rate ($cm^3\ min^{-1}$)
Q_l	=	Water circulation rate ($cm^3\ min^{-1}$)
q_g	=	Gas mole flow rate ($mole\ sec^{-1}$)
Re	=	Reynold number (-)
t	=	Time (sec)
TOC	=	Total organic carbon ($mg\ L^{-1}$)
V	=	Applied voltage (kV)
W	=	Water volume (cm^3)
w	=	Mole of water (mole)
ψ	=	Removal extent (-)
η_e	=	Electron efficiency (-)

CHAPTER 1

INTRODUCTION

1.1 Background

Nowadays, every country has brought a lot of new technologies to facilitate human beings, and those new technologies have slowly ruled our lives unconsciously. For example, in the developing countries, there are a lot of industries, petroleum industries and chemical industries, which have made the pollution to their communities. That is why we need to develop the processes and methods of pollution treatment. Also a healthy development can be fully achieved only in a good quality environment, and thus environmental protection has become one of the primary targets of society. Pollution problem is an important public issue. Wastewater and air pollution are the main causes we are currently facing their effects. Air pollution is the introduction of substances into the atmosphere as a result of human activity, which damages human health, living sources, ecosystems and material property and disturbs the proper use of the natural and human environment, and wastewater is the introduction of substances into the water.

There are so many kinds of pollution which is released from many sources, and the important one is volatile organic compounds (VOCs). VOCs can dissipate to atmosphere, natural water, and soil. Although some VOCs released to water will be rapidly evaporated, but some of them still dissolve in water and need the effective treatment. Similar to other countries, Thailand declared the environmental restriction to control the pollutants released from any sources. Even though the pollutant quality criteria does not cover all kind of pollutants, but some of them such as phenol, SO_2, NO_2, and a lot more have been regulated in Thailand.

Table 1.1 The typical waste compounds produced by commercial industries and agricultural activities including their sources and effects (Bruno et al., 1991; Kawamura, 1991; Gottschalk et al., 2000)

Type	**Source**	**Effect**
Phenol	Production of phenolic resins which are used in the plywood, construction, automotive, and appliance industries. Caprolactam and bisphenol A, which are intermediates in the manufacture of nylon and epoxy resins, respectively. Medicinal products.	Highly irritating to the skin, eyes, and mucous membranes in humans after acute inhalation or dermal exposures quite toxic to humans via oral exposure.
Benzene	Medical chemical, dyes, oil cloth, artificial leather, lacquers , Manufacturing of phenol and ethylbenzene	A carcinogen, highly toxic flammable
Toluene	Aviation gasoline and high octane blending stock, solvent for paints and coating, resin, rubber, medicine, dyes.	Flammable dangerous fire risk, toxic by ingestion, inhalation and skin absorption
Styrene	Polymer manufacture, fiberglass boat construction and repair, and in auto body fillers, polystyrene containers used for food products.	Nervous system effects such as depression, loss of concentration weakness, fatigue and nausea. liver and nerve tissue damage; cancer.
Sulfur dioxide	These gases are formed when fuel containing sulfur (mainly coal and oil) is burned, and during metal smelting and other industrial processes.	Breathing, respiratory illness, alterations in pulmonary defenses, and aggravation of existing cardiovascular disease, chronic lung disease

It is known that the volatile organic compounds generally appeared in both gas and liquid phase are for example benzene, phenol and acetaldehyde. To get rid of these types of compounds, there are a lot of complex units involving in the conventional method. There are many VOCs control methods of which each method has different advantages, disadvantages, and suitable condition. Similarly, the wastewater treatment methods have different proposition and how to select which method to treat wastewater depends on a lot of parameters, for example, the characteristic of wastewater and budget. VOCs and wastewater treatment methods with their features are demonstrated in **Tables 1.2** and **1.3**, respectively. Presently, it is widely known that the corona discharge reactor

can remove some gas contaminants at low concentration with very high efficiency. The wetted-wall corona discharge reactor, one type of corona discharge reactor proposed by Sano et al. (1996), can enhance the performance of the removal process. In this reactor, some of the negative ions produced by electron attachment are absorbed into a falling liquid film on the anode surface. In addition, the reactor can prevent reentrainment of particles at the anode and also prevent solid formation on the anode while other types of reactor may experience these problems. Moreover, the performance of corona discharge reactor is higher than that of conventional ozonation because the former can directly supply short–lived radicals and ions to form a strong oxidant for treatment of water. If we can treat gas and water containing organic compounds simultaneously, we will not only minimize the cost of the whole process , the time and the energy consuming, but also we will have an integrated process that can efficiently treat contaminated gas and water at the same time which is not too complex as conventional methods. Phenol and acetaldehyde are chosen as target contaminants since these compounds have been commonly used in the same petrochemical plants and some experimental data are available from previous works as well.

Table 1.2 Control methods of VOCs in gas phase. (Chaiyo, 2001)

Method	Suitable condition / requirement	Advantage	Disadvantage
After-burning (thermal combustion)	Uniform furnace temperature (800-900 °C). Residence time about 0.5~2 sec. High gas concentrations. Steady state operation.	Simple and widely available.	Unsuitable for unsteady state operation. Large furnace required.
Catalytic reaction (catalytic combustion)	Known unchanged gas species. High gas concentrations are preferable. Adequate residence time. Steady state operation.	Can be operated at relatively lower temperatures compared to thermal combustion. High selectivity of targeted gas species.	One catalyst type not effective simultaneously for several gas species. Combustion requires moderate to high temperatures Disposal of spent catalysts or regeneration.
Adsorption	Relatively low temperature and low space velocity. Low gas concentrations. Usually unsteady operation. Known types of gas species.	Steady and unsteady operations.	Regeneration is necessary to reduce costs. Relatively high pressure drop Continuous operation requires multiple units Disposal of solid adsorbents. Complicated operation.
Gas absorption	Low to very high temperature. Usually steady operation. Low to relatively high gas concentrations. Known types of gas species.	Can simultaneously remove particulate and gas species.	Difficult to find the appropriate liquid absorbent Regeneration is often necessary to reduce costs. Complicated operation. Disposal of liquid absorbent.
Corona discharge, electron attachment	Low space velocity. Dilute to low gas concentrations. Electronegative gas species and/or oxidizable species by ozone. Steady and unsteady operation.	Rapidly reach the steady state. Multiple removal mechanisms.	Relatively big reactor. High investment. High voltage entails risks, including explosion when the combustible gas concentration is high. Automatic cleaning of the anodic surface is difficult. Undesirable by-product gas may be produced.

Table 1.3 Control methods of VOCs in water phase. (Kawamura, 1991)

Methods	Limitation and characteristic of the methods
Air-stripping	Not applicable to treatment plants lacated in cold climates. Its exhaust pollutes the air. A high air to water ratio is required. Required a large surface area and contact time for mass transfer
Adsorption method	Adsorption rate depends on temperature. pH does not affect the adsorption rate. The absorbent must be regenerated.
Combination of aeration and adsorption	Aeration reduces the loading of contaminants. The frequency of regeneration is lower than adsorption only. The operation is more complicated
Ozonation	Can use for many proposition, for instant, disinfection and oxidation. High investment cost. Short operating time.

1.2 Objectives of Research Work

1.2.1 To develop the high–voltage electrical discharge technique for simultaneous treatment of gas and water

1.2.2 To investigate the influence of the concentrations of VOC in gas phase and of aqueous phenol as well as pH of the aqueous phase, corona discharge current, gas flow direction on the simultaneous treatment efficiency of gaseous VOC and aqueous phenol and on possible generation of byproducts by using a wetted-wall corona discharge reactor

1.2.3 To develop a dynamic model and simulation for simultaneous treatment of gas and water using the wetted-wall corona discharge reactor

1.3 Scopes of Research Work

1.3.1 Phenol is dissolved in de-ionized water to make synthetic aqueous phenol.

1.3.2 Acetaldehyde is mixed with a mixture of O_2 and N_2 to make synthetic gaseous VOC.

1.3.3 The reactor used in the research is the wetted-wall corona discharge reactor. Gaseous mixture goes through the reactor in one pass, whereas the wastewater is recycled through the reactor until sufficient treatment efficiency is achieved.

1.3.4 The conditions of experiment are as follows

Concentration of phenol in water : < 100 mg L^{-1}

Concentration of VOCs contaminants in gas : < 200 mol-ppm

Corona current : $0 – 2$ mA.

Gas flow rate : 100 cm^3 min^{-1}

Water circulation rate : 1400 cm^3 min^{-1}

1.3.5 The initial pH of water is adjusted to 2 – 14 by adding NaOH, H_3PO_4 or HCl.

1.3.6 The aqueous pollutant contaminants before and after treatment are analyzed by gas chromatography, high performance liquid chromatography, TOC analyzer and pH meter.

1.3.7 Gaseous species at the inlet and outlet of reactor are measured by gas chromatography, gas detector tube and iodometric method.

1.4 Expected Benefits from This Work

With simultaneous purification, not only an integrated process can be realized but also the cost of the whole process, the operation time and the energy consumption can be minimized. In addition, the obtained benefits from this research are the understanding of the influence of concentrations of VOC in gas phase and that of aqueous phenol as well as pH of the aqueous phase, corona discharge current and gas flow direction on the simultaneous treatment efficiency of gaseous VOCs and aqueous phenol and on possible generation of byproducts by using wetted-wall corona discharge reactor. Moreover, the dynamic model developed will be useful for scale-up of the system for practical application.

CHAPTER 2

LITERATURE REVIEW

2.1 Gas Purification Using High – Voltage Electrical Discharge

Gas purification involves the removal of vapor-phase impurities from a gas stream. Many methods for gas purification have been proposed, and the primary operation falls into one of the following three categories; 1) absorption into a liquid, 2) adsorption on a porous solid, 3) chemical conversion to another compound. In fact many research works to improve these processes are still going on.

High – voltage electrical discharge technology is one promising method of achieving ultrahigh purification. Application of this process with high - energy electrons has existed for over a hundred years, dating to the first electrostatic precipitator of Lodge (Oglesby and Nichols, 1978) and ozonizer of Simens (Horvath, 1980). The electrostatic precipitator (ESP) is a device – utilizing corona discharge for removing particulate pollutants in the form of either a solid (dust or fumes) or a liquid (mist) from a gas using the electrostatic force. One may realize that the corona – discharge reactor for the gaseous pollutant remover used in this work has the same working principle as ESP. Most information on ESP however focuses on the removal of particulate matter, whereas the reactor proposed in this work, utilizing low - energy electrons in gas discharge to induce electron attachment reaction and gas corona reactions, aims at purifying gaseous impurities from a gas stream. Moreover, simultaneous gas – water purification is also the aim of this research work.

Application of the electron attachment (a reaction of low energy electrons and gas molecules to produce negative ions) in a D.C. corona discharge reactor, first proposed by Tamon et al. (1989), is still innovative for gas separation processes nowadays.

Many publications on electron attachment and other reactions of electron with many kinds of gas molecules have appeared but most of them involve only the reaction kinetics (Moruzzi and Phelps, 1966, Caledonia, 1975 and Massey, 1976). In fact basic information on gas purification using electron attachment and the proposed use of the selectivity of electron to remove the electronegative gaseous molecules are still scarce.

Applications of high - voltage electrical discharge, so - call gas discharge technology, conducted to date are reviewed as follows.

Castle, Inculet, and Burgess (1969) discussed briefly about surface oxidation of discharge electrodes used in a wire – tube electrostatic precipitator. The rate of ozone generation in the precipitator with both stainless steel and copper wires was clarified. The reaction rate of ozone depended on the intensity of electron flux through the gas. The concentration of ozone generated was a linear function of current but decreased as the gas temperature increased.

Dorsey and Davidson (1994) reported an assessment of the contribution of contaminated wires and plates to ozone production in electrostatic air cleaners. It was found that runaway ozone generation due to contamination of electrode surfaces was a limiting factor in the long-term (7 weeks) effectiveness of electrostatic air cleaners.

The corona discharge degraded to streamers after only two weeks, causing increased ozone levels. Wire contamination alone can increase ozone generation. These findings have serious implications for the safe operation of electrostatic air cleaners.

Chemical Vapor Decomposition (CVD) occurring on a discharge wire of an electrostatic air cleaner causes the corona current to decrease more than 95% at the same voltage (after 180 hrs operation). This phenomenon was shown by Jan H. Davidson et al. (1998). Neither current drop nor deposition occurred when operated with clean or dry air (after 2 days).

Several types of DC energized point - electrode reactors have been developed and tested for gas chemistry applications. Although designed with different purposes in mind, the configurations could be put to other uses.

Castle, Kanter, Lee, and Kline (1984) tested a narrow – gap, multipoint-to-plane geometry device in which the gas passed through a corona discharge at high velocity (approximately 100 m/s). The upper multipoint electrode (cathode) was separated from the lower flat electrode (anode) by acrylic spacers that electrically isolated the electrodes and allowed visual observation of the corona. The narrow gap spacing ensured that the inter – electrode space was filled with corona induced plasma. However, the lateral spacing of the pins allowed major fractions of the gas flow to bypass the corona zones. A DC current was applied to the multipoint pins through current limiting resistors.

An experimental investigation has been conducted by Chang, Jen - Shih et al. (1988) to obtain electrode surface temperature profiles of cylindrical hollow electrodes under corona discharges. The result show that a slight temperature increases (about 5 Kelvin within the 10 W input for discharge power level) occurs near the edge of the cylindrical hollow electrodes. Thus, the corona discharge still can be categorized as a cold discharge region.

The pulsed electron technology has also been shown to be capable of generating ozone and active radicals and decomposing several unwanted gases as well as aerosol particles.

Higashi et al., (1985) and Weiss (1985) conducted the reduction of CO_2 the in exhaust gas from a diesel engine vehicle. It was shown that CO_2 concentration in a N_2 - CO_2 or even pure CO_2 gas could be reduced by DC and pulsed corona discharges, respectively. Further experiments for soot elimination and NO_x and SO_x reduction in a diesel – engine exhaust by a combination of discharge plasma and oil dynamics have been investigated by Higashi et al., (1991, 1992).

Chang (1989) and Chakrabarti et al. (1995) found that the removal of NO_x, SO_x, and aerosol particles could be achieved when NH_3 or H_2O was introduced into a pulsed streamer corona reactor. The pulsed electrons have been shown to cause reactions between oxidizing radicals such as OH, O, and O_3 on the one hand and NO_x and SO_x on the other hand at the concentrations found in flue gases to form several acidic aerosol particles with NH_3 or H_2O injections.

Mizuno, Clements, and Davis (1986) compared the performance of the pulsed streamer corona, DC corona, and electron – beam processes. It was found that a pulsed streamer corona discharge produced the radicals instead of a high – energy electron beam. A positive pulsed streamer corona discharge in a non-uniform electrode geometry showed better energy efficiency and higher removal performance than a DC corona discharge. Based on the delivered power, the pulsed streamer corona process removed more than 90% of SO_2 with at least two times better power efficiency than the energetic electron-beam process.

Masuda, Sato, and Seki (1984) developed a high – efficiency ozonizer using traveling wave pulse voltage. The test results relating to the pulse – induced ozone generation showed a great enhancing effect on the speed of reactions by positive pulse corona producing streamers bridging across the entire electrode gap. It was believed that the ozone generated in a corona discharge was a two step process: generation of oxygen free radicals by ionic processes and generation of ozone by free radical reactions. It was found that the ozone generation processes were substantially reduced by increasing the gas temperature, while the ozone loss processes were significantly enhanced by increasing the gas temperature. It was therefore recommended to operate an ozonizer in lower temperature conditions.

High – voltage pulser was used in a pulse-induced plasma chemical processing unit (PPCP unit). This pulser comprised a synchronous rotary spark gap that produced a very sharp negative pulse voltage. High electron energies could be achieved by both units since higher electric fields were allowed in surface – corona

and pulse - corona systems than in direct – current systems because of the breakdown limits of the discharge.

Eliasson, Hirth, and Kogelschatz (1987) applied a dielectric-barrier discharge for ozone generation from oxygen. The resulting efficiency of the generation was reported. A value of 1200 g/kWh was the theoretical ozone generation efficiency calculated by thermochemical theory. He also estimated the maximum ozone generation efficiency of 400 g/kWh for pure oxygen by analyzing a Boltzmann equation. The actual ozone generation efficiency was approximately 200 g/kWh for pure oxygen, which was very low compared to the theoretical values. It was because the discharge energy was consumed not only in producing the ozone but was also dissipated in heating the test gas and the electrodes of the ozonizer. Also some of the ozone produced was destroyed by the heat.

After the work of Eliasson et al., there has been attempt to improve the ozone generation efficiency. Ito et al., (1990) reported that the efficiency in the silent discharge showed a rise of 3-6% by the radiation of ultra-violet ray from the discharge in nitrogen gas. Later, Hattori et al., (1992) reported the superposition effect of two types of discharge in the same discharge space, silent and surface discharges, on ozone generation. Their ozonizer had two power sources with a variable-phase shifter. A 22-30% increase in the efficiency was observed in their ozonizer.

Yamamoto et al. (1996) demonstrated a new concept -single-stage, catalysis-assisted packed-bed plasma technology, to decompose CCl_4, one of the ozone-depleting substances. The objective of the concept was twofold: to enhance the

decomposition efficiency catalytically, and to selectively reduce the by-products. Either $BaTiO_3$ or $SrTiO_3$ pellets were packed in the ferroelectric packed - bed reactor employing an AC power supply. The configuration employed a unique one-stage catalysis/plasma process in which the $BaTiO_3$ pellets were coated or impregnated by active catalysts such as Co, Cu, Cr, Ni, and V. Enhancement of the CCl_4 destruction and the conversion of by-product CO to CO_2 were demonstrated using Ni catalyst in the one-stage plasma reactor.

The so - called non - thermal plasma including corona discharge has been widely studied

A non – thermal plasma chemical process with an AC powered ferroelectric packed – bed reactor was again tested by Zhang, Yamamoto, and Bundy (1996). In this work, the targeted gases to be decomposed were ammonia and odorous compounds gathered from animal houses. The plasma reactor packed with $BaTiO_3$ pellets produced high energy free electrons and radicals, which in turn, decomposed the targeted compounds. Four important parameters affecting the reactor performance were investigated: gas residence time, power voltage, power frequency and initial ammonia concentration.

Tamon, Sano, and Okazaki (1989) proposed a novel method of gas separation based on electron attachment. Two kinds of separation devices using either photocathode or glow discharge as electron source were constructed. They reported high efficiency for the removal from nitrogen of SF_6 at very low concentrations. Recently, Tamon et al. (1995) used two types of corona discharge reactors;

deposition-type and sweep-out – type reactors, to remove from nitrogen dilute sulfur compounds, dilute iodine and oxygen. They also discussed the purification mechanism and presented simulation models for predicting the removal efficiency. Subsequently, Tamon et al. (1996) investigated the influence of coexisting oxygen and water vapor on the removal of six sulfur compounds from nitrogen. They discovered that the presence of oxygen and water vapor increased the removal efficiency.

Sano et al. (1996) used a new type of corona-discharge reactor, the wetted-wall reactor, and the conventional deposition-type reactor to remove iodine and methyl iodide from nitrogen. The removal mechanism of I_2 and CH_3I in the reactor was also discussed. In the wetted – wall reactor, negative ions produced by electron attachment were absorbed into the liquid film on the anode resulting in the change of chemical species in the liquid so that gas absorption increased t raise the removal efficiency. In the removal of methyl iodide by the wetted – wall reactor, the reaction byproduct, iodine, was not produced in the reactor, and the removal efficiency became high compared with the deposition – type reactor.

Kittisak Larpsuriyakul et al. (1996) and Wiwut Tanthapanichakoon et al. (1998) reported experimental results regarding the influence of the structure of the corona-discharge reactor on the removal of dilute gases. The effects of the reactor structure, namely the cathode diameter, the anode shape, and the number of cathodes, were investigated. The results revealed that the thicker the cathode diameter, the higher the removal efficiency. In contrast, the smaller the reactor diameter among three equivolume reactors, the higher the removal efficiency. As for the number of

cathodes in a single reactor vessel, the single-cathode reactor always exhibited higher removal efficiency than the 5-cathode one.

Paisarn Khongphasarnkaln (1998) investigated the application of electron attachment to the removal of dilute gaseous pollutants using a corona-discharge deposition-type reactor. It has been found that the presence of O_2 enhanced the removal efficiency of each impurity gas. The enhancement was experimentally shown to be attributable to the ozone reaction in the removal of $(CH_3)_3N$ from O_2-N_2 mixed gas. Water vapor also enhanced the removal efficiency of $(CH_3)_3N$ and CH_3CHO. Furthermore, The high selectivity of electron attachment to electro negative gas molecules was utilized in the simultaneous removal of dilute $(CH_3)_3N$-CH_3CHO, NH_3-CH_3CHO, SO_2-$(CH_3)_3N$, SO_2-CH_3CHO, NO_2-CH_3CHO and CO_2 - CH_3CHO from the air in the single reactor. Compared to single impurity removal, it has been shown that the presence of SO_2 enhanced the removal efficiency but retarded that of CH_3CHO in the single reactor. Some reaction by-products generated could be avoided by using two independently operated reactors in series. In the case of coexisting of NO_2, it was noted that the lower the inlet NO_2 concentration, the lower the discharge current that still yielded beneficial effect. At higher discharge currents, the retarding effect of CO_2 on CH_3CHO removal was obviously significant.

Han S. Uhm (1999) investigated the influence of the chamber temperature on the properties of the corona discharge system. It was found that the critical voltage V_c required for the corona discharge breakdown was inversely proportional to the chamber temperature T. The electrical energy w_c required for corona discharge breakdown was inversely proportional to the square of the chamber temperature T.

Thus, the electrical energy consumption for the corona discharge system decreased significantly as the temperature increased. The plasma generation by corona discharge in a hot chamber was much more efficient than that in a cold chamber.

Wiwut Tanthapanichakoon et al. (2001) investigated the common gas species emitted during cremation. Even ultra – low concentrations of some organic compounds can still cause malodor. They summarized past and recent experimental results on the removal of sulfur compounds, nitrogen compounds and organics compounds, which indicated that the presence of oxygen and/or water vapor in N_2 gas contribute to an increase in the removal efficiency in many cases. Conversely, temperature elevation negatively affected the removal of SO_2.

Sano et al. (2001) applied a reactor using DC corona discharge of negative polarity to remove sulfur dioxide from oxygen – nitrogen mixture in the presence or absence of water vapor for temperatures ranging from room temperature to 350^{o}C. It was observed that increasing the reactor temperature cause a decrease in the removal efficiency. Mixing water vapor with the process gas resulted in an increase of the removal efficiency. The effect of the presence of water vapor on improving the removal efficiency was significant under low temperature conditions, while it was relatively moderate under high temperature conditions.

Masaaki Okubo et al (2001) investigated the removal of acetaldehyde (CH_3CHO) and ammonia (NH_3), which is another odor component of cigarette smoke. In the experiment, the ac barrier – type plasma reactor was used. In the experimental, more than 90% of acetaldehyde removal efficiency was obtain under

dry air and N_2 environment. For NH_3 removal, almost 100% removal efficiency was obtained with minimum reaction byproduct under dry air environment.

Wiwut Tanthapanichakoon et al. (2003) investigated a corona discharge reactor is employed to remove acetaldehyde (CH_3CHO) from N_2 and air from room temperature up to 300^oC. The more dilute the inlet concentration, the higher the removal efficiency. The presence of either oxygen or water vapor always enhances the removal of acetaldehyde from N_2.

Wiwut Tanthapanichakoon et al. (2004) investigated the individual and combined effect of O_2 and H_2O vapor on the separate and simultaneous removal of styrene and NH_3 from N_2 at elevated temperatures via corona discharge reaction. The presence of O_2 in N_2 always enhances the removal of styrene and / or NH_3 from N_2. The presence of H_2O in N_2 generally enhances the removal of styrene and / or NH_3 but its presence retards of NH_3 when H_2O concentration is too high or the temperature is 300^oC. The combined effect of O_2 and H_2O is found to substantially retard the removal of styrene and / or NH_3 compared to the sole effect of coexisting O_2.

2.2 Water Purification Using High - Voltage Electrical Discharge

Water treatment involves the removal of liquid-phase impurities from liquid solution. Many methods for water treatment have been proposed, and the primary operation falls into one of the following categories; 1) Physical operation, 2) Chemical processes, 3) Biological processes. The oxidation with ozone, one of the above chemical processes, is widely used to treat wastewater. Because ozone is a strong oxidant, it can decompose many kinds of organic and color compounds, control taste and odor, and have a very short disinfection time. In fact, there are many ways to produce ozone. The conventional method is the plasma or corona discharge technique. Air and/or oxygen are fed to ozonator to generate ozone, and then ozone transfers to the reactor in which the wastewater is treated.

According to the conventional ozonation, a part of ozone with almost all radicals and ions produced by ozonator are lost during they drift from ozonator to the reactor which set apart since these species are not stable. Furthermore, ozone has a low solubility in water. Thus, bubbling of ozone into water is still not good enough to obtain high efficiency. In addition, molecular ozone selectively attacks organic contaminants. At a high pH range, molecular ozone decomposes rapidly to form radicals. These radicals are nonselective oxidants and have a higher oxidation power than molecular ozone. This finding initiated the concept of advanced oxidation processes.

Advanced Oxidation Processes (AOPs)

AOPs aim at the in – situ production of strong oxidizers. Among the oxidizers, of interest are hydroxyl radical (OH), atomic oxygen (O), ozone (O_3) and hydrogen peroxide (H_2O_2). Hoeben (2000) reported that several techniques for production of these species as follows.

O_3 / UV – In this technique, OH radicals are produced from ozone, water and UV photon. Ozone is produced on location by an ozonizer, which converts atmospheric or pure oxygen into ozone by corona discharges.

Hydrogen Peroxide / UV and Fenton Oxidation – Hydrogen peroxide is decomposed by UV photons into hydroxyl radicals. Also, the reaction of hydrogen peroxide with iron (II) ions produces hydroxyl radicals; this reaction is known as the Fenton reaction.

Photocatalytic Oxidation – Hydroxyl (OH) and hydroperoxyl (HO_2) radicals are produced by Photocatalytic oxidation at an irradiated semiconductor surface in contact with water. Excitation of electrons in the surface layer by UV photon will promote electrons from the valence band to the conductivity band. In this way, electron – deficient holes (h^+) are created in the valence band and free electrons will be available in the conductivity band. Water is absorbed onto the surface, resulting in the formation of H^+ and OH^- ions. Subsequently, OH radicals are produced by oxidation of water or hydroxyl ions, while HO_2 radicals are obtained from the reaction of seperoxide anion (O_2^-) with H^+.

Wet – Oxidation – Water with dissolved oxygen is used to oxidize the target compound. The process can be performed at e.g. subcritical or supercritical conditions. Metal ions can be added to catalyze the oxidation. OH radicals are produced from dissociation and oxidation of water. Hydroperoxyl radicals and hydrogen peroxide are also produced and play an important role on decomposition of target compound.

Radiolysis – Irradiation of water by high – energy photons or electrons dissociates water molecules into hydroxyl radicals and hydrogen atom, or ionizes water molecules. Ionized water molecules react with water to produce OH radicals. By saturation of the water with nitrous oxide (N_2O), solvated electrons are converted into OH radicals. Also, the target compound is dissociated or ionized.

Ultrasonic Irradiation – The introduction of ultrasonic energy into a liquid causes electrohydraulic cavitation. The applied frequency range is from 15 kHz up to 1 MHz. The cavitation process involves the oscillation of the radii of pre – existing gas cavities by the periodically changing pressure field of ultrasonic waves. The rapid implosion of the eventually instable gas bubbles causes adiabatic heating of the bubble vapor phase. In this way, localized and transient high temperatures and pressures are reached e.g. p>300 bar and T>3300 K in aqueous solution. These vigorous conditions invoke dissociation and pyrolysis of the liquid phase molecules and the present target compounds. Water will be dissociated into hydroxyl radicals and hydrogen atoms, when organic compounds are dissociated into radicals and functional groups like carboxyl and nitro groups are removed.

Electrical Discharge – The discharge of electric energy into a dielectric medium may cause dissociation, ionization and excitation of the dielectric molecules or atoms. Depending on the energy input, the produced plasma is thermal or non – thermal. In thermal plasma the ionization level is high, about 10^{-2}. Examples of thermal electrical discharge are lightning and arc discharges. Typical numbers of electron density (n_e) and electron energy (T_e) for lightning discharges are about n_e = $1x10^{17}$ – $5x10^{17}$ cm^{-3} and T_e = 2.2 eV (corresponding to 25000 K). Corona and glow discharges are non – thermal plasmas. Their ionization level is very low, about 10^{-6}. The electron density and electron energy of a corona plasma are about n_e = 10^{13} cm^{-3} and T_e = 10 eV, respectively. Corona discharge in water produces hydroxyl radicals and hydrogen atoms from the dissociation and ionization of water molecules. The OH radicals produced directly decompose organic compounds in water. By another approach, corona discharge in gas above water can produce gaseous corona species such as radicals and ions. These gaseous species react with water molecules to produce reactive hydroxyl radical in water which contribute to decomposition of aqueous target compounds.

Besides above – mentioned techniques, the combination of AOPs such as microwave irradiation in UV / H_2O_2 process by Do – Hung Han et al. (2004) and ultrasonic irradiation in the presence of TiO_2 particle by Masaki Kubo et al. (2004) was proposed to enhance the performance of the wastewater treatment systems.

Among these AOPs, corona discharge is considered as the one of promising method in term of high decomposition and energy efficiencies. In this work, corona

discharge reactor is used for waste water treatment, gas treatment and simultaneous gas – water treatment.

Applications of corona discharge for wastewater purification conducted to date are reviewed as follows.

Sharma et al. (1993) carried out the preliminary study of pulsed streamer corona discharge for the degradation of phenol in aqueous solution. The isothermal batch reactor and semi – batch reactor with the continuous addition of oxygen bubbling were used in this study. In the experiments where no oxygen was bubbled through the reactor, the phenol breakdown was independent of pH, thus indicating significant OH radical formation directly from the corona discharge. The addition of iron was found to significantly enhance phenol degradation; this may be due to Fenton's reaction arising from hydrogen peroxide formed directly by the corona discharge. . In the experiments where oxygen was fed to the reactor, it appeared that two simultaneous reaction pathways contributed to phenol degradation. The first pathway consisted of corona – induced aqueous phase reactions and the second pathway arose from ozone production in the gas phase with subsequent mass transfer into the liquid phase.

Hoeben (2000) investigated the applicability and technical feasibility of pulsed positive corona discharges for the degradation of organic materials at low concentration in aqueous solution. The model compounds used in this study were phenol, atrazine, malachite green and dimethyl sulfide. Intermediate products of phenol decomposition were analyzed in order to construct the oxidation pathway model and to account for the composition of the phenol oxidation product mixture.

The influence of different corona parameters and reactor configurations has been determined from phenol conversion and malachite green decolorization measurements.

Won-Tae Shin et al., (2000) investigated the use of a novel pulseless corona discharge system combined with electrohydrodynamic spraying of oxygen to form microbubble. Experimental result indicated that organic compound such as phenol and methylene blue were removed. The major species are hydroxyl radical, atomic hydrogen species and ozone.

Sano et al., (2002) proposed a novel corona discharge reactor, wire to plate reactor. The concept of reactor is the combination of ozonator and reactor together. The water purification principle is the utilization of radicals and ions for the degradation of contaminant in water. This proposed method is much more effective than the ozonation treatment. The result demonstrated that the negative polarity showed the higher efficiency than positive polarity. The results showed that concentration of gaseous oxygen and gas flow rate have significant effects on efficiency of the reactor. Sano et al. (2003a) continued to investigate the influence of dissolved inorganic additives on the efficiency of the phenol degradation in this reactor.

Sano et al. (2003b, 2004) proposed the wetted - wall corona discharge reactor for decomposition of organic compounds in water. Even though the novel reactor proposed by Sano et al. (2002) can obtain a high efficiency but the active area used in the corona process is only between wire and plate. Thus the wetted – wall reactor

which consists of wire cathode set along the center of the cylindrical anode. By this reactor, the higher performance can be obtained because of the more active area. The influence of corona region length, water circulation rate, the gap between cathode and anode significantly affected the decomposition efficiency. Influence of current density and applied voltage has also been investigated.

Yin – Sheng Chen et al. (2004) used the pulsed high – voltage discharge plasma for degradation of phenol in aqueous solution. It is found that phenol degradation can be raised considerably by increasing the peak voltage of the corona and the repetition rate of the pulse or increasing pH of solution. The additions of oxygen and $FeSO_4$ were found to enhance phenol degradation.

2.3 Modeling and Simulation of Above Systems

Modeling and simulation of gas purification in a corona discharge reactor.

Mukkavilli S. et al. (1988) proposed a model for the electrostatic corona discharge reactor in a pin – plate configuration in order to describe the fundamental chemistry and physics governing the discharge behavior, and to predict the reactor performance. In this approach, the electric field strength was estimated assuming a space – charge free field. A two – term spherical harmonic expansion was used to solve the Boltzman equation for the electron energy distribution function (EEDF) and calculate the electron – molecule reaction rates using collision cross – section data. Species continuity equations were solved for the dry and wet air systems to predict

ozone and NOx. The calculations indicated that the Maxwell EEDF cannot be used as it overpredicts the electron molecule rate coefficients by several orders of magnitude.

Tamon et al. (1995) proposed the new concept of gas purification by electron attachment. Removal of six sulfur compounds, oxygen and iodine from nitrogen were conducted to verify the concept of gas purification. Simulation models were used to estimate removal efficiencies of these compounds, by taking into account electron attachment, and experimental constants of the model were determined. The removal efficiency correlated by the models agrees well with the experimental one.

Stathiamoorthy G. et al. (1999) conducted the experiment and simulation studies on removal of nitrogen oxides from dry nitrogen gas and dry air with and without ethylene using a pulsed streamer corona discharge reactor. A kinetic model was developed to characterize the chemical reactions taking place in the reactor using a combination of the CHEMKIN and KINEMA programs. Concurrently, an experimental program to determine NO removal was conducted. The electron density for the reactions of N_2 and O_2 by electron – molecule collisions were obtained by fitting the model to the experimental data. Then the model was used to predict the concentrations of various species, including NO, NO_2, N_2O, O_3 and byproducts of ethylene decomposition.

Modeling and simulation of water purification in a corona discharge reactor.

Joshi A.A. et al. (1995) determined the rates of formation of radical and molecular species, specifically hydrogen radicals, hydrogen peroxide and aqueous

electrons involved in the pulsed streamer corona process in the aqueous phase. The reactor model for describing the pulsed streamer corona discharge process in the aqueous phase was developed. In this model, the kinetics of the process is described by a set of reactions where the pseudo - steady state assumption was made for all radicals and ionic species.

Won-Tae Shin et al., (2000) modeled the kinetic rate of phenol degradation in a pulseless corona discharge process. Modeling results showed that the dominant species of the pulseless corona – discharge reactor are hydroxyl radical and aqueous electron. Several radical species produced in this process were also identified experimentally. The major species are hydroxyl radical, atomic hydrogen species and ozone.

The combination of pulse corona discharge and suspended activated carbon for aqueous phenol decomposition was proposed by David R. Gremonpre et al. (2003). Experimental studied showed that phenol can be effectively degraded with a wide range of reactor conditions; however, the most efficient removal of phenol occurred when activated carbon and ferrous sulfate solutions were utilized in the liquid phase corona reactor. Through the experimental measurement and a mathematic model accounting for adsorption, mass transfer and surface reaction on the activated carbon, it was that there is a strong possibility that activated carbon participates in catalytic reactions with phenol and its primary byproducts.

CHAPTER 3

FUNDAMENTAL KNOWLEDGE

3.1 Corona Discharge

The self–sustaining discharge of electrons in a non-uniform electric field between a thin wire and a coaxial cylinder is called a corona discharge. This name is descriptive of the glowing light effects found when the applied voltage is several kilovolts. High vacuum is not always required and corona discharge can be generated at or near atmospheric pressure. The gas pressure needs not be low for the discharge to occur, but at low gas pressure the corona is not visible. The luminous part of the discharge is usually restricted to a region close to the wire surface, which may be positive or negative with respect to the cylinder. Positive and negative coronas can be distinguished by the applied positive or negative voltage of the central electrode.

Coronas are by no means only artificially produced. It is the natural phenomenon of the glow or corona surrounding the sun but is only visible during a total solar eclipse. In addition, nature produces them between and within electrically charged clouds. A theory on cloud electrification attributes this process to the corona on and around ice particles in the clouds. According to this theory, corona is not only the effect but also the cause of the appearance of charged clouds and therefore of lightning and thunderstorms.

In a corona discharge reactor, there are three regions in the void space between the anode and cathode as shown in **Figure 3.1**. In the high electron energy region, free electrons are emitted from the cathode surface and rapidly accelerated. Surrounding gas molecules will be ionized after collision with these free electrons and negative ions are produced. In the transient region, the electron energy is just enough to dissociate gas molecules to produce neutral radicals. In the vast region of low-energy

electrons, electrons are prone to be captured after collision with gas molecules. Cluster formation and electron attachment reaction generally take place in this region.

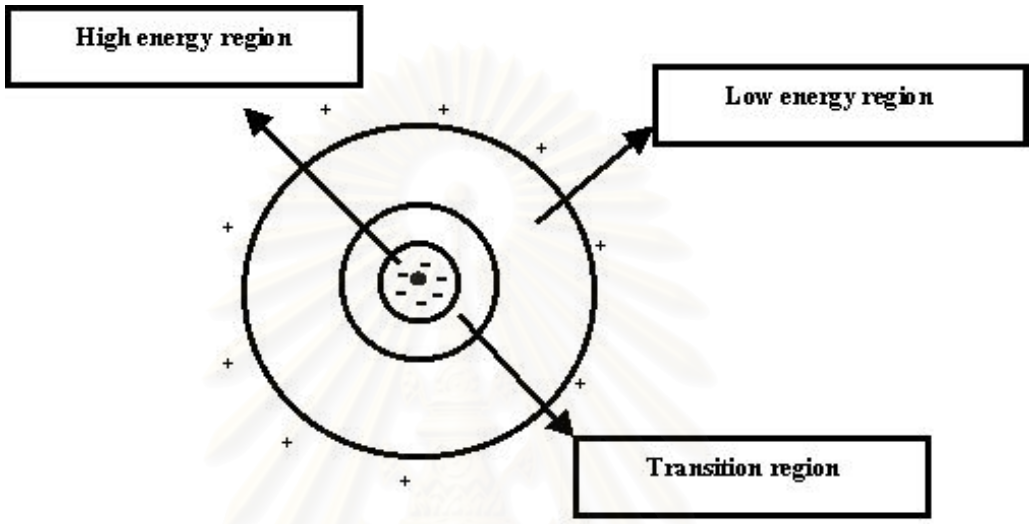

Figure 3.1 The regions of corona discharge reactor

3.2 Corona Discharge Reactions

3.2.1 Dissociation and Ionization

Ionization of gas molecules in corona discharge takes place when high–energy electrons collide with the gas molecules, producing some extra electrons and positive ions. When the energy level of the electrons is not high enough to ionize the gas molecules, these energetic electrons can dissociate gas molecules to produce radicals. In addition, dissociative ionization of gas can also take place when the electron's

energy is appropriate. A mixture of an electron-ionizing or electron –dissociating gas, AB, is considered in the corona discharge reaction region.

Ionization:	$e + AB \rightarrow AB^+ + 2e$	(3.1)
Dissociation:	$e + AB \rightarrow A + B + e$	(3.2)
Dissociative ionization:	$e + AB \rightarrow A^+ + B^- + e$	(3.3)

The dissociation and ionization are expected to take place in the corona plasma zone in which the electron energy is higher than 1.85 eV. It should be noted that the ionization energy and bonding energy of oxygen are 12.06 and 5.12 eV, and those of nitrogen are 15.6 and 9.76 eV, respectively.

3.2.2 Electron Attachment Reaction

When low-energy electrons collide with electronegative gas molecules, some electrons are captured by the gas molecules, and negative ions are formed. This phenomenon is called "electron attachment" (Massey, 1976). Electron attachment depends on the electron energy level, the structure of the gas molecule, and its electron affinity. There is a huge difference between the electron attachment probability of the gas molecules and that of the carrier gas. This high selectivity is reflected in the production of negative ions (Caledonia, 1975; Massey, 1976, 1979). Therefore, electronegative impurities of very dilute concentration become negative ions by electron attachment, and they can effectively be separated from the neutral gas (for example, N_2) in an electric field.

In contrast, if an electron whose energy is too low reaches the molecular orbital, the electron can not be captured by the molecule. It is necessary to take into account the moderate (appropriate) range of electron energy when the attachment probability is to be enhanced. A great deal of effort has been devoted to generate or utilize electrons with a variety of energy range via quite a number of gas-discharge devices. However, the appropriate range of electron energy contributing exclusively to electron attachment generated by such devices has not been clarified because of the limitation of measurement devices and/or techniques.

At the exact moment when an electron is captured by a gas molecule, the molecule would be placed at an excited state. To become stable, the molecule must release the excess energy in quanta, for example, by collision with another electron, by collision with another gas molecule, by being decomposed, or by radiation. Various processes for the electron attachment reaction have been reported (Moruzzi and Phelps, 1966) as shown by Eqs. (3.4), (3.5), and (3.6). A mixture of an electron-attaching gas, AB, and an appropriate third body, M, is considered in these processes.

Dissociative attachment: $e + AB \rightarrow A^- + B$ (3.4)

Three-body attachment: $e + AB + M \rightarrow AB^- + M$ (3.5)

Radiative attachment: $e + AB \rightarrow AB^- + h\nu$ (3.6)

Since the electron attachment probability of the gas molecule is also dependent upon its electron affinity, it is reasonable to expect that a molecule that contains one or more atoms with high electron affinity would have high probability of electron attachment. For example, in a comparison between SF_6 and N_2, the electron affinities

of S, F, and N are 200 kJ/mol, 333 kJ/mol, and –26 kJ/mol, respectively. So it is not surprising that the probability of electron attachment for SF_6 molecule is reportedly 10^{11} times that of N_2 molecule (Hickman and Fox, 1956). This huge difference in the electron attachment probability among various kinds of gas molecules results in high selectivity in the formation of the corresponding negative ions. Therefore, even a specific gas component whose concentration is extremely low can effectively be separated from the main (neutral) gas in an electric field by utilizing the electron attachment reaction. Also one can expect the method based on electron attachment to be one of the most efficient methods of gas purification.

3.3 Simultaneous Gas – Water Treatment Concept

When a corona discharge is applied to the reactor, the energetic electrons are emitted from the wire cathode and accelerated to the anode along the electric field. During theirs drift, dissociation and ionization of oxygen can produce O radical in the high strength electric field adjacent to the cathode as shown in Eq. (3.7) (Peyrous et al., 1989; Loiseau et al., 1994). In the low strength electric field next to the high electric zone, the dissociative electron attachment to oxygen can also produce O and O^- as shown in Eq. (3.8) (Chanin et al., 1962; Moruzzi et al., 1966). Reaction of oxygen with O radical would produce ozone in Eq. (3.9). When the O and O^- reach the interfacial water and subsequently react with water molecule, reactive OH radical is expected to be produced in water as described by Eqs. (3.10) and (3.11) (Hoeben et al., 2000; Sano et al., 2002).

$$O_2 + e^- \rightarrow O + O + e^- \quad (3.7)$$

$$O_2 + e^- \rightarrow O^- + O \quad (3.8)$$

$$O_2 + O \rightarrow O_3 \quad (3.9)$$

$$O^-_{(gas)} + H_2O \rightarrow OH^-_{(aq)} + OH_{(aq)} \quad (3.10)$$

$$O_{(gas)} + H_2O \rightarrow OH_{(aq)} + OH_{(aq)} \quad (3.11)$$

The simultaneous treatment concept of the wetted – wall corona discharge reactor is illustrated in **Figure 3.2**. When gas stream is introduced to the reactor, the acetaldehyde is absorbed into the aqueous phenol solution. Then, aqueous solution containing phenol and acetaldehyde flow through the corona zone as a falling thin film on the inner surface of the anode cylinder. In the corona zone, the OH radical together with ozone simultaneously decomposes both aqueous phenol and acetaldehyde.

$$OH_{(aq)}/O_{3(aq)} + \text{organic compounds}_{(aq)} \rightarrow \text{product} \quad (3.12)$$

If the gaseous acetaldehyde is remaining in the gas stream, it is expected to be removed in the gaseous corona zone by radical reaction (Sano et al., 1997; Butkovskaya et al., 2000), ozonation, and cluster formation (Sano et al., 1997).

The treated solution is circulated through the reactor, while the gas containing acetaldehyde is steadily supplied. By this system, acetaldehyde can be continuously absorbed into the solution since acetaldehyde in water can be continuously degraded. Meanwhile, phenol along with its intermediate products could be completely decomposed to be CO_2 and H_2O as final products by the circulation system.

In fact, the gaseous acetaldehyde can be fed into the reactor either by introducing to gas phase over the water bubbling or through the water. When the gas stream is bubbled into the water, the acetaldehyde is expected to be completely removed from gas stream by absorption. Absorbed acetaldehyde in water is simultaneously decomposed by OH radical, resulting in sustainable absorption. The influence of gas flow direction, including method of gas introduction to the reactor is shown in the results and discussion section.

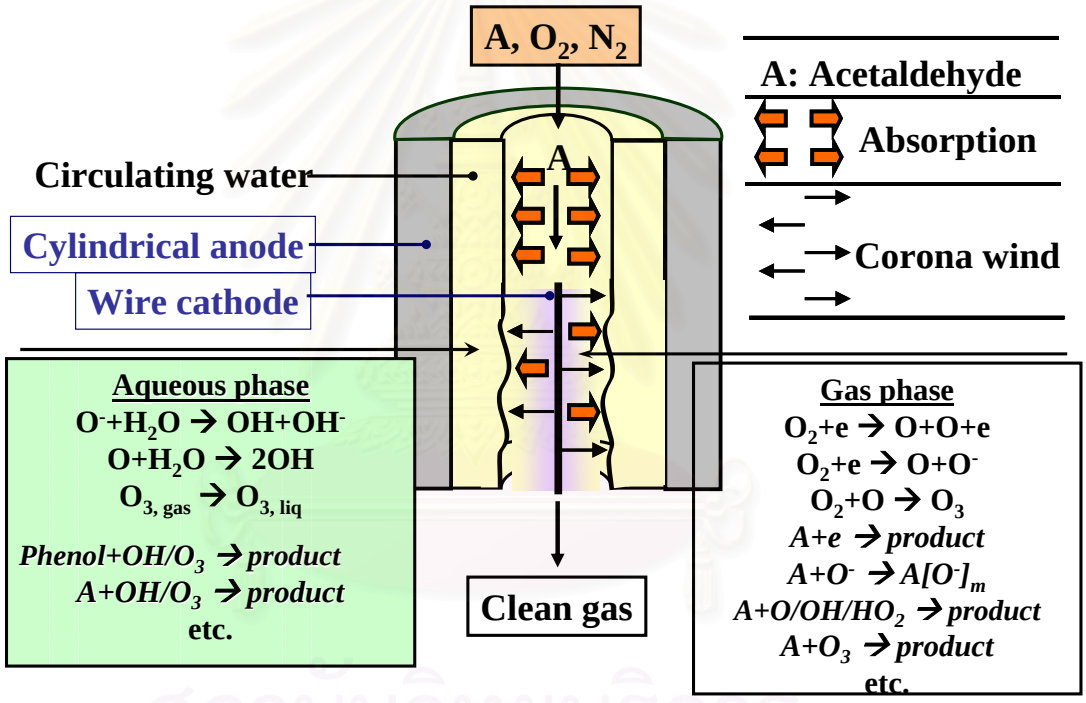

Figure 3.2 Simultaneous treatment concept of Gaseous acetaldehyde and aqueous phenol using a wetted – wall corona discharge reactor

3.4 Type of Corona Discharge Reactors

In some cases certain kind of negative ions produced by electron attachment would drift towards but do not easily adhere to the anode surface. Thus they end up as uncaptured negatively charged or uncharged impurities at the outlet of the conventional deposition – type reactor, and cause a decrease in their removal efficiency. It is therefore essential to find out how to effectively remove such negative ions at the anode. This has motivated Tamon et al. to propose three types of reactor, as shown in **Figure 3.3.**

3.4.1 Deposition–type reactor

Some negative ions readily adhere to the anode surface of the reactor after releasing their negative charges there. In this case they may form solid particles or react with the metallic anode. The solid particles form a thin deposition layer on the anode surface. Thus, the so–called deposition – type or (simple) reactor is adequate for the removal of these negative ions. Periodic cleaning of the anode surface or its replacement is often necessary to maintain high removal efficiency.

3.4.2 Sweep–out–type reactor

In some uncommon cases certain negative ions do not easily deposit on the anode surface but change back to the original uncharged molecules after releasing electrons at the anode surface. In such cases, the deposition-type reactor is not suitable because the original molecules of the gas impurities are not removed but

diffuse back to the main gas stream. To solve this problem, the sweep-out-type reactor, which uses a porous pipe wall made of sintered metal as anode is recommended. A small portion of the carrier gas around the anode surface is swept out by suction through this pipe to restrict backward diffusion of the concentrated electronegative impurities so that the removal efficiency would be kept high. The swept-out stream with a much higher concentration of the gas impurities can then be treated using a suitable conventional method.

3.4.3 Wetted–wall reactor

Another option to remove negative ions at the anode surface is the wetted-wall reactor. Negative ions reaching the anode of the reactor can be absorbed into a down-flowing liquid film on the vertical anode surface. This absorption of the ions improves the removal efficiency. The most important advantage is the self-cleaning of the anode, which makes it suitable even for dirty gas streams containing both dust and gaseous pollutants. The major drawback is the need for a liquid (mostly water) treatment and recycles system.

Recently, this reactor is applied for wastewater purification by Sano et al. (2003). The organic compounds in aqueous solution were used to make a liquid film. Direct contact of gas corona species with water molecules produces reactive OH radicals which contribute to decomposition of the target compounds in water. The OH radical is known as the most powerful oxidant in the advance oxidation processes (AOPs).

With these special features, the wetted – wall reactor is used in this research for both separate treatment of gaseous acetaldehyde, that of aqueous phenol and simultaneous treatment of gaseous acetaldehyde and aqueous phenol.

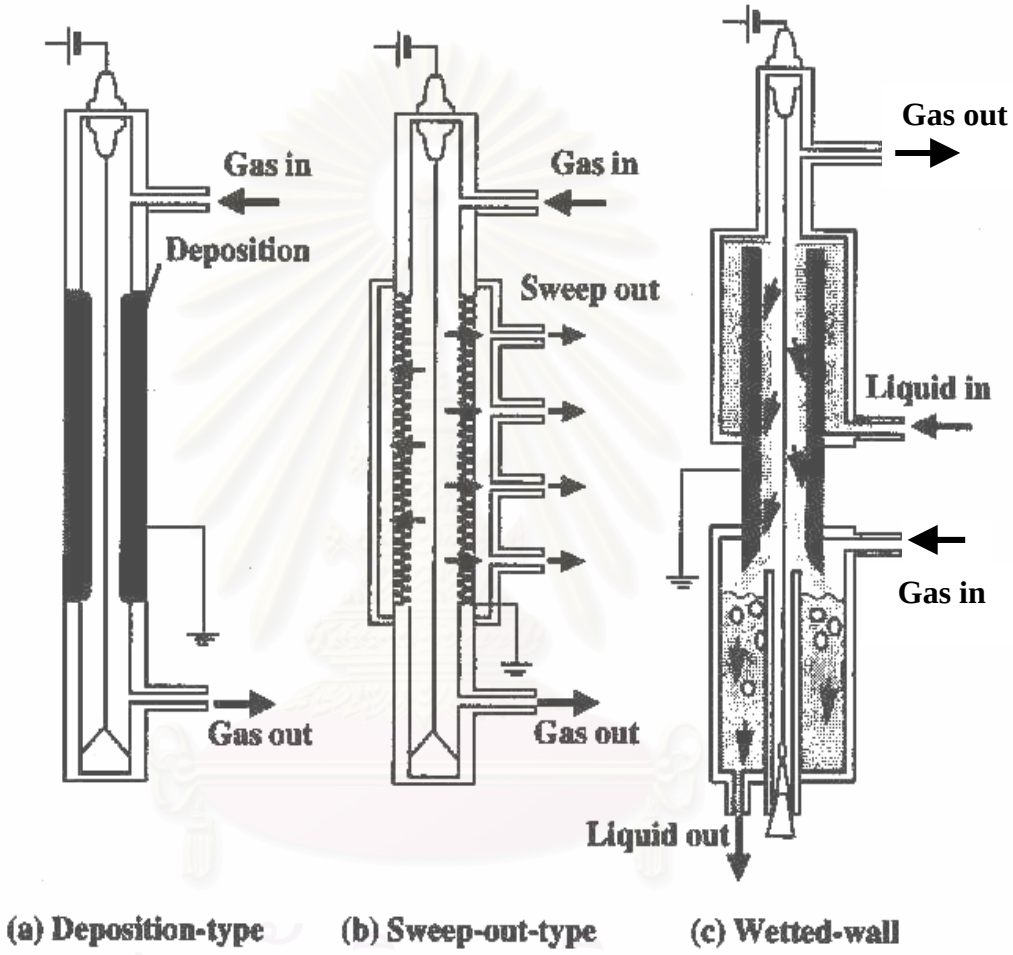

Figure 3.3 Types of corona–discharge reactor

CHAPTER 4

EXPERIMENTAL PROCEDURE

4.1 Test Materials and Chemicals

The specification of test materials and chemicals used in this research work were shown in **Table 4.1.**

Table 4.1 The specifications of test materials and chemicals

Type	Use	Purity / Grade
Acetaldehyde (g)	Sample gas	Acetaldehyde 361 ppm balanced with N_2
Oxygen (g)	Coexisting gas	Industrial grade
Nitrogen (g)	Carrier and diluents gas to reactor	UHP* 99.999 % min
Nitrogen (g)	Carrier gas for GC	UHP* 99.999 % min
Hydrogen (g)	For flame ignition	HP*, 99.99%
Air Zero (g)	For flame ignition	N / A
Phenol	Sample liquid	Analytical grade
Acetic acid	Sample liquid	Analytical grade
NaOH	For adjusting pH of solution	Analytical grade
HCl	For adjusting pH of solution	Analytical grade
H_3PO_4	For adjusting pH of solution	Analytical grade
HNO_3	For adjusting pH of solution	Analytical grade

* UHP = Ultra high purity, HP = High purity

4.2 Experimental Setup

Figures 4.1 (a) and 4.1 (b) show the actual arrangement of the wetted – wall reactor and experimental apparatus used in this work, while **Figures 4.2 (a)** and **4.2 (b)** present their schematic diagrams.

Figure 4.1 (a) Arrangement of present wetted – wall reactor

Figure 4.1 (b) Arrangement of the experimental apparatus

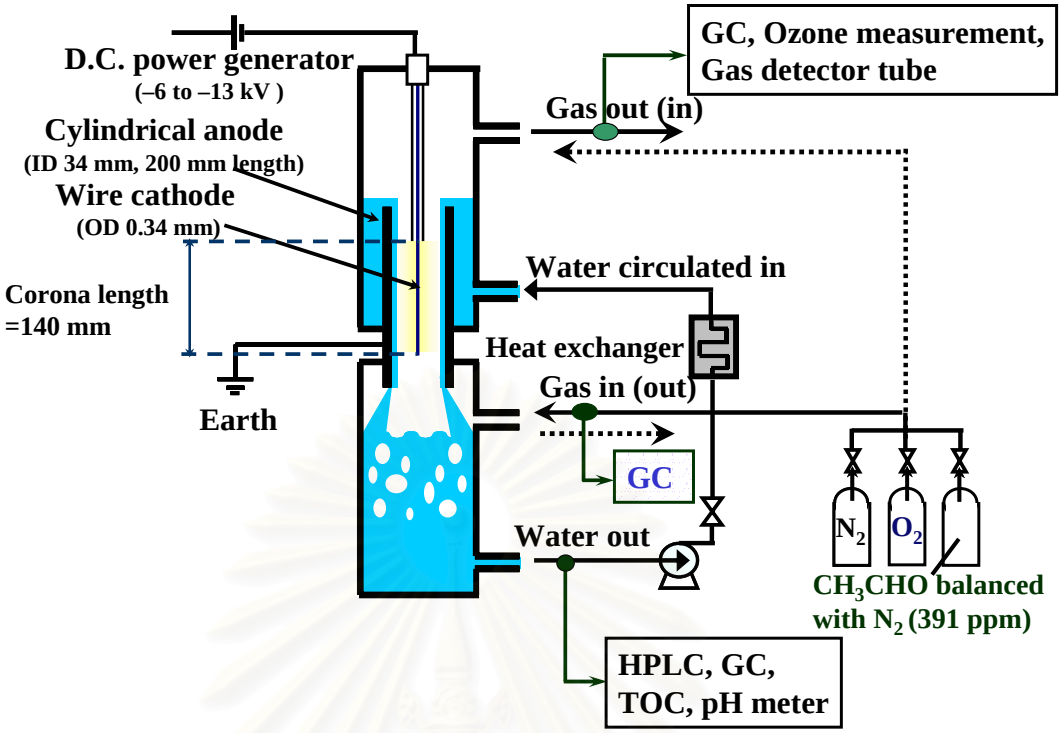

Figure 4.2 (a) Schematic diagram of the experimental set-up for separate treatment of gaseous acetaldehyde or aqueous phenol

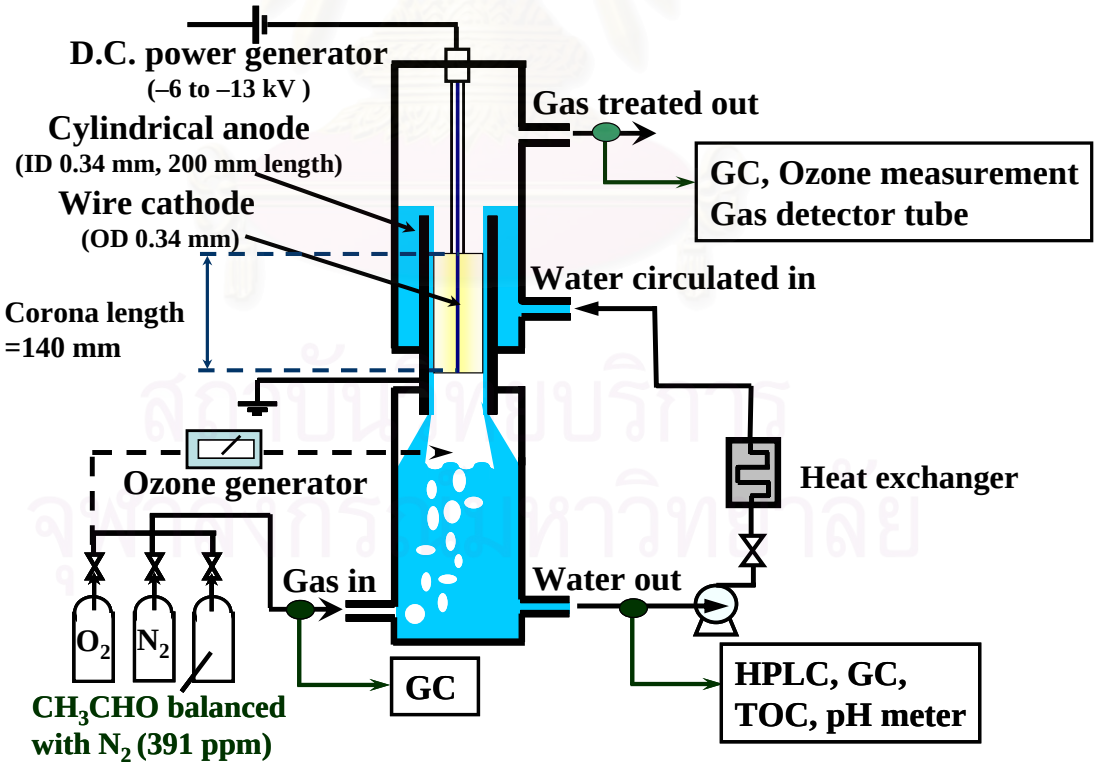

Figure 4.2 (b) Schematic diagram of the experimental set-up for simultaneous treatment of gaseous acetaldehyde and aqueous phenol

As shown in **Figures 4.2 (a)** and **4.2 (b**), a stainless steel (SUS) wire cathode (0.34 mm diameter) was sustained along the center of a SUS cylindrical anode (34 mm inner diameter; 200 mm length). By using the high – voltage D.C. generator shown in **Figure 4.3**, a high voltage of –8 to –13 kV was applied on the cathode to generate corona discharge. The effective length of axial corona discharge was fixed at 140 mm for all experiments. Throughout all runs, the gas flow rate, water flow rate and volume of circulating water were controlled at 100 $cm^3 min^{-1}$, 1400 $cm^3 min^{-1}$ and 1000 cm^3, respectively. The water circulation rate used here was found as the optimal flow rate for decomposition of aqueous phenol by using the wetted-wall corona discharge reactor used in this research work (Sano et el., 2003). At this flow rate, the water could be circulated at 84 cycles an hour. The water film thickness, Reynolds numbers (*Re*) of water and gas streams in the absence of corona discharge were, therefore, calculated as 0.4 mm, 870, and 4, respectively. The temperature of the water was controlled at 10 ^oC by passing it through a heat exchanger unit.

4.2.1 Separate Treatment of Gaseous Acetaldehyde

Standard acetaldehyde gas balanced with N_2 was mixed with O_2 and N_2 from gas cylinders and then fed either upward or downward through the reactor in one pass, whereas water, originally deionized, was circulated as a falling film on the inner surface of the grounded anode. The concentration of acetaldehyde and that of oxygen were varied in the ranges of 0 – 200 mol-ppm and 0 – 21%, respectively.

4.2.2 Separate Treatment of Aqueous Phenol

When the removal of phenol was conducted, phenol solution was used as circulating water. The gas mixture of O_2 and N_2 was fed to the reactor at above water layer, flowing upward through the reactor. The concentration of phenol was varied in the range of 0 – 100 mg L^{-1}.

4.2.3 Simultaneous Treatment of Aqueous Phenol and Gaseous Acetaldehyde

Gas mixture of acetaldehyde, oxygen, and nitrogen was fed to the reactor by bubbling into the water reserved below the corona zone. The solution was prepared by dissolving phenol into de-ionized water. The concentration of acetaldehyde was varied in the range of 0 – 200 mol-ppm. Meantime, the concentration of phenol was varied in the range of 0 – 100 mg L^{-1}.

When the effect of pH was investigated, the pH of the solution ranging from 2-13 was adjusted by adding H_3PO_4, HCl, HNO_3 or NaOH.

Ozone (O_3) can be produced in the presence of O_2 under the corona discharge in the reactor. In the experiments 4.2.1, 4.2.2 and 4.2.3, O_3 around 2000 mol-ppm maximum was detected in the treated gas. Thus, the contribution of ozone to the purification of phenol and acetaldehyde was first separately evaluated without corona discharge to perform this experiment. O_2 (21 cm^3 min^{-1}) is separated from the main gas stream before being fed to an ozone generator to produce ozone at approximately 1% by mole. Subsequently, it is fed to the bottom part of gas corona zone. Whereas the main gas stream, 125 mol-ppm acetaldehyde balanced with nitrogen at 79 cm^3 min^{-1}, is bubbled through the wetted-wall reactor. When the ozone mixes with the main gas stream in the reactor, the ozone concentration was diluted to approximately 2000 mol-ppm, and total gas flow rate was determined at 100 cm^3 min^{-1}. Under these conditions, the concentrations of all gas components become similar to those used in the experiments with the corona discharge.

To compare the removal efficiency obtained from the wetted – wall reactor and the deposition reactor, the deposition type reactor as shown in **Figure 3.3 (a)** was constructed for conducting the separate experiment on removal of gaseous

acetaldehyde. The deposition reactor used here consisted of a cylindrical anode and a coaxial wire cathode of the same dimensions as the wetted-wall reactor.

Since corona wind was generated during the corona discharge, it could affect the reactions inside the reactor. The corona wind velocity inside the reactor was evaluated as an indicator of the degree of gaseous turbulence in the reactor by measuring the pressure difference between the dynamic pressure in the corona wind and the static pressure outside the reactor by a Pitot tube. The measurement was conducted under the condition that gas flow was fed into the reactor without feeding water onto the wall of the reactor. This was because the Pitot tube inserted into the corona zone through the anode disturbed the water film.

Figure 4.3 High - voltage DC generator

4.3 Analytical Methods

The gas composition at the inlet and outlet of the reactor were analyzed by a gas chromatograph (Shimadzu, GC-9A or GC-14B) equipped with an FID detector. Gaseous ozone concentration was measured by KI method. To determine the gaseous ozone concentration, the outlet gas was sampled (4 cm^3) and bubbled into a 1 mol/L KI solution (5 cm^3), and then a UV/VIS spectrophotometer (Shimadzu, UV-1600PC) was used to measure the photoabsorptivity at 288 or 353 nm to estimate the ozone concentration. Gaseous byproducts such as NO_x and CO were measured by gas detector tube (GASTEC Co., Ltd. and Kitagawa Co., Ltd.).

A high performance liquid chromatograph (HPLC) with a UV-VIS detector (Shimadzu, SPD-10AVP) and the FID gas chromatograph were used for analyses of phenol, acetaldehyde, and intermediate products in the circulating water. For HPLC analysis, an adsorption column, Devolosil (Nomura chemical – ϕ 4.6 mm x 50 mm), was operated at fixed temperature 20 ^oC. The UV-VIS detector was set at 277 nm. The carrier liquid was 0.1% aqueous phosphoric acid mixed with acetonitrile (2%). Total organic carbon (TOC) and pH of the circulating water were measured by a TOC analyzer (Shimadzu, TOC-5000) and a pH meter (Horiba, pH meter F-22), respectively.

Table 4.2 Operating conditions of FID gas chromatograph

Sample	Column temperature (^oC)	Injection temperature (^oC)	Detector temperature (^oC)	Retention time (min)	Column Packing Type
CH_3CHO	150	160	160	4.5	Porapak Q
CH_2O	150	160	160	3.5	Porapak Q
CH_3CO_2H	140	160	160	10	Peg 6000 Flusin T

Table 4.3 Retention time of aqueous species analyzed by HPLC

Sample	Retention time (min)
Phenol	13
Hydroquinone	2.5
1,4-benzoquinone	4.6
Resorcinol	4.8
Catechol	6.9

Figure 4.4 Gas chromatograph GC-9A

Figure 4.5 Gas chromatograph GC-14B

Figure 4.6 High performance liquid chromatograph (HPLC)

Figure 4.7 TOC analyzer TOC-5000

Figure 4.8 UV/VIS spectrophotometer UV-1600PC

4.4 Experimental Procedure

To carry out the experiments, the following implementation steps must be carried out carefully because of the high risk of physical injury caused by the high voltage supplied to the reactor.

a. Ensure that the reactor is securely grounded and each unit of the experimental apparatus is also securely connected.
b. Check the gas line for the experiment (feed gas balance nitrogen, O_2, acetaldehyde)
c. Introduce the water into the reactor, and then circulate the water via pump at flow rate of interest.
d. Mix the above streams in the gas mixing device and measure the total flow rate with the soap film flow meter.
e. Feed the gas mixture to the inlet of the reactor.
f. Turn on the high voltage DC generator, adjust the discharge current as desired, and then keep the current stable throughout each experimental run.
g. Take gas samples at the inlet and outlet of the reactor and analyze their concentrations. Simultaneously, take water samples for analysis.
h. After finish the experimental run, Turn off the DC generator after the completion of the experiment. Be careful that high voltage does not remain in the reactor.
i. Stop gas flow and take off the water from the reactor.
j. Clean the reactor by introducing fresh deionized water and circulating it in the reactor for about 1 hr.
k. Take out the water.

CHAPTER 5

RESULTS AND DISCUSSION

5.1 Voltage – Current Characteristics

Figure 5.1 shows the voltage–current (V–I) characteristics of the wetted-wall corona discharge reactor at various oxygen concentrations. In the absence of O_2, the corona voltage increased very slightly from 6.5 to 7.5 kV, while the corona current is increased widely from 0.25 to 2 mA. In contrast, in the presence of 1% oxygen, the corona voltage sharply increases from around 8 to 15 kV when the current is increased from 0.1 to 2 mA. The increase in oxygen concentration from 1 to 21% causes higher corona voltage requirement. The high electron affinity of O_2, which easily induces the formation of oxygen ions, would be one of the reasons of this voltage elevation. It should be reminded that electron affinity of O_2 is significantly larger than that of N_2. They are 1.78 and –2.58 eV, respectively. These values were calculated by the density functional calculation at B3LYP/6-31G level. Because the ion mobility is much lower than electron mobility (Chen and Davidson, 2003), the voltage required to maintain the corona discharge in presence of oxygen is significantly higher than that in its absence. The difference of the required voltages between in presence and in absence of the falling water film on the anode was insignificantly smaller than 2%.

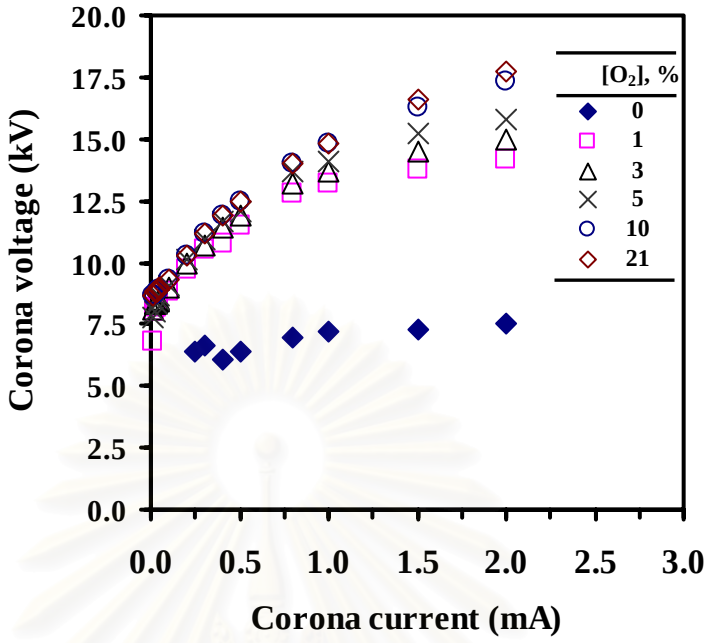

Figure 5.1 V–I characteristic of wetted-wall corona discharge reactor at various oxygen concentrations.

5.2 Treatment of Gaseous Acetaldehyde

5.2.1 Effect of Corona Current

Figure 5.2 shows the outlet concentration of gaseous acetaldehyde $C_{a\text{-}g}$ during the discharge operation. The influence of the corona discharge current, varied from 0.02 to 0.3 mA, on the purification of acetaldehyde laden air is investigated here. Even in the absence of corona discharge, $C_{a\text{-}g}$ initially drops to essentially zero because acetaldehyde is readily absorbed into fresh water. However, $C_{a\text{-}g}$ significantly rises with time as the water is incessantly contaminated with acetaldehyde. When the corona discharge is generated, for instance at the discharge current of 0.1 mA, $C_{a\text{-}g}$ continues to gradually increase at early stage but levels off at around 8 mol-ppm after 200 min. However, if the applied discharge current is lower

than 0.1 mA, the effect of corona discharge becomes weak and C_{a-g} does not level off at a constant value. It should be noted out that the decomposition of the feed acetaldehyde takes place mainly in the aqueous phase as discussed in the latter section.

When the discharge current increases, the asymptotic value of C_{a-g} is found to slightly increase. The result may be attributed to corona induced turbulence in the gas stream flowing inside the reactor, which affects the residence time distribution (RTD) of the gas in the reaction zone. When the ion wind induces turbulence, the RTD in the reactor becomes closer to that of a continuous stirred tank reactor (CSTR), which possesses a much broader RTD than a laminar flow model, or plug flow reactor (PFR), with the same mean residence time. This phenomenon is known to result in a lower conversion efficiency (Bird et al., 1960) and is the reason why a higher *I* yields a lower acetaldehyde removal efficiency.

When corona discharge is generated, electrons are emitted from the wire cathode and then drift to the anode. In the small region of high strength electric field adjacent to the wire cathode, electron impacts on gas molecules produce short-lived radicals such as O as shown in Eq. (5.1) (Peyrous et al., 1989; Loiseau et al., 1994). During the drift process, low – energy electrons collide with gas molecules and electron attachment reactions are expected to take place, as shown in Eq. (5.2). In addition, ozone is produced, as in Eq. (5.3) (Moruzzi and Phelps, 1966).

$$O_2 + e^- \rightarrow O + O + e^- \qquad (5.1)$$

$$O_2 + e^- \rightarrow O^- + O \qquad (5.2)$$

$$O_2 + O \rightarrow O_3 \qquad (5.3)$$

In the reactor, the gas stream also contains water vapor. Thus electron attachment to H_2O vapor should produce OH^- and H^-, whereas dissociation of H_2O should produce OH and H radicals (Moruzzi and Phelps, 1996; Peyrous et al., 1989). Acetaldehyde not absorbed into the aqueous phase would be removed by the reactions with ions, radicals (Sano et al., 1997; Butkovskaya and Setser, 2000; Tomas, Villenave and Lesclaux, 2001), and ozone (Sano et al., 1997) generated by corona reactions in the gas phase as shown in Eqs. (5.4) – (5.8)

$$OH + CH_3CHO \rightarrow CH_3CO + H_2O \quad (5.4)$$

$$HO_2 + CH_3CHO \rightarrow \text{product} \quad (5.5)$$

$$O + CH_3CHO \rightarrow \text{product} \quad (5.6)$$

$$O_3 + CH_3CHO \rightarrow \text{product} \quad (5.7)$$

$$O^- + CH_3CHO \rightarrow O^-[CH_3CHO]_m \quad (5.8)$$

Since the observed values of the $C_{a\text{-}g}$ shown in **Figure 5.2** depend mostly on the absorptivity of the gaseous acetaldehyde into the circulating water, $C_{a\text{-}g}$ is thought to depend on the pH of the water during the operation. In **Figure 5.3**, the pH values of the water during the discharge operation are plotted. Based on a starting pH value of around 6 – 7, they gradually decrease in around 200 min before stabilizing at around pH 4.5 – 5.5. This may be ascribed to the fact that HNO_3 is produced during the discharge operation (Hoeben, 2000; Sano et al., 2003). It should be noted that the final value and decreasing rate of the pH depend on the applied corona discharge current. To investigate the influence of pH on the absorption rate, the initial pH of the circulating water was varied from 4 to 6.5 by adding HNO_3. In the absence of discharge current, acetaldehyde laden air is passed through the wetted-wall reactor

and $C_{a\text{-}g}$ is measured at adequate time intervals. Influence of pH on the absorptivity of acetaldehyde is shown in **Figure 5.4**. In these experiments, the observed difference in the acetaldehyde absorption rate is negligible in this pH range. Therefore it may be considered that the absorptivity of acetaldehyde is not significantly affected by the pH of the water during the operation.

The reaction scheme of production of OH radical is shown in Eqs. (5.9)-(5.11) (Sano et al., 2002). The OH radical along with O_2H and ozone are expected to contribute to the decomposition of acetaldehyde in water as shown in Eq. (5.12).

$$O^-_{(gas)} + H_2O \rightarrow OH^-_{(aq)} + OH_{(aq)} \quad (5.9)$$

$$O_2^-{}_{(gas)} + H_2O \rightarrow OH^-_{(aq)} + O_2H_{(aq)} \quad (5.10)$$

$$O_{(gas)} + H_2O \rightarrow OH_{(aq)} + OH_{(aq)} \quad (5.11)$$

$$OH_{(aq)}, O_2H_{(aq)}, O_{3(aq)} + CH_3CHO_{(aq)} \rightarrow \text{product} \quad (5.12)$$

In **Figure 5.5**, the concentrations of aqueous acetaldehyde $C_{a\text{-}l}$ at various discharge currents are depicted against corona – discharge time. As expected, $C_{a\text{-}l}$ increases with time in the absence of corona discharge. When corona discharge is generated, the increase in $C_{a\text{-}l}$ is retarded by its decomposition. The rate of decomposition of the aqueous acetaldehyde becomes greater as I increases. It may be ascribed to the fact that, when I increases, more radicals, ions, and ozone are produced by the higher density of electrons. Similar to the effluent concentration of gaseous acetaldehyde shown in **Figure 5.2**, $C_{a\text{-}l}$ becomes stabilized after about 200 min at 0.1 and 0.3 mA, but keeps increasing at 0.02 mA. These results indicate that the current higher than 0.1 mA is required to stop the accumulation of the aqueous acetaldehyde. In other words, if the discharge current is too low, stable purification of acetaldehyde

laden air cannot be achieved because the unceasing accumulation of the aqueous acetaldehyde inhibits the gas – phase removal of acetaldehyde by gas absorption. It should be noted that, according to overall mass balance of acetaldehyde in the blank test, the deposit of acetaldehyde on the wall of anode is negligible.

Figure 5.6 (a) shows the concentrations of liquid – phase TOC and of aqueous acetaldehyde during the discharge operation for the cases of both upflow and downflow. The current 0.5 mA was used here, which is the optimized value to degrade stable organic compounds in water under the present dimension of the reactor, as previously reported (Sano et al., 2003). When corona discharge is not generated, both TOC and acetaldehyde concentrations increase with time due to gas absorption. As expected, their values in either case of upflow and downflow are essentially the same. When corona discharge is generated, the increases of TOC and acetaldehyde are significantly attenuated. However, though $C_{a\text{-}l}$ becomes stabilized, TOC continues to gradually increase. This indicates that some byproducts which are more stable than acetaldehyde are accumulated in the water. To identify the byproducts, the circulating water is analyzed with the GC and HPLC. The detected byproduct has the same retention time with acetic acid whereas the presence of formaldehyde is slightly detected at the outlet of the reactor. Acetic acid is a common byproduct of the oxidation treatment of aqueous acetaldehyde (Jacob, Gottlied and Prather, 1989).

The kinetic rate constants of acetaldehyde and acetic acid toward ozone and radical OH in water are listed in **Table 5.1**. Based on the rate constants, it is considered that acetic acid is more stable than acetaldehyde. To back up our assertion, we carried out experiment on the decomposition of aqueous acetic acid. One liter of aqueous acetic acid (50 mg L^{-1}) was decomposed in stationary air in the

wetted-wall reactor with I = 0.5 mA and Q_l =1400 cm^3 min^{-1}. The result shows that about 20% of TOC is slowly degraded in 8 h. Since O_3 is produced up to 2000 – 2500 ppm in our reactor, the contribution of O_3 toward the decomposition of aqueous acetaldehyde was also evaluated experimentally, as explained in the experimental section. The result explores that decomposition of aqueous acetaldehyde by O_3 does not play a significant role in the present condition.

To avoid the non–stop accumulation of TOC in the circulating water, the influent concentration of gaseous acetaldehyde $C_{a\text{-}g\ inl}$ was intentionally decreased. **Figure 5.7** shows the change in TOC concentration at various $C_{a\text{-}g\ inl}$. Here the current is maintained at 0.5 mA and the gas flow direction is upward. The result shows that, when $C_{a\text{-}g\ inl}$ is decreased, the increasing rate of TOC is reduced. The value of TOC becomes stabilized when $C_{a\text{-}g\ inl}$ is 50 mol-ppm. To maintain a stable TOC level, the generation rates of the aqueous acetaldehyde and its byproducts must equal their decomposition rates. It should be noted that the maximum $C_{a\text{-}g\ inl}$ to avoid the non-stop accumulation of TOC would depend on the experimental conditions such as corona current, water flow rate, gas flow rate and gas flow direction.

Table 5.1

Kinetic rate constants of decomposition of aqueous acetaldehyde and acetic acid toward ozone (k_{O3}) (Bruno et al., 1991) and OH radical (k_{OH}) (Buxton et al., 1988)

Substance	k_{O3} ($M^{-1}s^{-1}$) (nondissociated Form)	k_{OH} ($M^{-1}s^{-1}$)
Acetaldehyde	1.5	$7.3x10^8$
Acetic acid	$3x10^{-5}$	$1.6x10^7$

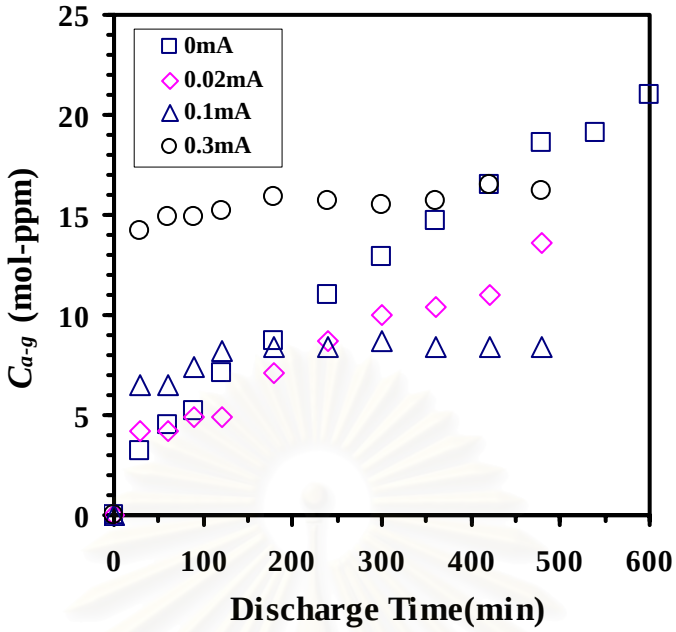

Figure 5.2 The concentration of acetaldehyde in treated gas during corona discharge operation. $C_{a\text{-}g\ inl}$=200 mol-ppm, Gas flow direction:Upflow

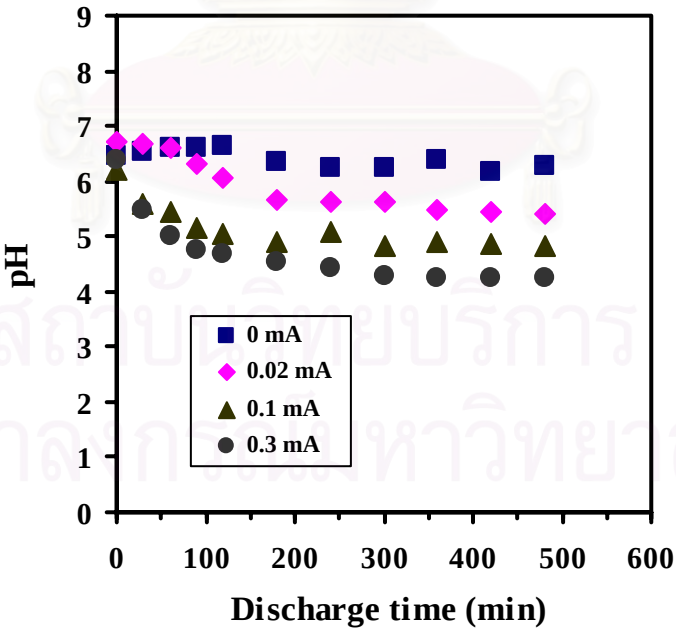

Figure 5.3 Change of pH of water against discharge time. $C_{a\text{-}g\ inl}$=200 mol-ppm, Gas flow direction:Upflow.

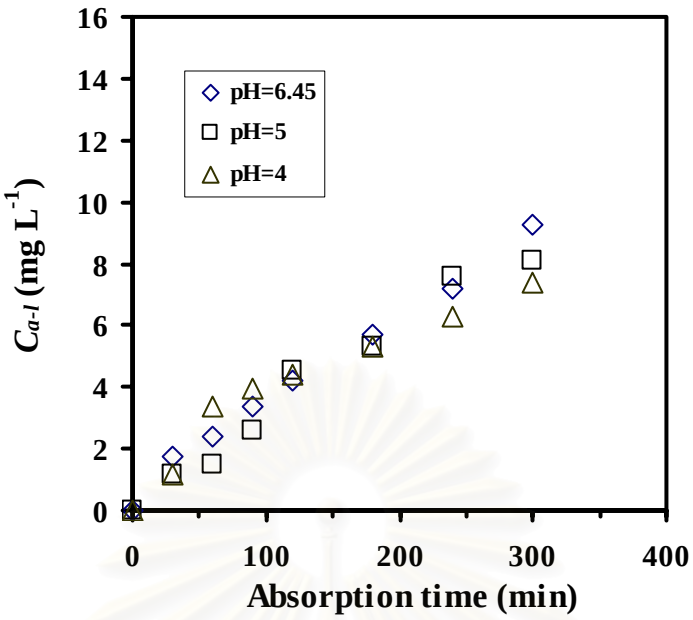

Figure 5.4 Influence of pH on absorptivity of acetaldehyde. $C_{a\text{-}g\ inl}$ =200 mol-ppm, Gas flow direction:Upflow.

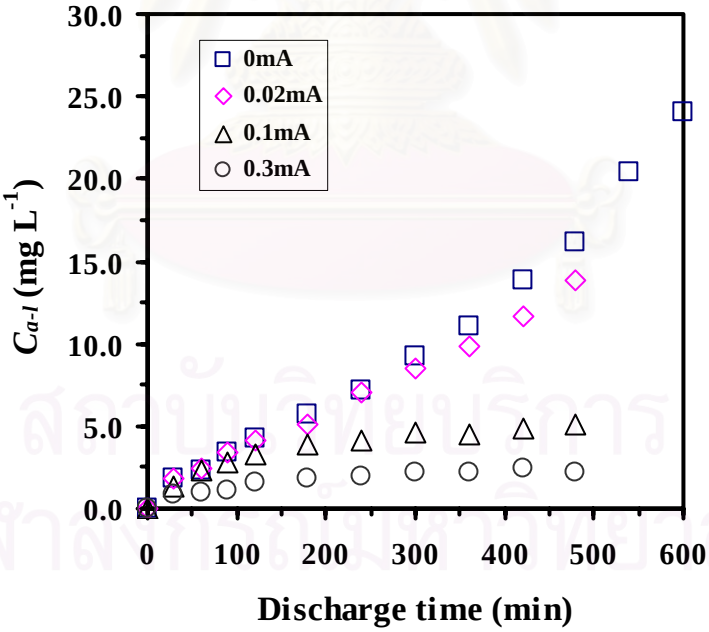

Figure 5.5 The concentration of acetaldehyde in circulating water during corona discharge operation. $C_{a\text{-}g\ inl}$=200 mol-ppm, Gas flow direction:Upflow.

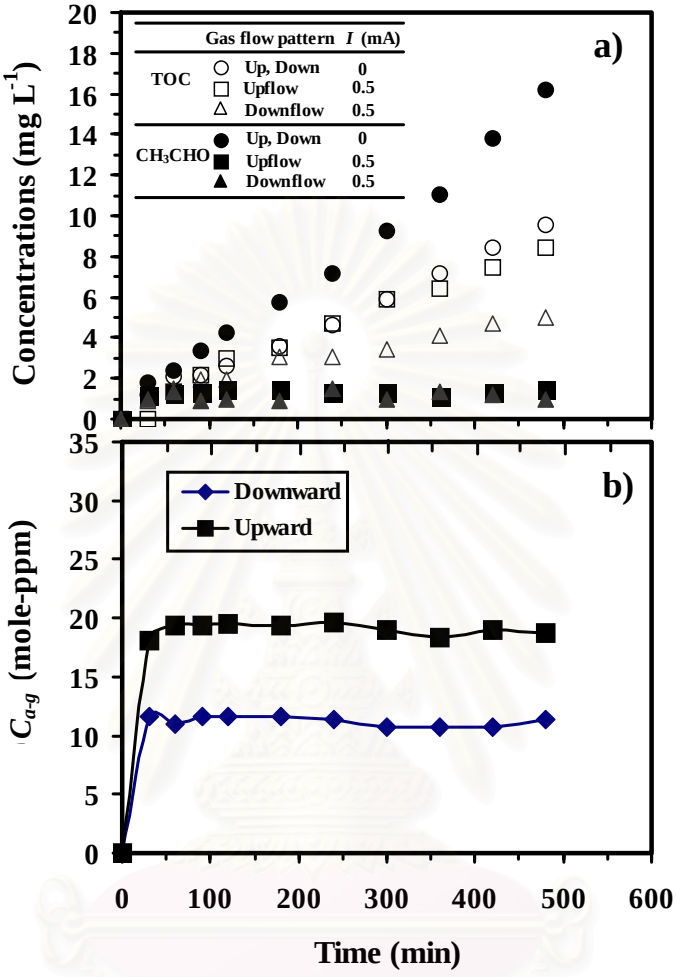

Figure 5.6 Influences of gas flow directions on a) TOC and aqueous acetaldehyde and on b) gaseous acetaldehyde removals. $C_{a\text{-}g\ inl}$=200 mol-ppm.

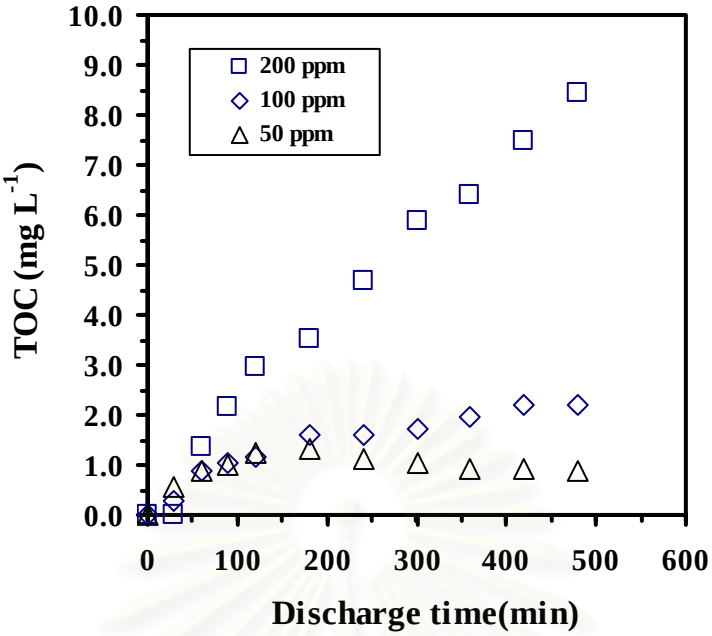

Figure 5.7 TOC concentration in water against discharge time at various inlet concentrations of gaseous acetaldehyde. *I*=0.5 mA, Gas flow direction:Upflow.

5.2.2 Effect of Influent Acetaldehyde Concentration

Figures 5.8 and **5.9** show the concentrations of gaseous acetaldehyde at outlet of the reactor and that of aqueous acetaldehyde during the discharge operation when the inlet concentration of acetaldehyde $C_{a\text{-}g\ inl}$ is varied from 50 – 200 mol-ppm. From **Figure 5.8**, the results show that $C_{a\text{-}g}$ remains almost constant at higher value when the $C_{a\text{-}g\ inl}$ increases. Similarly, $C_{a\text{-}l}$ remains almost constant at higher value when the $C_{a\text{-}g\ inl}$ increases as seen in **Figure 5.9**.

Although $C_{a\text{-}l}$ can keep constant in the water phase, the TOC of water still increases with discharge time when the $C_{a\text{-}g\ inl}$ is so high at 200 mol-ppm. To keep steady – state concentration of TOC, the $C_{a\text{-}g\ inl}$ is decreased to 50 mol-ppm under the present condition as explained in the previous section.

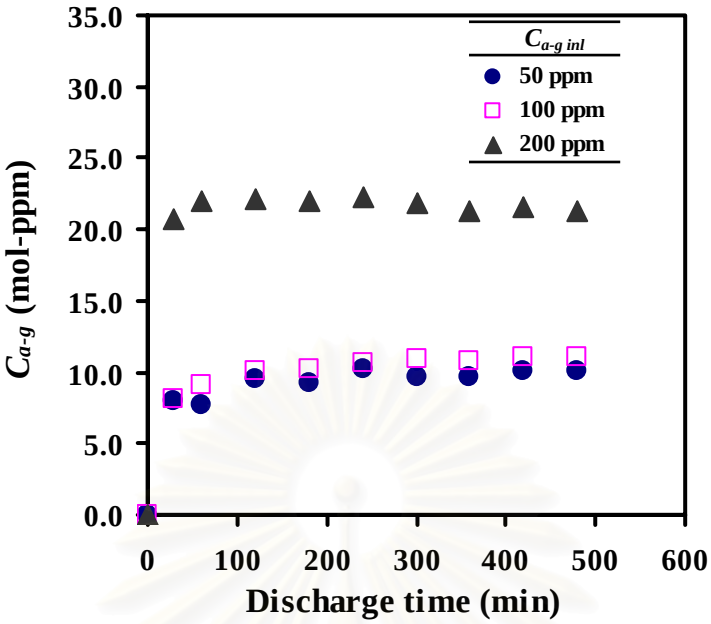

Figure 5.8 The outlet concentration of gaseous acetaldehyde against discharge time at various inlet concentrations of gaseous acetaldehyde. *I*=0.5 mA, Gas flow direction:Upflow.

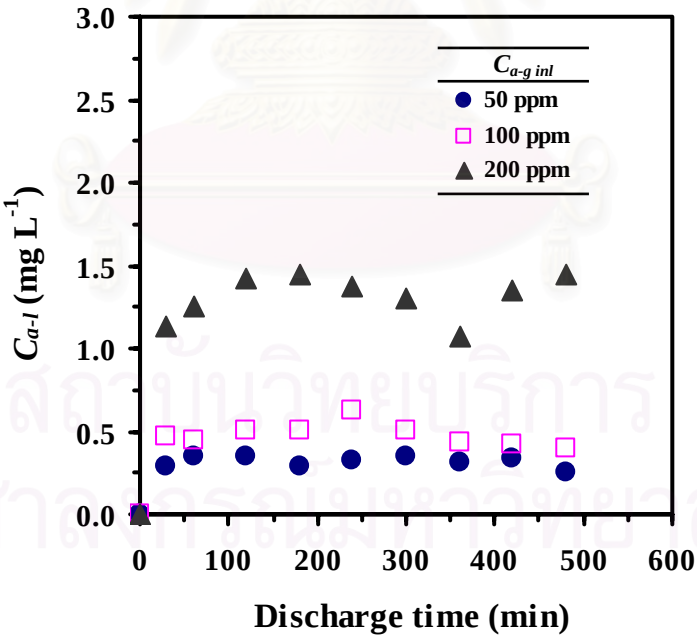

Figure 5.9 The concentration of aqueous acetaldehyde against discharge time at various inlet concentrations of gaseous acetaldehyde. *I*=0.5 mA, Gas flow direction:Upflow.

5.2.3 Effect of Gas Flow Direction

According to **Figure 5.6 (a)**, the downflow shows obviously higher decomposition rate of aqueous acetaldehyde and TOC than the upflow. To explain this result, the concentration profile of gaseous acetaldehyde along the reactor length in the absence of corona discharge was investigated experimentally, as shown in **Figure 5.10**. Apparently significantly more unabsorbed gaseous acetaldehyde remains to penetrate deeper into the corona zone in the case of downflow than upflow due to the present structure of the reactor. Therefore, when gas flow direction is upward, the removal of acetaldehyde is dominated by the reaction in the water phase because most gaseous acetaldehyde is absorbed into water before it reaches the corona zone. On the other hand, when the gas flow direction is downward, the removal reactions also take place significantly in the gas phase. It is logical to consider that the combined decomposition of gaseous and aqueous acetaldehyde improves the purification performance of the reactor.

In **Figure 5.10**, it should be noted that the concentration profile of gaseous acetaldehyde in the rector was obtained in a condition without corona discharge. When corona discharge occurs, the gas phase zone which is disturbed by ion – wind should be expanded to outside the corona zone (ion drift zone) because of convective effect. Therefore, it should be reminded that the excessive discharge current causing significant gas turbulence can raise the outlet concentration of acetaldehyde as explained in the previous section although the most acetaldehyde can be absorbed in water before it reaches the corona zone.

As seen in **Figure 5.6 (b)**, the downflow shows higher removal extent of gaseous acetaldehyde than the upflow. This is because the absorption of gaseous

acetaldehyde into the water can be accelerated by the enhanced water purification when the gas flow direction is downward. When the decomposition of absorbed acetaldehyde is enhanced, the driving force of absorption is also enhanced, resulting in improvement of absorption rate. In addition, the gas reactions should improve the removal of acetaldehyde.

O_3 is known to be produced from O radical and O_2 in the gas corona zone. If reaction of O with acetaldehyde does take place, then the observed O_3 concentration should be lowered. According to the ozone analysis, the effluent concentrations of ozone in the cases of upflow and downflow are $2.2x10^3$ and $1.6x10^3$ ppm, respectively. The results of gas-phase O_3 analysis confirm that the reaction between O radical and gaseous acetaldehyde take place to a significant extent when the gas is fed downward.

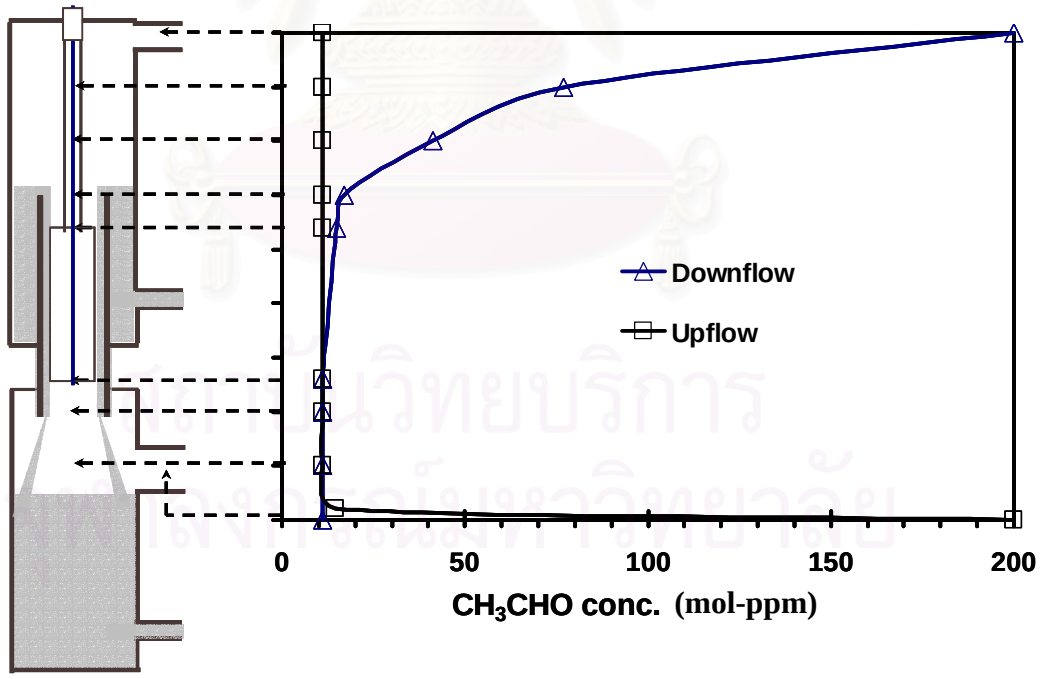

Figure 5.10 Acetaldehyde concentration profile in gas stream along the reactor. I=0 mA, $C_{a\text{-}g\ inl}$=200 mol-ppm, Time=4 hrs.

5.2.4 Effect of Oxygen Gas

5.2.4.1 Influence of oxygen on removal of gaseous acetaldehyde

Figure 5.11 shows the outlet concentration of gaseous acetaldehyde $C_{a\text{-}g}$ during the discharge operation at various oxygen concentrations ranging from 0 to 21% at a fixed corona current with downward gas flow. The inlet concentration of gaseous acetaldehyde here is at 200 mol-ppm. Without the corona discharge, $C_{a\text{-}g}$ is initially zero, which shows that acetaldehyde is readily absorbed into fresh water. However, $C_{a\text{-}g}$ rapidly increases with time because the water is continuously contaminated with acetaldehyde. When the corona discharge is generated in the gas stream with 5% oxygen, this increase in $C_{a\text{-}g}$ is drastically suppressed. At early time of operation, the $C_{a\text{-}g}$ becomes steady state at around 5 mol-ppm. This feature can also be noticed at 10, 21% oxygen concentrations. The $C_{a\text{-}g}$ increases as the oxygen concentration becomes greater. When oxygen does not coexist in gas stream, $C_{a\text{-}g}$ still increases with elapsed time. It is considered that the rate of acetaldehyde absorption is not stable because the aqueous acetaldehyde can be accumulated in the water and it inhibits the gas absorption. This result indicates that the oxygen plays a significant role on the removal of acetaldehyde in the wetted – wall corona discharge reactor. The ozone concentrations measured at oxygen concentrations 5, 10, and 21 % were respectively 200, 757, and 1622 ppm. This clearly shows that the increase in ozone concentration does not contribute the acetaldehyde removal. The reason why increase in oxygen inhibits the removal of acetaldehyde is explained later in this section.

In **Figure 5.12**, the removal extent ψ of acetaldehyde defined by Eq. (5.13) is plotted against corona discharge current, I.

$$\psi = (C_{a\text{-}g\ inl} - C_{a\text{-}g}) / C_{a\text{-}g\ inl} \quad (5.13)$$

where $C_{a\text{-}g\ inl}$ is the inlet concentration of gaseous acetaldehyde and $C_{a\text{-}g}$ is the time-averaged outlet concentration of acetaldehyde at steady state. The results clearly show that an increase in oxygen inhibits the removal extent at corona currents 0.3 and 0.5 mA. Focusing upon 5% oxygen concentration, the removal extent increases when the current increases from 0.1 to 0.5 mA. It was reasonable that the higher current provides a higher electron flux, resulting in more effective acetaldehyde removal. However, when oxygen concentration is 10 or 21%, the increase in the current does not provide a higher removal extent.

The inhibition of acetaldehyde removal by the increase in oxygen concentration could be attributed to corona – induced turbulence in the gas stream inside the reactor. To evaluate the degree of turbulence in gas stream, the velocity of corona wind was measured. The corona wind velocity is depicted against the oxygen concentration in **Figure 5.13**. When the current is either 0.3 or 0.5 mA, the increase in oxygen concentration leads to a significant increase in the corona wind velocity. Nonetheless, the corona wind velocity does not significantly increase when current is 0.1 mA. The corona-induced turbulence inside the corona reactor should affect the gas residence time distribution (RTD) in the reaction zone. It is considered that when the turbulence induced by corona wind becomes stronger, the RTD in the reactor should behave more likely that in a continuous stirred tank reactor (CSTR), which results in a much broader RTD compared with a plug flow reactor (PFR). It is common knowledge that, with the exception of the zero-order reaction, the CSTR possesses a lower conversion than the PFR based upon the same space – time (Bird et al, 1960).

It should be noted that the negative effect on removal extent of admixing oxygen could not be observed when the current was as low as 0.1 mA. This is compatible with that the corona – induced turbulence is not affected by O_2 concentration in the low current range.

5.2.4.2 Influence of oxygen on removal of absorbed acetaldehyde in water

Figure 5.14 shows the concentrations of aqueous acetaldehyde $C_{a\text{-}l}$ at various oxygen concentrations during the discharge operation. In the absence of corona discharge, $C_{a\text{-}l}$ obviously increases with time, suggesting that acetaldehyde is accumulated in the water by absorption. When corona discharge is generated, the increase in $C_{a\text{-}l}$ is attenuated by the decomposition of aqueous acetaldehyde. When the oxygen concentration was increased from 5 to 10%, $C_{a\text{-}l}$ becomes constant at a lower value. It is reasonable that with more oxygen coexisting in the corona zone, more O radical could be produced not only because of the high O_2 concentration but also due to the elevated voltage. As a result, the production of aqueous radical OH is enhanced, resulting in the higher decomposition rate of aqueous acetaldehyde. However, when oxygen is further increased from 10 to 21%, $C_{a\text{-}l}$ does not decrease further. This is because the elevated corona-induced turbulence disturbs the surface of the falling water film, resulting in less uniform spatial distribution of the gas corona. The reduced spatial uniformity of the gas corona attenuates the decomposition efficiency of an aqueous organic compound in water was revealed by Sano et al. (2003). The aqueous acetaldehyde is not so effectively decomposed in absence of oxygen.

Since aqueous acetaldehyde is converted to other organic compounds as intermediate byproducts, the total organic carbon TOC was monitored against the decomposition time. **Figure 5.15** shows the concentrations of TOC in the aqueous phase during the discharge operation at various oxygen concentrations. The figure reveals that, when the oxygen concentration is increased in the range of 5 to 10%, the TOC decomposition rate becomes greater. However, when the oxygen concentration is further increased from 10 to 21%, TOC decomposition rate does not significantly increase. This is because the smoothness of the water film surface was disturbed, resulting in less spatial uniformity of the corona.

Although the aqueous acetaldehyde concentration becomes stable as shown in **Figure 5.14**, the TOC concentration still increases with time. This result shows that there are some byproducts that are more stable than acetaldehyde accumulated in the water. The byproducts existing in the circulating water were identified by GC and HPLC. As a result, acetic acid which is common in the oxidation treatment of aqueous acetaldehyde (Jacob et al., 1989; Bruno et al., 1991) is detected as the dominant one. Other byproducts are quantitatively negligible compared with acetic acid.

To determine the effect of accumulating acetic acid in water on the removal of acetaldehyde by the present reactor, acetic acid is dissolved into the circulating water at 50 mg L^{-1} (equivalent to 20 mg L^{-1} TOC). **Figure 5.16** shows the concentration of gaseous acetaldehyde at outlet of the reactor and that of aqueous acetaldehyde in the circulating water against discharge time when pure de – ionized water or acetic acid solution is used as circulating water. The result shows that the concentration of gaseous acetaldehyde is kept constant at the same level for both cases. Similarly, the difference in aqueous acetaldehyde concentration between with and without acetic

acid contamination is negligible. This indicates that the removal of gaseous acetaldehyde can be sustained during the corona discharge operation even if acetic acid may be accumulated at high concentration in circulating water.

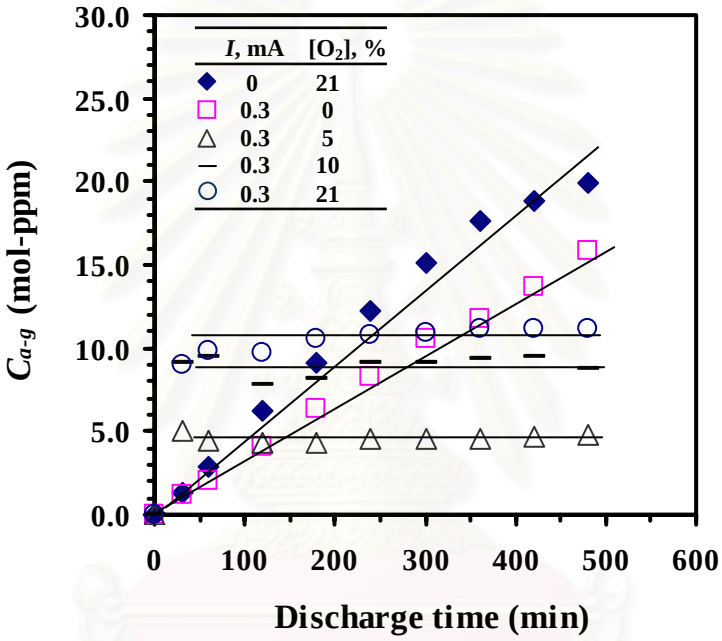

Figure 5.11 The concentration of acetaldehyde in treated gas during corona discharge operation at various oxygen concentrations. $C_{a\text{-}g\ inl}$=200 mol-ppm, Gas flow direction=Downward.

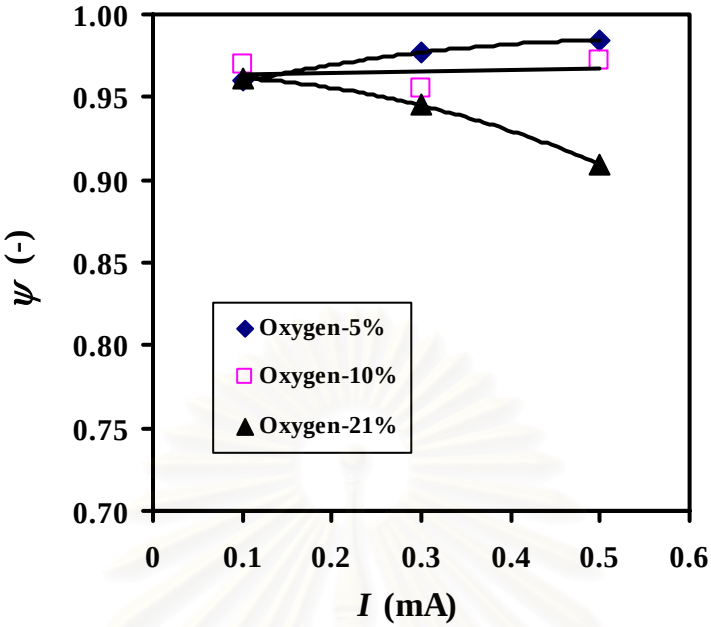

Figure 5.12 Removal extent of gaseous acetaldehyde against corona discharge current at various oxygen concentrations. $C_{a\text{-}g\ inl}$=200 mol-ppm, Gas flow direction=Downward.

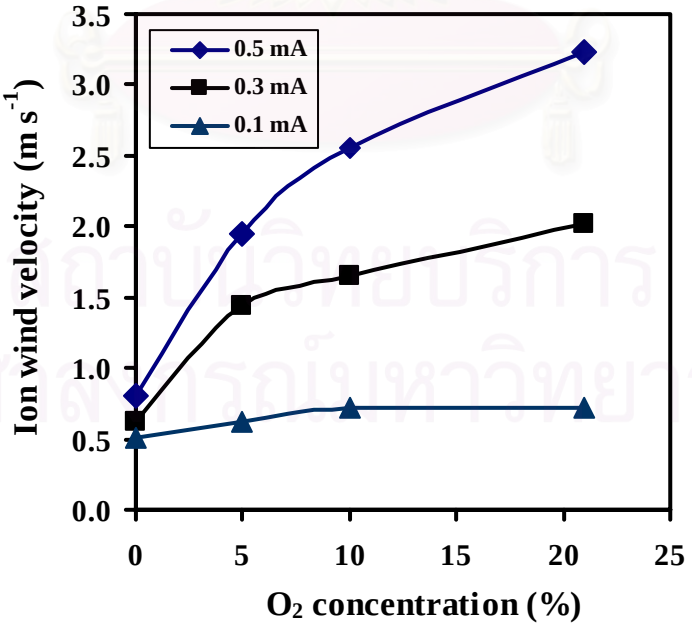

Figure 5.13 Effect of oxygen on corona wind velocity. Q_g=100 cm^3 min^{-1}.

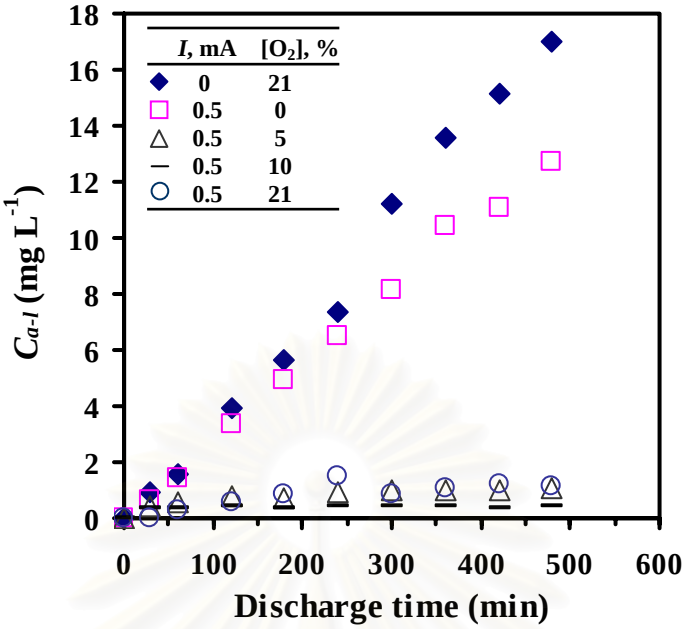

Figure 5.14 The concentration of acetaldehyde in circulating water during corona discharge operation at various oxygen concentrations. $C_{a\text{-}g\ inl}$=200 mol-ppm, Gas flow direction=Downward.

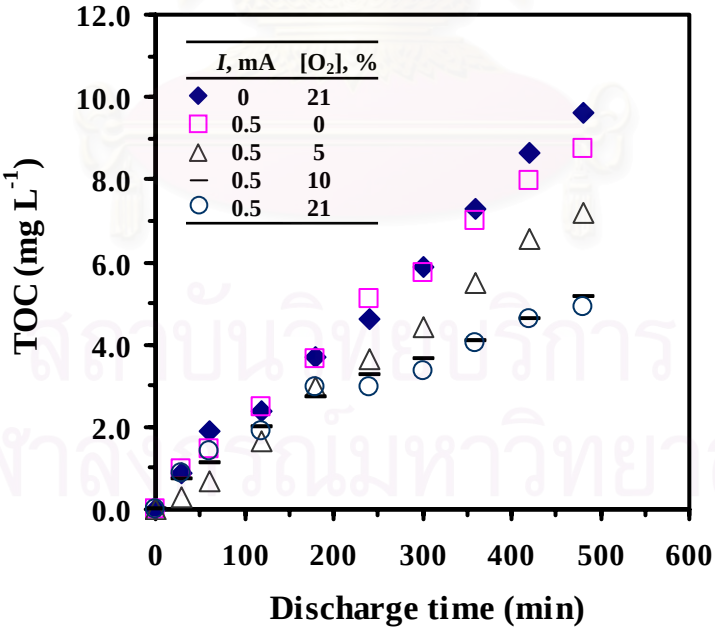

Figure 5.15 TOC concentration in water against discharge time at various oxygen concentrations. $C_{a\text{-}g\ inl}$=200 mol-ppm, Gas flow direction=Downward.

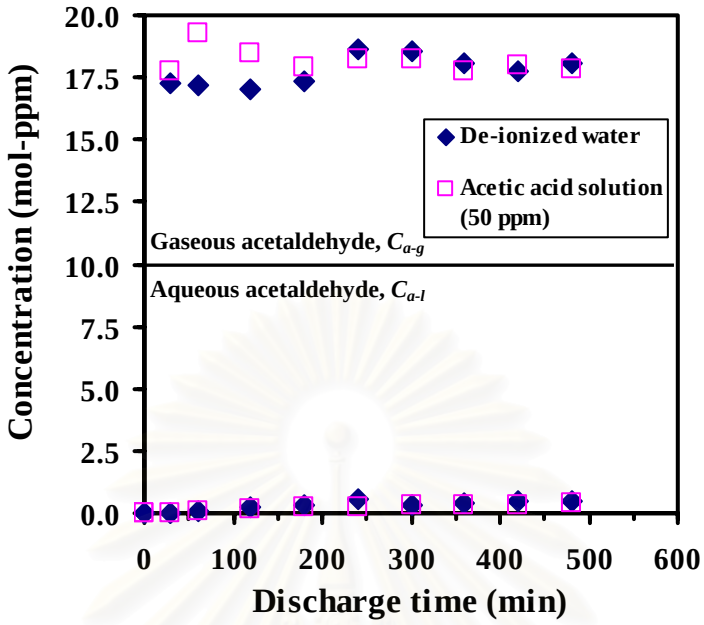

Figure 5.16 Effect of accumulating acetic acid on gaseous and aqueous acetaldehyde removals. I=0.5 mA, $C_{a\text{-}g\ inl}$=200 mol-ppm Oxygen=21%, Gas flow direction=Downward.

5.2.5 Effect of pH: Type of Inorganic Additives

The effects of inorganic additives, NaOH and HCl dissolved into the circulating water were investigated on the removal of gaseous acetaldehyde by the present reactor. In **Figure 5.17**, the concentration of aqueous acetaldehyde against absorption time in the absence of corona discharge is shown. It is obvious that dissolved NaOH and HCl enhance the absorptivity of acetaldehyde into water. In contrast, it was found that HNO_3 does not significantly affect the absorptivity of acetaldehyde as shown in the previous section. In fact, HNO_3 was produced in water during the corona operation, leading to the decrease in pH of water (Hoeben et al., 2000; Sano et al., 2002). When current is 0.1 mA, the pH of water decreased from around 6 – 6.5 to 5, corresponding to 10^{-5} mol L^{-1} HNO_3.

Figure 5.18 shows the outlet concentration of gaseous acetaldehyde during the discharge operation with various dissolved additives. The effect of dissolved inorganic compounds in water is investigated at corona current 0.1 mA with upward gas flow. It was found that NaOH enhances the removal of acetaldehyde from the gas stream, whereas HCl retards the removal of gaseous acetaldehyde. When NaOH concentration is further increased from 10^{-3} to 10^{-1} mol L^{-1}, the removal extent of gaseous acetaldehyde is increased from 97.1 to 98.5%.

In considering the effect of HCl, removal of gaseous acetaldehyde is attenuated even if HCl elevates its absorptivity. It is considered that absorbed acetaldehyde may be accumulated in circulating water, and the raised concentration of aqueous acetaldehyde may consequently inhibit the absorption of gaseous acetaldehyde into water. The concentrations of aqueous acetaldehyde $C_{a\text{-}l}$ in circulating water with dissolved NaOH, HCl and without additives during the discharge operation are shown in **Figure 5.19**. As expected, when 10^{-4} mol L^{-1} HCl is dissolved in the water, $C_{a\text{-}l}$ rapidly increases with time and becomes higher than when de–ionized water free of additives is used. This confirms that the increase of $C_{a\text{-}l}$ could reduce the absorption rate of gaseous acetaldehyde, leading to the inhibition of removal of gaseous acetaldehyde. The reason why HCl lessens the decomposition of aqueous acetaldehyde could be explained as follows – when HCl is dissolved into the water, dissociated Cl^- could be reacted with OH radical as given by Eq. 5.14 with a rate constant of 4.3×10^9 L mol^{-1} s^{-1} (Buxton et al., 1988).

$$OH + Cl^- \rightarrow ClOH^- \qquad (5.14)$$

In addition, OH radical could react with some derivatives of Cl^- such as ClO^- and ClO_2^- which might be produced in the aqueous phase at high reaction rate (Buxton et al., 1988). Therefore, these reactions may take place and inhibit the decomposition of aqueous acetaldehyde by OH. It is consistent that adding HCl can inhibit the decomposition of aqueous phenol (Sano et al., 2004).

Focusing on the effect of NaOH, despite the accelerated absorption of acetaldehyde, the concentration of aqueous acetaldehyde is reduced. This result suggests that the decomposition rate of the aqueous acetaldehyde can be enhanced by addition NaOH. The enhancement by adding NaOH could be attributed as follows – when NaOH is added into the water, dissociated OH^- could be produced and then acts as an initiator to accelerate the decay of ozone to form the oxidant such as hydroxyl radical, OH (Buxton et al., 1988; Bruno et al., 1991). Besides the acceleration in OH production by NaOH, the reactivity of OH radical with organic compounds may be enhanced by the dissolved NaOH. Eventually, the decomposition of acetaldehyde in water is enhanced. This result is consistent that addition of NaOH can enhance the decomposition of aqueous phenol (Sano et al., 2004).

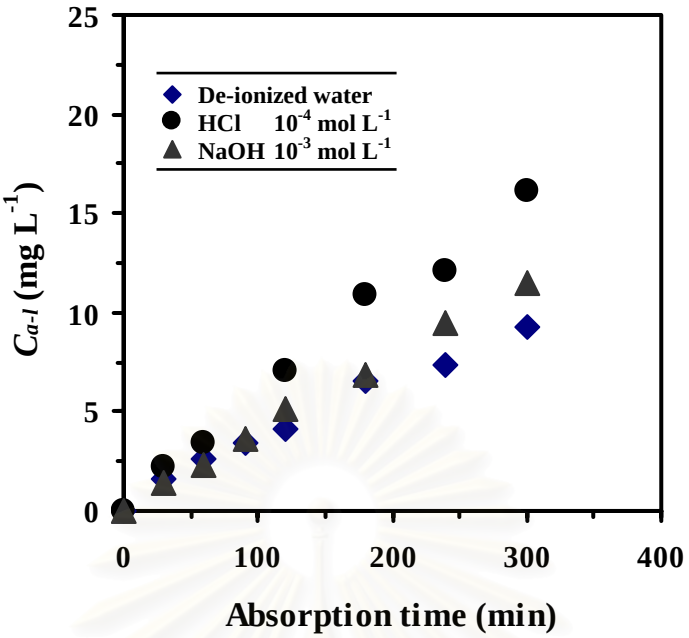

Figure 5.17 Influence of dissolved inorganic additives on absorptivity of acetaldehyde. $C_{a\text{-}g\ inl}$=200 mol-ppm, Gas flow direction=Upward.

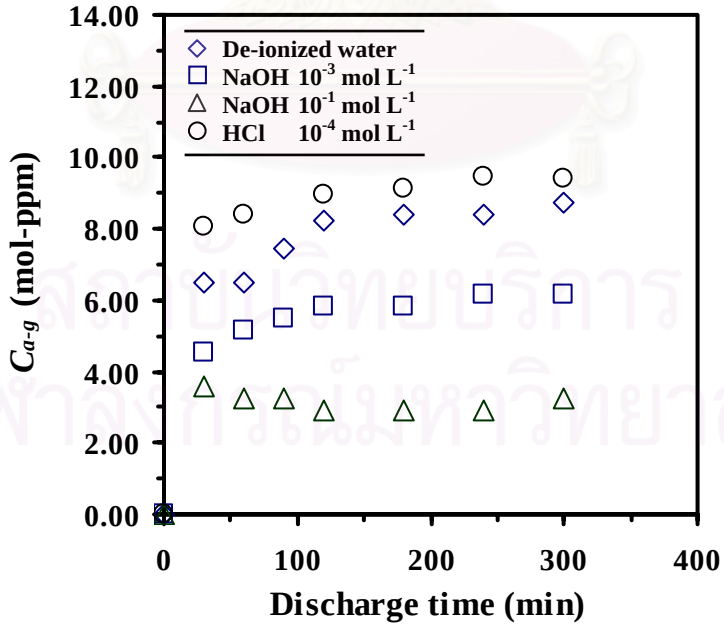

Figure 5.18 Effect of additives on the concentration of acetaldehyde in treated gas during discharge time. I=0.1 mA, $C_{a\text{-}g\ inl}$=200 mol-ppm, Gas flow direction=Upward.

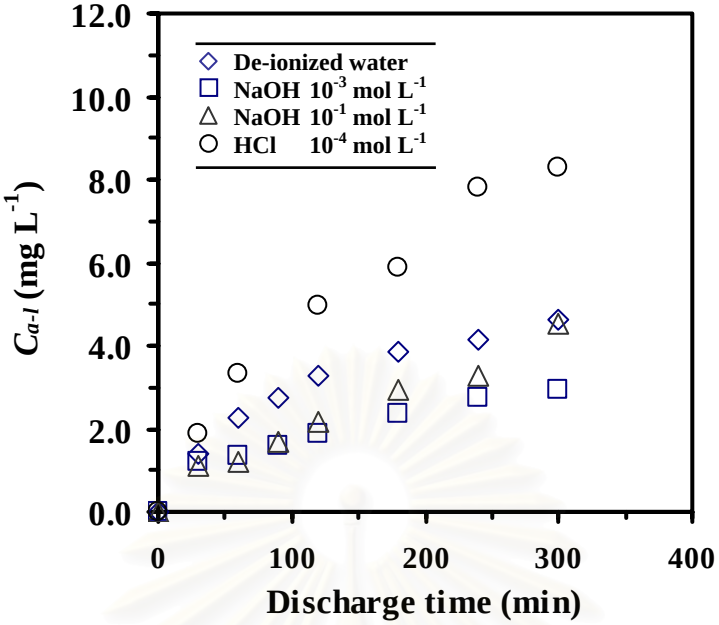

Figure 5.19 Influence of additives on the accumulation of acetaldehyde in circulating water. I=0.1 mA, $C_{a\text{-}g\ inl}$=200 mol-ppm, Gas flow direction=Upward.

5.2.6 Comparison of Removal Extent and Byproduct Formation between Wetted-Wall Type and Dry-Deposition Type

The removal extent of acetaldehyde ψ, defined by Eq. (5.13), is plotted against corona discharge current, I, in **Figure 5.20.** The deposition type reactor used here consists of a cylindrical anode and a coaxial wire cathode of the same dimensions as the wetted-wall reactor. Since this reactor does not have the wetted wall, acetaldehyde is removed from the gas stream solely by gas – phase corona discharge reaction. Compared with the deposition type, the wetted – wall type exhibits a clearly higher removal extent when the discharge current is low. This is because the absorption of gaseous acetaldehyde enhanced the removal extent. When gas downflow is applied, the removal extent in the wetted-wall reactor is higher than that of deposition reactor at corona currents less than 0.5 mA.

To investigate the influence of water vapor on the removal of acetaldehyde, we conducted experiments on the removal of gaseous acetaldehyde in the deposition – type corona discharge reactor in the absence and in presence of water vapor. Our results confirm that water vapor enhances the removal efficiency. When water vapor exists in the corona zone, related gaseous radicals and ions are produced as explained previously. These radicals and ions are shown experimentally to contribute to the removal reaction of acetaldehyde.

Figure 5.21 compares the GC chromatograms of gas analysis between the wetted-wall type and deposition type corona discharge reactors. Chromatograms a, b, c, and d stand, respectively, for the influent and effluent gas stream of the deposition-type reactor in the absence of water vapor, the effluent gas stream of the deposition-type reactor in the presence of 2.3% water vapor, and the effluent gas stream of the wetted-wall reactor. The only significant detected byproduct from the deposition type reactor has the same retention time as formaldehyde, whereas other byproducts are negligible. On the other hand, the formaldehyde which is detected in the deposition type reactor becomes negligible in the wetted – wall type. It should be noted that, though highly soluble, formaldehyde is not detected in the water after the corona discharge operation. This result may be ascribed to the following. In the deposition reactor, removal reactions of acetaldehyde take place in the gas phase, which produce formaldehyde as a byproduct. In contrast, formaldehyde is not detected significantly in both the gas and water phases in the wetted – wall reactor. This suggests that the main decomposition reaction which takes place in the water phase does not produce formaldehyde. Instead, it produces mainly acetic acid as byproduct.

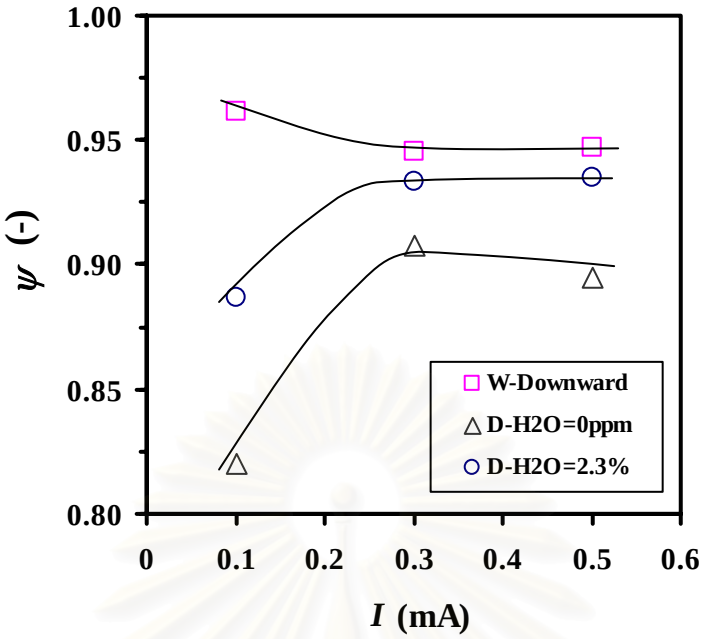

Figure 5.20 Removal extent of gaseous acetaldehyde against corona discharge current. W=Wetted-wall type, D=Deposition type, $C_{a\text{-}g\ inl}$=200 mole-ppm, Q_g=100 $cm^3\,min^{-1}$

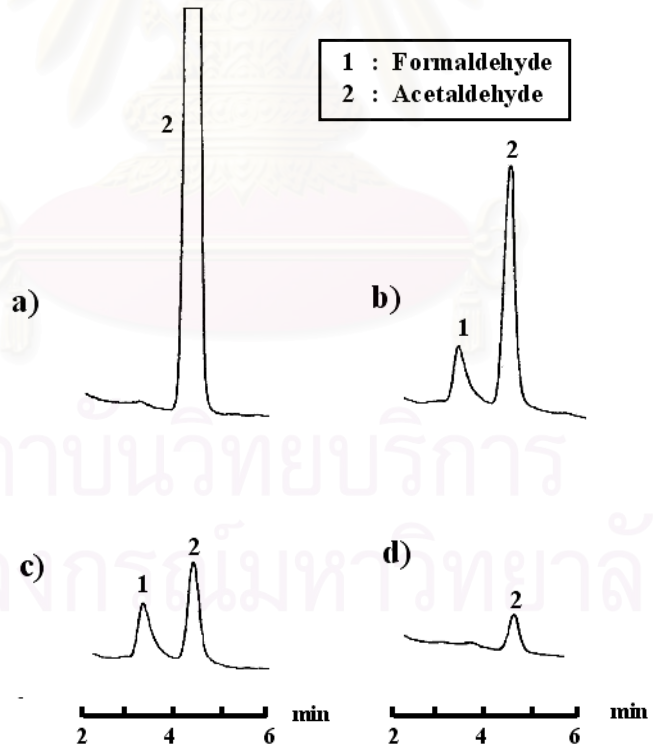

Figure 5.21 GC chromatograms of gas analysis. a) influent gas stream, b) effluent gas stream of the deposition-type reactor in the absence of water vapor, c) the effluent stream of the deposition-type reactor in the presence of 2.3% water vapor, and d) the effluent stream of the wetted-wall reactor. I=0.1 mA, $C_{a\text{-}g\ inl}$=200 mol-ppm.

5.2.7 Energy Utilization: Electron Efficiency and Energetic Efficiency

The electron efficiency η_e and energetic efficiency *J*, defined by Eqs. (5.15) and (5.16), are calculated to evaluate the removal efficiency in the wetted – wall reactor.

$$\eta_e = \left(q_g(C_{a\text{-}g\ inl} - C_{a\text{-}g}) - w\frac{dC_{a\text{-}l}}{dt} \right) N / N_e \qquad (5.15)$$

$$J = \left(q_g(C_{a\text{-}g\ inl} - C_{a\text{-}g}) - w\frac{d\,C_{a\text{-}l}}{dt} \right) / IV \qquad (5.16)$$

where q_g is the total gas mole flow rate; $C_{a\text{-}g\ inl}$, inlet concentration of gaseous acetaldehyde; $C_{a\text{-}g}$, outlet concentration of gaseous acetaldehyde; *w*, mole of water; $C_{a\text{-}l}$, concentration of aqueous acetaldehyde; *t*, discharge time; *N*, Avogadro's number; N_e, the number of electrons produced by corona discharge per unit time; *I*, discharge current; and *V*, applied voltage. N_e is obtained from the discharge current as in Eq. (5.17)

$$N_e = I / e \qquad (5.17)$$

where *e* is the elementary charge. η_e and *J* are based on the combined decomposition of gaseous and aqueous acetaldehyde by corona discharge. η_e represents the average number of acetaldehyde molecules removed by one electron, and *J* represents how many moles of acetaldehyde are degraded by unit energy. The values of η_e and *J* obtained at steady state when $dC_{a\text{-}l}/dt=0$ are shown in **Table 5.2**. Obviously the wetted-wall type attains a higher η_e and *J* than the deposition one, revealing that the wetted-wall reactor is more promising for acetaldehyde removal.

Compared with other high voltage discharge systems with our results, some reports showing higher energetic efficiencies can be found. For example, Mizuno et al shows 1.87×10^{-7} mol J^{-1} using non – thermal pulsed plasma combining with TiO_2 (Mizuno et al., 1995). However, it should be noted that the experimental condition used in their group is different from our work. For example, the inlet concentration used in their work is 1 mol-ppm, whereas energy efficiency in our work is obtained with the inlet concentration 200 mol-ppm. If the extremely low concentration is used, the energy requirement is expected to be decreased since the discharge current and applied voltage can be decreased to lower values. In addition, the absolute efficiency can be further improved when some operational parameters are changed, for example the absorptivity of target components, pH in water, and discharge patterns such as non-thermal plasma. The advantage of our work is that there are no significant gaseous byproducts in treated gas. At this stage, rather than pursuing the highest removal efficiency among conventional methods, it is important to notice that this study proposes the potential ability of the wetted-wall discharge reactor for simultaneous purification of gas and water to degrade organic compounds in both phases.

Table 5.2

The electron efficiency η_e and energetic efficiency J of removal of acetaldehyde in air at steady state

Reactor type	η_e (-)	J (10^{-9} mol J^{-1})
Dry deposition	11.0	12.1
Wetted-wall (Upflow)	12.8	14.0
Wetted-wall (Downflow)	12.9	14.0

$C_{a\text{-}g\ inl}$=200 mol-ppm, I=0.1 mA, Q_g=100 cm^3 min^{-1}, Q_l=1400 cm^3 min^{-1}, W=1000 cm^3

5.3 Treatment of Aqueous Phenol

5.3.1 Effect of Corona Current

Figure 5.22 shows typical results of decomposition of aqueous phenol using a wetted – wall corona discharge reactor when the initial concentration of phenol is 30 mg L^{-1}. The corona current used here is 0.3 mA. The result shows that phenol concentration rapidly decreases towards zero within around 3 h, while TOC still remains in the solution approximately at 65% of its initial amount. The TOC remaining in water, after phenol is completely decomposed, indicates that there are other byproducts produced in water. The analyses of byproduct will be shown and discussed in the forthcoming section.

The influence of corona current on decomposition of aqueous phenol is shown in **Figures 5.23** and **5.24**. The time-course concentrations of aqueous phenol and TOC at various corona currents during discharge operation are depicted in these figures. As clearly demonstrated, aqueous phenol rapidly decreases toward zero within around 10 h, while TOC still remains in water at about 13 mg L^{-1} when the corona current is attained at 0.1 mA. When the corona current is increased up to 0.5 mA, the decreasing rate of phenol and that of TOC are significantly accelerated.

Removal ratios of phenol and TOC against varied corona current are depicted in **Figure 5.25**. The currents varied from 0.1 – 1.0 mA are used for phenol degradation when initial phenol concentration is fixed at 30 mg L^{-1}. The result shows that increase of current from 0 to 0.5 mA enhances the removal ratios of both phenol and TOC. This is because the production of radicals and ions produced in the plasma – corona region is accelerated. However, the currents higher than 0.5 mA up to 1 mA inversely provide the extent of removal. This is because the elevated corona–induced

turbulence disturbs the surface of the falling water film, resulting in less uniform spatial distribution of the gas corona. The reduced spatial uniformity of the gas corona attenuates the decomposition efficiency of an aqueous organic compound in water (Sano et al., 2003).

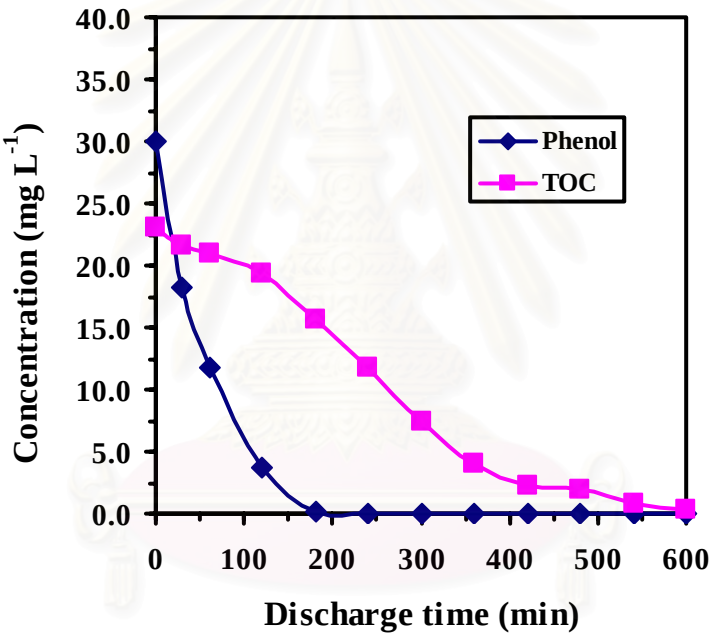

Figure 5.22 Decomposition of aqueous phenol using direct contact of corona discharge. $C_{p\text{-}l\ ini}$ = 30 mg L^{-1}, I=0.3 mA.

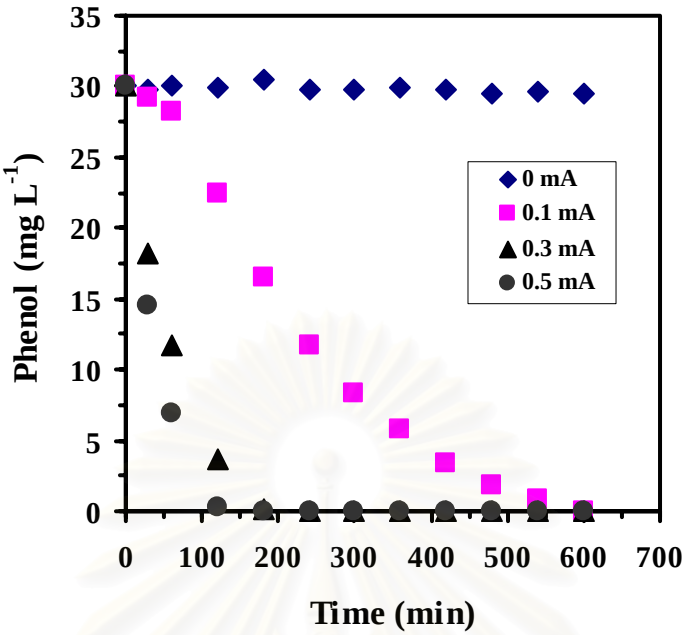

Figure 5.23 The time-course concentrations of aqueous phenol at various corona currents during discharge operation. *I*=0.3 mA.

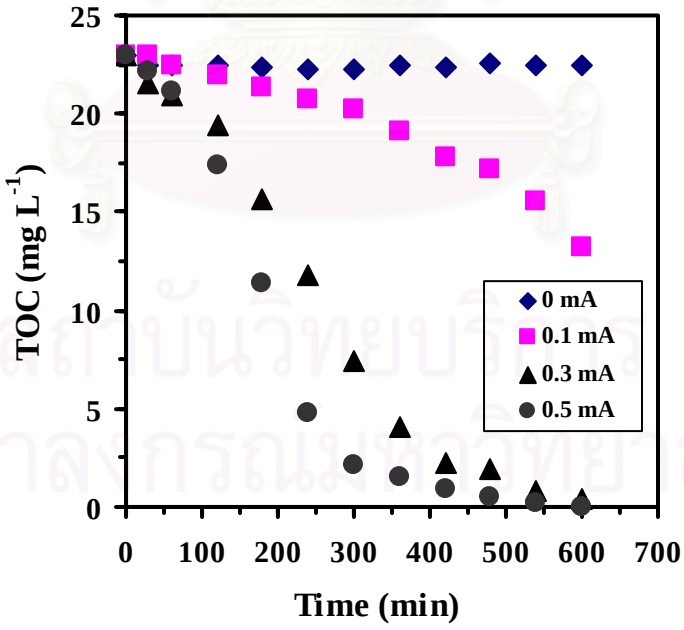

Figure 5.24 The time-course concentrations of TOC at various corona currents during discharge operation. *I*=0.3 mA.

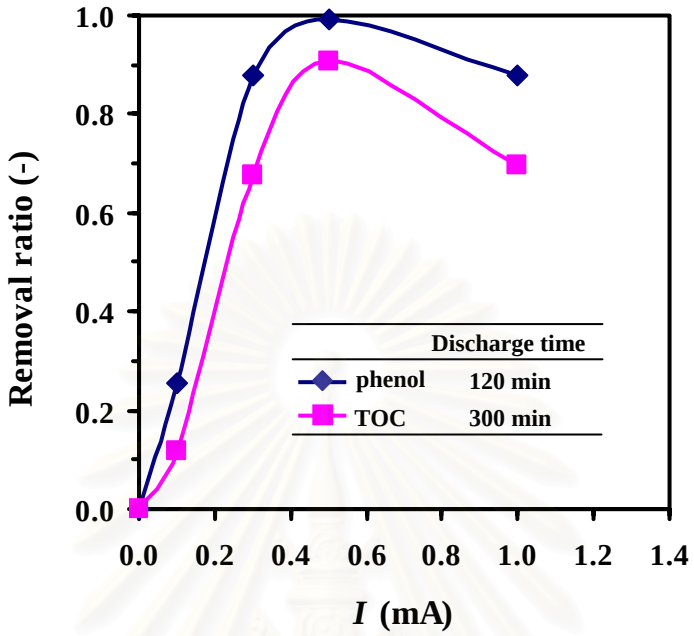

Figure 5.25 Removal ratio of phenol and TOC at various corona currents during discharge operation. I=0.3 mA.

5.3.2 Effect of Initial Phenol Concentration

The influence of initial phenol concentration on decomposition of aqueous phenol and TOC is shown in **Figure 5.26** and **Figure 5.27**. Initial phenol concentrations varied from 15 – 100 mg L^{-1} are used for phenol degradation when the corona current is fixed at 0.3 mA.

Also in these figures, the normalized concentrations of phenol and that of TOC at varied initial concentrations with fixed 30 ppm $C_{a\text{-}g\ inl}$ are depicted. The phenol normalized concentration sharply decreases with discharge time. Increase initial phenol concentration results in lower phenol and TOC removal rate. The maximum removal rate was found at 15 mg L^{-1} $C_{p\text{-}l\ inl}$. Similarly, TOC normalized concentration decreases as discharge time increases. However, the decreasing rate of TOC normalized concentration is much slower than that of phenol normalized concentration throughout this range of initial phenol concentrations. This result suggests that the reactor can be efficiently used at the low concentration of phenol under the condition studied here.

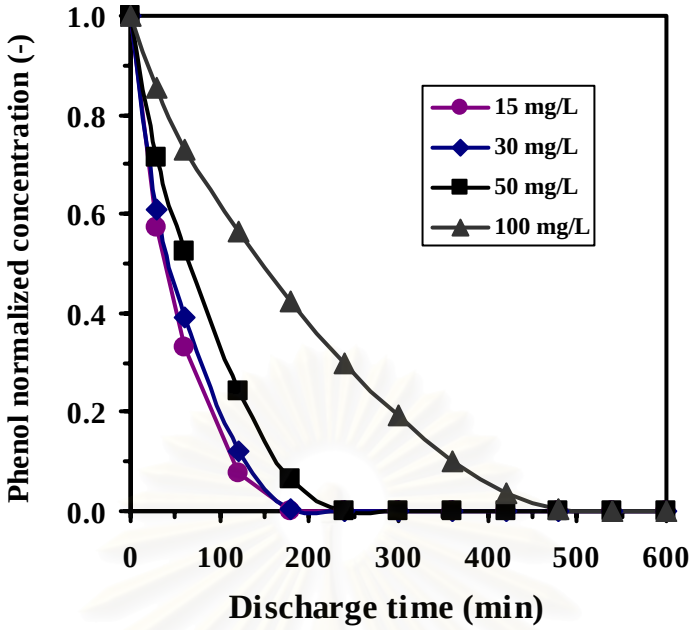

Figure 5.26 Phenol normalized concentrations during corona discharge operation at various initial concentrations of phenol. *I*=0.3 mA.

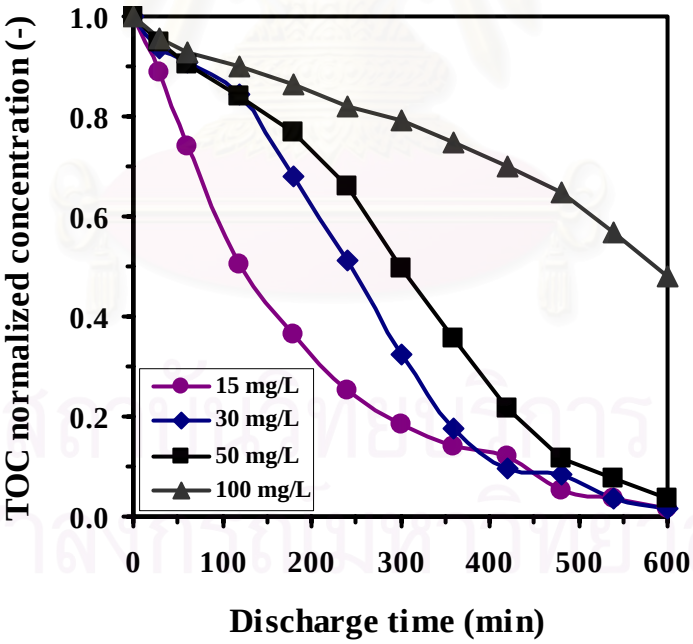

Figure 5.27 TOC normalized concentrations during corona discharge operation at various initial concentrations of phenol. *I*=0.3 mA.

5.3.3 Effect of Ozonation

Influences of direct ozonation on the simultaneous purification of phenol and TOC are shown in **Figure 5.28**. It is clearly demonstrated that shows the concentration of phenol and TOC in water against operation time. The oxygen gas is fed through the ozone generator and then introduced to the reactor by bubbling via the water reservoir under the corona zone. It should be noted that the concentration used here, 2000 ppm, is almost the same as that detected in the treatment of phenol by corona discharge.

The result shows that ozone can completely decompose phenol within around 6 h, approximately 2 times slower than corona discharge. However, rates of TOC degradation by ozonation are slower than that determined by corona discharge. Acetic acid, a significant stable byproduct of phenol decomposition, cannot efficiently be degraded via direct ozonation.

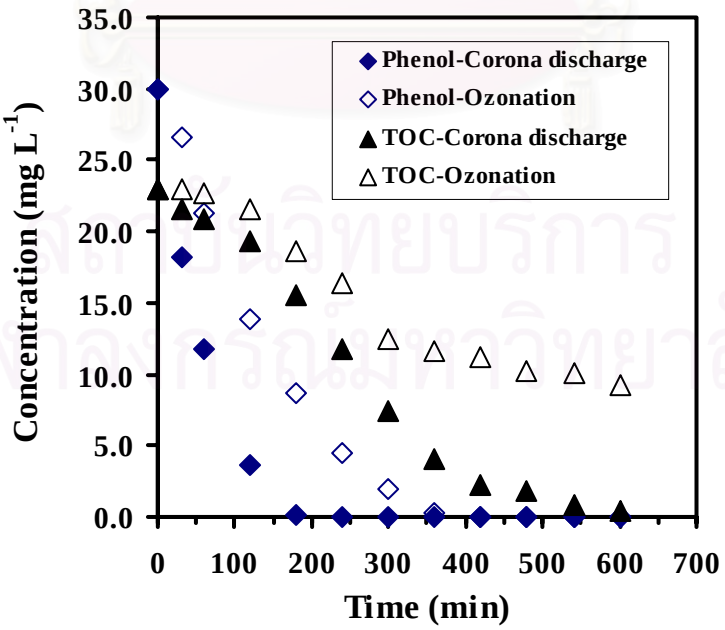

Figure 5.28 Changes of phenol and TOC concentrations during treatment operation compared between corona discharge system and ozonation system.

5.3.4 Byproduct Formation

Figure 5.29 shows the concentrations of phenol, TOC and intermediate byproducts detected during simultaneous system against corona discharge time. The corona current is fixed at 0.3 mA when $C_{p\text{-}l\ ini}$ and $C_{a\text{-}g\ inl}$ are at 30 mg L^{-1} and 100 mol-ppm, respectively. **Figure 5.30** particularly shows the concentrations of intermediate byproducts during corona discharge operation.

As a result, hydroquinone, 1,4-benzoquinone, resorcinol and catechol are detected as common intermediate byproducts by HPLC during the corona discharge operation. These byproducts could be completely mineralized within around 4 h. Moreover, it is found that small amount of aqueous acetaldehyde is detected from decomposition of phenol within around 5 h. Acetic acid is considered to be a final intermediate product of phenol decomposition.

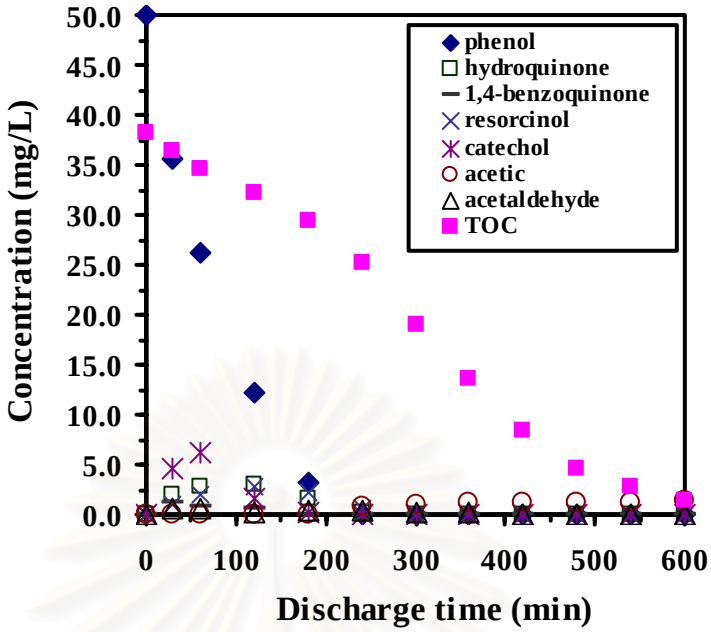

Figure 5.29 Concentrations of phenol, TOC and intermediate byproducts detected during simultaneous system against corona discharge time. I=0.3 mA, $C_{p\text{-}l\ ini}$=30 mg L^{-1}, $C_{a\text{-}g\ inl}$=100 mol-ppm.

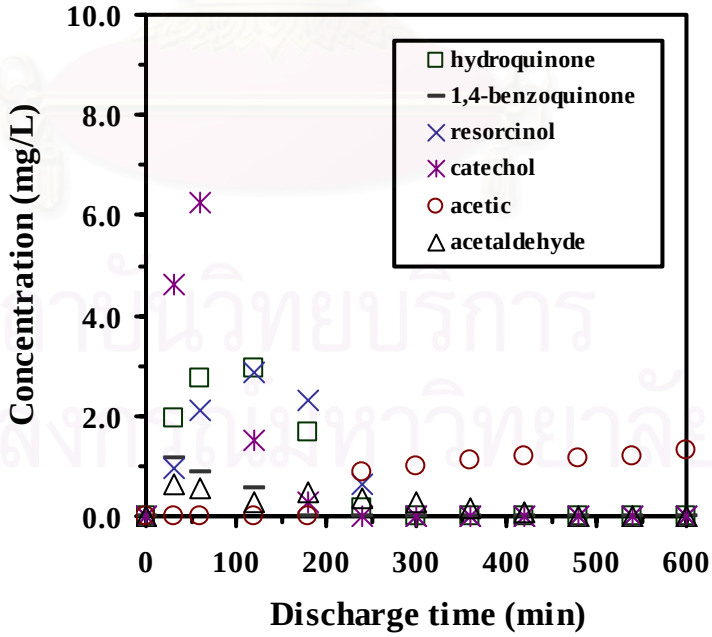

Figure 5.30 Concentrations of intermediate byproducts detected during simultaneous system against corona discharge time (extent of Figure 5.29 in larger scale). I=0.3 mA, $C_{p\text{-}l\ ini}$=30 mg L^{-1}, $C_{a\text{-}g\ inl}$=100 mol-ppm.

5.4 Simultaneous Treatment of Gaseous Acetaldehyde and Aqueous Phenol

5.4.1 Effect of Influent Acetaldehyde Concentration

The influence of influent acetaldehyde concentration on simultaneous treatment is shown in **Figure 5.31**. Concentrations of aqueous phenol, $C_{p\text{-}l}$, aqueous acetaldehyde, $C_{a\text{-}l}$, and TOC are shown against discharge time with varied inlet concentrations of gaseous acetaldehyde, $C_{a\text{-}g\ inl}$. The influent acetaldehyde concentrations varied from 30 – 200 mol-ppm are used for phenol degradation when discharge current, *I*, and applied voltage, *V*, are 0.3 mA and 11.8 kV, respectively. In **Figure 5.31 (a),** concentration of phenol are rapidly decreased toward zero within around 3 h at the inlet concentration of acetaldehyde in the range of 0 – 200 mol-ppm. The decomposition rates of phenol are not significantly affected by acetaldehyde in this range. However, it might be possible that the excessively high concentration of acetaldehyde at inlet could inhibit the decomposition of phenol. Regarding the concentration of aqueous acetaldehyde, **Figure 5.31 (b)** shows that the $C_{a\text{-}l}$ slightly increased at the early operation time for all runs and then the $C_{a\text{-}l}$ gradually decreases. The higher $C_{a\text{-}g\ inl}$ causes higher remaining $C_{a\text{-}l}$.

Since both phenol and acetaldehyde are converted to other byproducts, TOC are monitored as shown in **Figure 5.31 (c)**. The result shows that TOC can be efficiently degraded when the inlet concentration of acetaldehyde is at 30 ppmv. The concentrations of acetaldehyde higher than 100 mol-ppm obviously inhibit the TOC degradation rate. This implies that some stable products are accumulated in the treated water. According to the aqueous analysis by GC and HPLC, the acetic acid was detected as a significant byproduct. Acetic acid occupied more than 50% of the residual TOC after 8 h operation time.

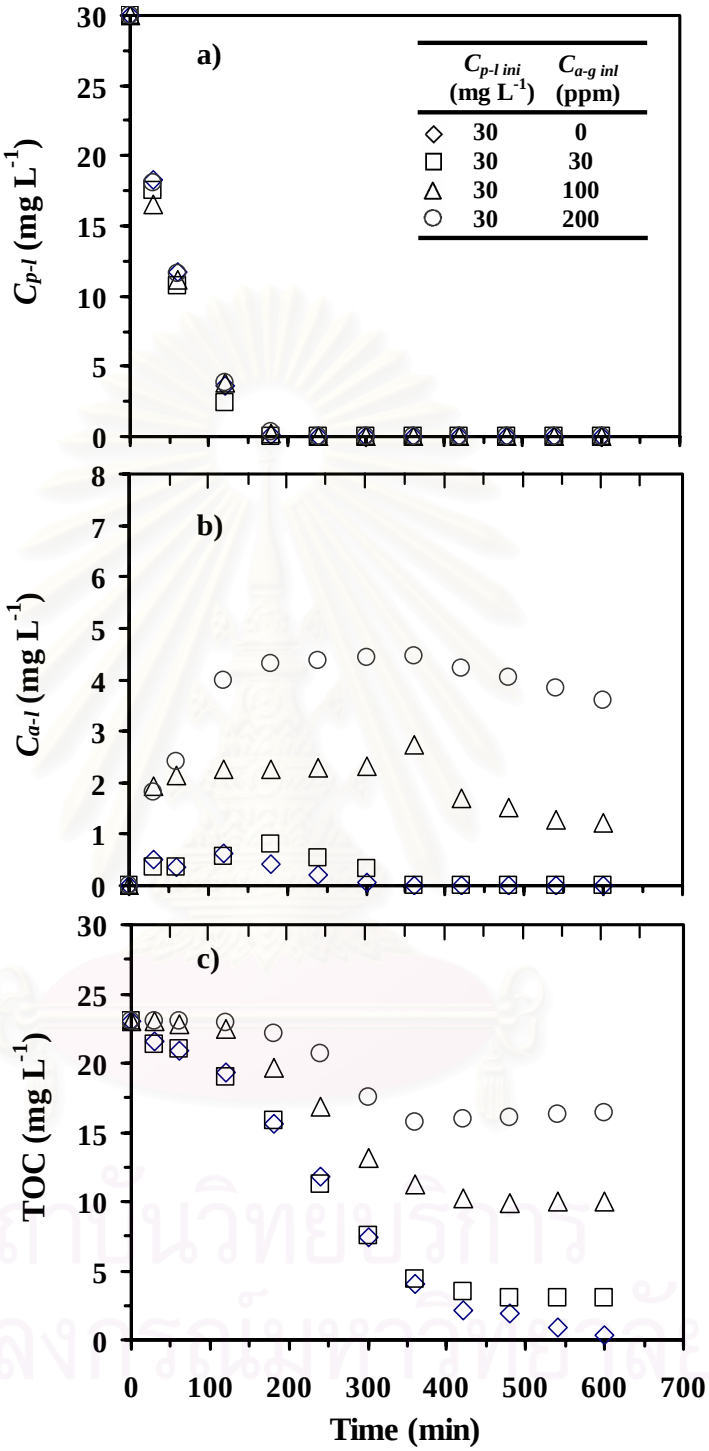

Figure 5.31 The concentration of a) aqueous phenol, b) aqueous acetaldehyde and c) TOC, during corona discharge operation at various inlet concentrations of gaseous acetaldehyde for fixed initial concentration of phenol. *I*=0.3 mA.

5.4.2 Effect of Initial Phenol Concentration

The influence of initial phenol concentration on decomposition of aqueous phenol is shown in **Figure 5.32** and **Figure 5.33**. **Figure 5.32** shows the phenol normalized concentration during simultaneous treatment at various initial concentrations of phenol ranging from 15 – 100 mg L^{-1} for fixed inlet concentration of gaseous acetaldehyde at 30 mol-ppm. Here, the corona current is fixed at 0.3 mA.

The phenol normalized concentration sharply decreases towards zero with discharge time while the concentration of aqueous acetaldehyde remains essentially at zero throughout the operation. The decreasing rate of the normalized concentration increases with the lower inlet concentration. The maximum removal rate was found at 15 mg L^{-1} $C_{p\text{-}l\ ini}$. This result suggests that the reactor can be efficiently used for the low concentration of phenol under the present condition.

The concentrations of TOC during simultaneous treatment at various initial concentrations 15 – 50 mg L^{-1} with fixed 30 mol-ppm $C_{a\text{-}g\ inl}$ are depicted in **Figure 5.33**. Decrease in TOC is considerably slower than that of phenol. This is because TOC includes more stable compounds than phenol. TOC is found to remain almost constant after about 500 minutes for all cases. At the steady state, TOC generation in water only comes from acetaldehyde and its intermediate product (acetic acid), and equals the TOC degradation rate. Evidently, if the initial phenol concentration is much higher than 50 mg L^{-1}, the time required for the TOC to reach an asymptotic value is expected to increase significantly.

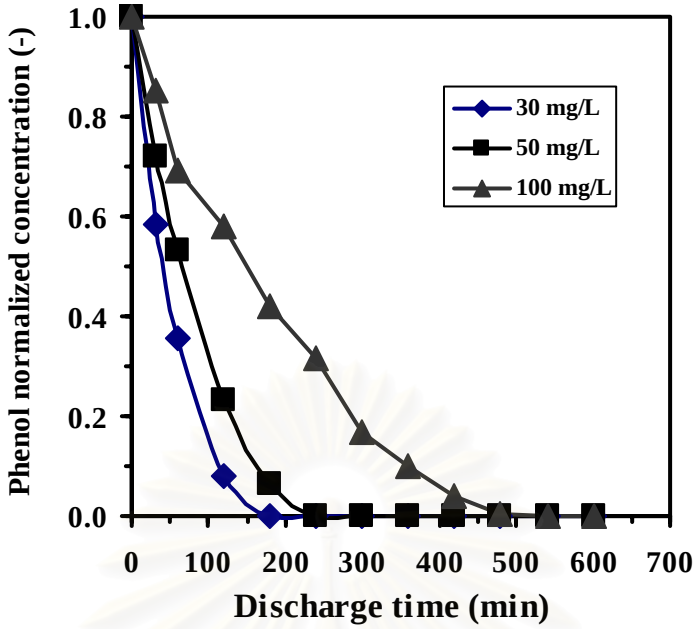

Figure 5.32 Phenol normalized concentrations during corona discharge operation at various initial concentrations of phenol for fixed inlet concentration of gaseous acetaldehyde. $C_{a\text{-}g\ inl}$=30 mol-ppm, I=0.3 mA.

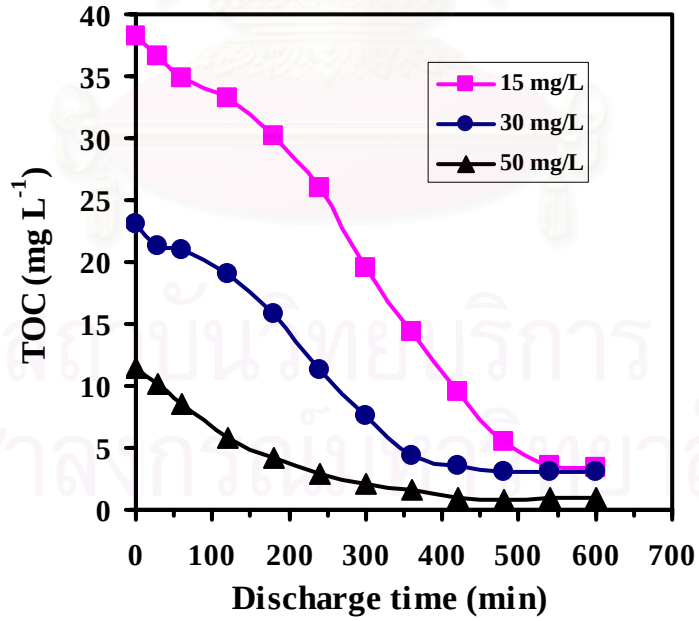

Figure 5.33 The concentrations of TOC during corona discharge operation at various initial concentrations of phenol for fixed inlet concentration of gaseous acetaldehyde. $C_{a\text{-}g\ inl}$=30 mol-ppm, I=0.3 mA.

5.4.3 Effect of pH

Figures 5.34 (a), (b), and **(c)** show the influence of the pH of the solution on simultaneous purification process in terms of aqueous acetic acid, phenol and acetaldehyde concentration, respectively. H_3PO_4 and NaOH were used to adjust pH of solution at 2 to 13. In **Figure 5.34 (a)**, when pH was raised up to 11, the concentrations of acetic acid significantly decreased. On the other hand, the pH ranging from 2 – 10 does not strongly affect the decomposition of acetic acid. Not only the decomposition of acetic acid but also the decomposition of aqueous phenol and acetaldehyde are strongly enhanced by adding NaOH as shown in **Figures 5.34 (b)** and **(c)**. When NaOH is added into the water, dissolved OH^- would accelerate the decay of ozone to form hydroxyl radical, OH, which could enhance the decomposition of acetic acid in water (Gottschalk et al., 2000). Furthermore, NaOH might enhance the reactivity of organic compounds in water while H_3PO_4 is considered to be an inert species (Sano et al., 2004).

5.4.4 Effect of Ozonation

The influences of direct ozonation on the simultaneous purification are shown in **Figure 5.35**. It should be noted that the concentration used here is almost same as that detected in the simultaneous treatment above. The experimental operation was explained in the experimental section. In **Figure 5.35 (a)**, the removal extent of gaseous acetaldehyde is shown against time. Without corona current, the removal extent gradually decreases with time since the absorbed acetaldehyde in water inhibits

the absorption rate. With ozonation, the removal extent decreases slightly slower than that obtained by absorption. This result shows that direct ozonation does not significantly contribute to the removal of gaseous acetaldehyde. In contrast, when the corona discharge is generated, the removal extent can reach 100% through the operation time. **Figure 5.35 (b)** shows the concentration of aqueous acetaldehyde during operation. As expected, with ozonation, the concentration of acetaldehyde increases with time, resulting in the increase of outlet concentration of gaseous acetaldehyde. When the corona discharge is generated, the concentration of aqueous acetaldehyde can be kept almost constant, resulting in steady state removal extent of gaseous acetaldehyde.

Figure 5.35 (c) shows the concentration of phenol and TOC in water against operation time. The result shows that ozone can completely decompose phenol within around 6 h, approximately 2 times slower than corona discharge. However, TOC degradation by ozonation gently decreases compared with that by corona discharge because acetic acid cannot effectively be decomposed by direct ozonation. The effect of direct ozonation is not significant in the corona discharge system studied here.

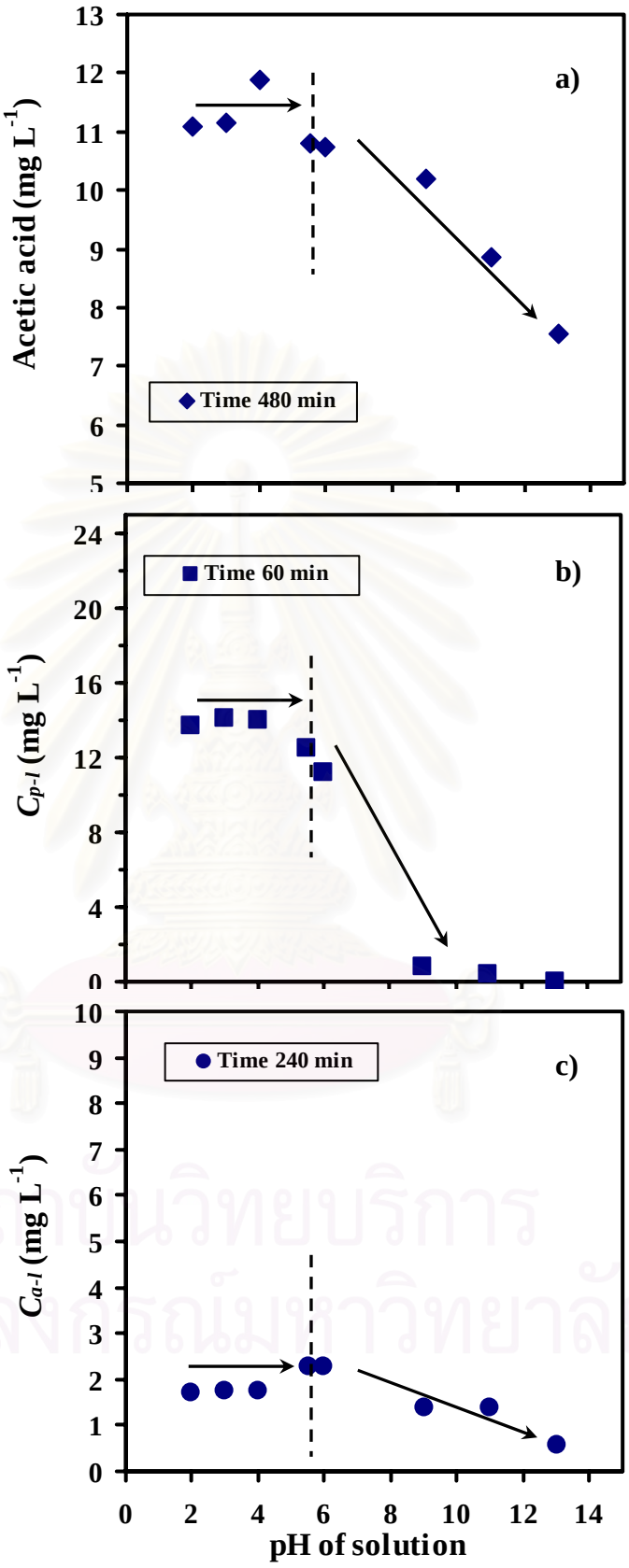

Figure 5.34 Influence of pH of solution on the simultaneous purification: a) aqueous acetic acid concentration at 480 min, b) aqueous phenol concentration at 60 min, and c) aqueous phenol concentration at 240 min. $C_{p\text{-}l\ ini}$=30 mg L^{-1}, $C_{a\text{-}g\ inl}$=100 mol-ppm, I=0.3 mA.

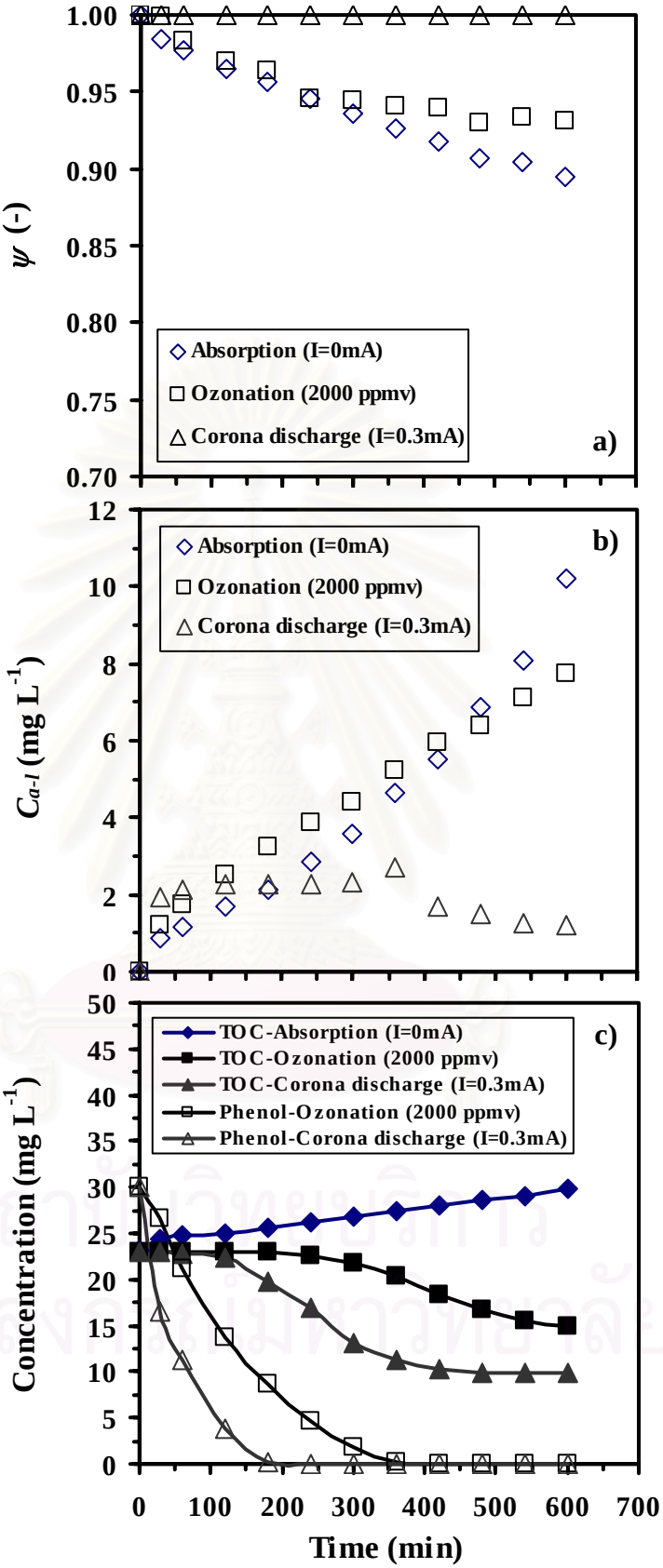

Figure 5.35 Influence of ozonation on the simultaneous purification during operation: a) removal extent of gaseous acetaldehyde, b) aqueous acetaldehyde concentration, and c) TOC and phenol concentrations in water. $C_{p\text{-}l\ ini}$=30 mg L^{-1}, $C_{a\text{-}g\ inl}$=100 mol-ppm, I=0.3 mA.

5.4.5 Byproduct Formation

The intermediate byproducts during the simultaneous treatment using corona discharge technique are shown in **Figure 5.36**. Hydroquinone, 1,4-benzoquinone, resorcinol, and catechol were detected as common intermediate byproducts by HPLC during the discharge operation. These byproducts could be completely mineralized within around 4 h. Thus, it was considered that decomposition of phenol along with these intermediates might inhibit the decomposition of absorbed acetaldehyde at the early time operation. Moreover, when decomposition of phenol was conducted without feeding of gaseous acetaldehyde, it was found that small amount of aqueous acetaldehyde was detected from decomposition of phenol within around 5 h. This presence of acetaldehyde corresponds to the $C_{a\text{-}l}$ detected when $C_{a\text{-}g\ inl}$ is fed to the system at 30 mol-ppm. It was reported that acetaldehyde is one of byproducts in the intermediate pathway of decomposition of phenol by pulsed corona discharge (Hoeben et al.; 2000). Acetic acid is found as a major product after primary intermediates are completely degraded. After about 7 h of treatment, acetic acid possessed approximately 75% of TOC.

Gaseous acetaldehyde at outlet was not be detected throughout the discharge operation for all experiments. This suggests that acetaldehyde is completely absorbed into the solution. If the acetaldehyde remains in the gas stream, it could be removed by gas corona reactions. According to the gas analysis by GC, there are no significant gaseous byproducts detected at the outlet gas stream.

The corona reactor was used to removal gaseous acetaldehyde or aqueous phenol separately to evaluate the acetic acid formation pathway. The concentrations of acetic acid are plotted as a function of time in **Figure 5.37**. The result shows that

acetic acid accumulated in water is mainly converted from acetaldehyde rather than phenol. Acetic acid is considered to be a final intermediate product of decompositions of acetaldehyde and phenol.

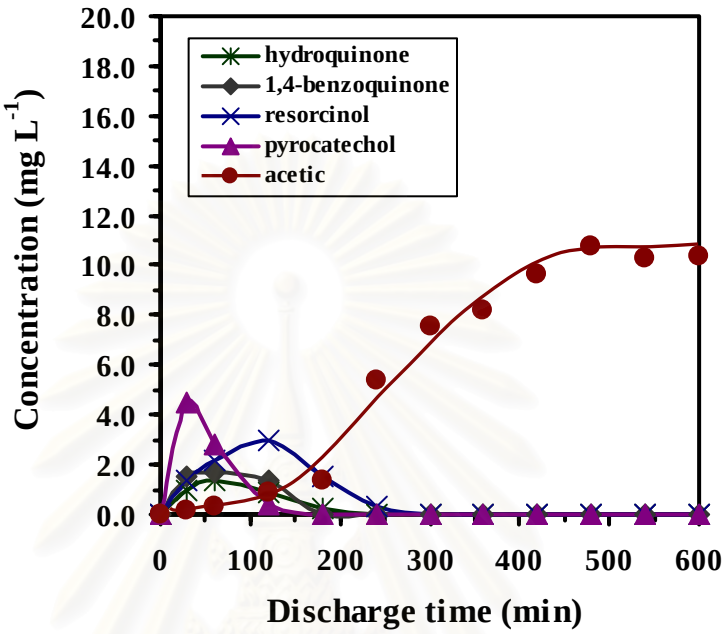

Figure 5.36 Concentrations of intermediate byproducts detected during simultaneous system against corona discharge time. I=0.3 mA, $C_{p\text{-}l\ ini}$=30 mg L^{-1}, $C_{a\text{-}g\ inl}$=100 mol-ppm.

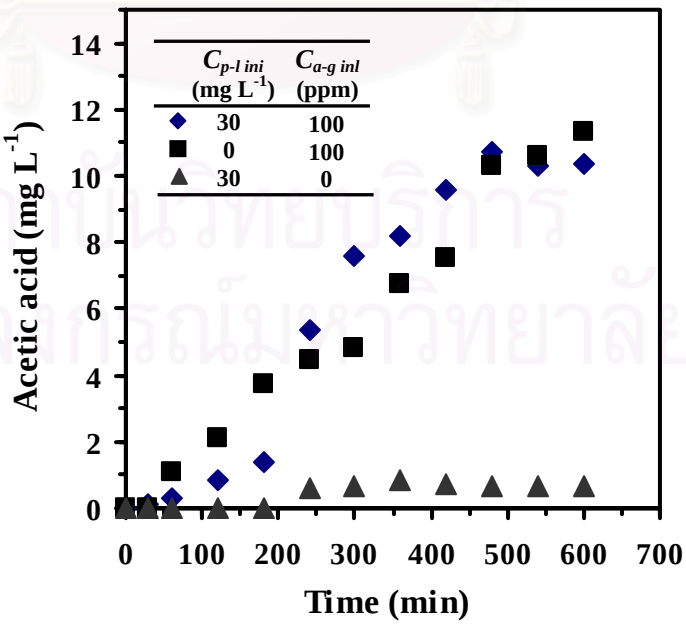

Figure 5.37 The concentrations of acetic acid during corona discharge operation. I=0.3 mA.

CHAPTER 6

MODELING AND SIMULATION

A dynamic model for simultaneous treatment of aqueous phenol and gaseous acetaldehyde in cylindrical wetted–wall corona discharge reactor was proposed to predict the changes of concentration of organic species in the system. The influence of gaseous acetaldehyde inlet concentration and aqueous phenol initial concentration as well as their major intermediate products on the simultaneous treatment were investigated. Then, simulation results were compared with experimental data. The proposed model will be useful for scale–up of the system for practical application.

6.1 Concept of mass transfer phenomena and reaction pathway

Figure 6.1 shows the basic concept of mass transfer phenomena and formation of aqueous OH radical via direct contact with gas corona discharge. Corona discharge is generated by applying a high dc voltage onto the wire cathode with negative polarity. Subsequently, energetic electrons are emitted from the wire cathode and accelerated towards the anode along the electric field. During their drift, dissociation and ionization of oxygen can produce O radical in the high strength electric field adjacent to the cathode as shown in Eq. (6.1) (Peyrous et al., 1989; Loiseau et al., 1994). In the low strength electric field next to the high electric zone, dissociative electron attachment to oxygen can also produce O and O^- via Eq. (6.2) (Moruzzi and Phelps, 1966). Reaction of oxygen with O radical would produce ozone via Eq. (6.3). It should be noted that O_2^-, O_3^-, and some ions can also be produced by

corona discharge reactions. However, among those ions, O^- is considered to be a dominant species in the dc corona discharge (Ushijima, Nishioka and Sadakata, 2004).

When O and O^- reach the interfacial water and dissolve into it, they subsequently react with water molecules to produce reactive OH radical in water as described in Eqs. (6.4) and (6.5) (Colussi, Weavers and Hoffmann, 1998; Hoeben, 2000; Sano et al., 2003). In addition, OH, H_2O_2, and some radicals can also be produced in the gas corona zone since water vapor is present in the gas phase. These gaseous species along with ozone would also transfer into the water. It should be noted that OH radical can be generated by radiolysis in the pulsed corona discharge (Joshi et al., 1995; Hoeben, 2000) and in the pulseless corona discharge (Shin et al., 2000). In these works, the corona was directly generated in water by submerged corona spot. However, as previous report in section 5.2.4, aqueous acetaldehyde could not be decomposed by the present reactor in the absence of oxygen under corona discharge. This indicated that production of OH by radiolysis in the present reactor is negligible.

When the gas stream is bubbled through the phenol solution, acetaldehyde is absorbed into the aqueous phenol solution. As a result, aqueous solution containing phenol and acetaldehyde flows through the corona zone as a falling thin film on the inner surface of the anodic cylinder. In the corona zone, ions and radicals produced by gas corona are continuously supplied to the solution in order to form the hydroxyl radical. Meantime, aqueous organic compounds are continuously decomposed. If some gaseous acetaldehyde remains in the gas stream, it is expected to be removed in the gaseous corona zone by radical reactions (Sano et al., 1997; Butkovskaya and Setser, 2000; Tomas et al., 2001), ozonation, and cluster formation (Sano et al., 1997).

Decomposition pathways of phenol by oxidation processes such as radiolysis (Joshi et al., 1995; Grymonpre et al., 1999; Shin et al., 2000), oxidation by hydroxyl (Hoeben, 2000; Chen et al., 2004) and by ozone (Bruno et al., 1991), and ultrasonic irradiation (Masaki et al., 2004) have been studied. Based on the above-mentioned studies, **Figure 6.2** showed that phenol was first oxidized to polyhydroxybenzenes and subsequently to quinones. Both continued to yield ring–cleavage products i.e. aldehyde and carboxylic acid groups. Finally, carboxylic acids, such as, formic and acetic acids were converted to carbon dioxide. As for the decomposition pathway of aqueous acetaldehyde, it is reported that aqueous acetaldehyde is mainly decomposed to acetic acid before being mineralized to carbon dioxide by the oxidation process (Jacob et al., 1989).

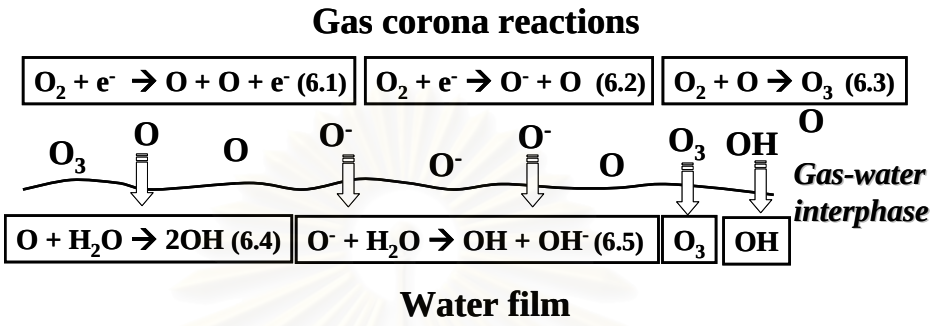

Figure 6.1 Concept of mass transfer phenomena and formation of OH radical in water.

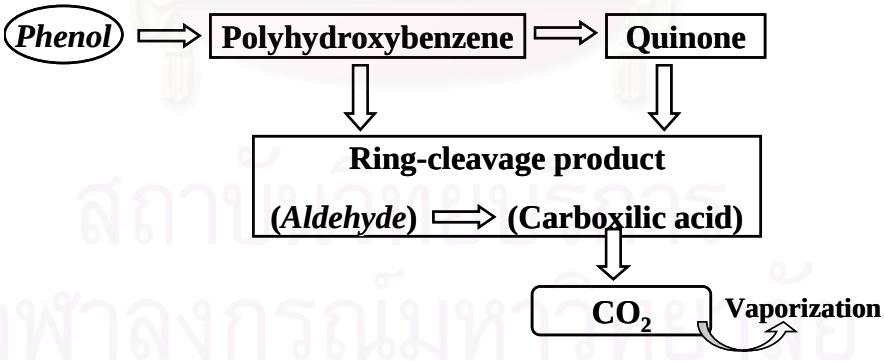

Figure 6.2 Reaction pathways of phenol and acetaldehyde.

6.2 Modeling and Simulation

Based on the decomposition pathways mentioned in the previous section, the reaction scheme is proposed as shown in **Table 6.1**. The assumptions used in developing the model are as follows: 1) The reactor is assumed to be an isothermal well-mixed reactor since the decomposition of phenol and acetaldehyde is expected to fully take place in the reservoir under the corona zone. Gas bubbling and water stream falling down the anode makes the reservoir behave like a well-mixed reactor. The water volume in the reservoir occupies approximately 60% of the total volume of solution; 2) Gaseous acetaldehyde is completely absorbed into the water before the bubbles rise through the reservoir. Thus, all acetaldehyde is decomposed in the aqueous phase; 3) Volume of the solution circulated in the system is constant; 4) Reactive OH radical concentration is assumed to reach pseudo-steady state, and is determined from experimental data. The OH pseudo–steady state assumption was successfully used for the simulation of phenol decomposition in radiolysis process (Joshi et al., 1995; Grymonpre et al., 1999; Shin et al., 2000). The direct ozonation is not involved in the system here since its reaction rate constant is six time in order of magnitude lower than that of OH (Bruno et al., 1991). It should be noted that vaporization of phenol along the operation is negligible. Molar species material balance in the liquid phase gives 6 first–order ordinary differential equations as shown in **Table 6.2**. A system of the above differential equations is numerically integrated using the fourth–order Runge–kutta method. The rate constants involved in the reaction are all obtained through the literature, except k_1 which is estimated through model fitting with the experimental data.

Table 6.1 Decomposition of organic species in aqueous phase

Eqs.	Reactions	Rate constant ($M^{-1}s^{-1}$)	Reaction rate	Ref.
1	Acetaldehyde + OH $\xrightarrow{k_1}$ Acetic acid	9.8×10^9	$k_1[AD][OH]$	Parameter estimation
2	Acetic acid + OH $\xrightarrow{k_2}$ product	1.6×10^7	$k_2[AA][OH]$	Buxton et al., 1988
3	Phenol + OH $\xrightarrow{k_3}$ Catechol	7×10^9	$k_3[PH][OH]$	Walling and Goosen, 1973
4	Phenol + OH $\xrightarrow{k_4}$ Hydroquinone	6.5×10^9	$k_4[PH][OH]$	Shin et al., 2000
5	Phenol + OH $\xrightarrow{k_5}$ Resorcinol	1×10^9	$k_5[PH][OH]$	Shin et al., 2000
6	Catechol + OH $\xrightarrow{k_6}$ product	1.1×10^{10}	$k_6[CC][OH]$	Bielskie et al., 1985
7	Hydroquinone + OH $\xrightarrow{k_7}$ product	1×10^{11}	$k_7[HQ][OH]$	Shin et al., 20008
	Resorcinol + OH $\xrightarrow{k_8}$ product	1×10^{10}	$k_8[RC][OH]$	Hoigne and Barder, 1979

Table 6.2 Molar species material balance in aqueous phase

$d[AD]/dt$	=	$q_g C_{a\text{-}g\ inl} / W - k_1[AD][OH]$
$d[AA]/dt$	=	$k_1[AD][OH] - k_2[AA][OH]$
$d[PH]/dt$	=	$-(k_3 + k_4 + k_5)[PH][OH]$
$d[CC]/dt$	=	$k_3[PH][OH] - k_6[CC][OH]$
$d[HQ]/dt$	=	$k_4[PH][OH] - k_7[HQ][OH]$
$d[RC]/dt$	=	$k_5[PH][OH] - k_8[RC][OH]$

6.3 Comparison of simulation and experimental results

Aqueous concentration of OH radical and rate constant k_1 are determined by experimental data as 2.8 x 10^{-10} ppm and 9.8 x 10^9 M^{-1} L^{-1}, respectively. Reaction rate of aldehyde group toward OH is reported at 10^9 M^{-1} L^{-1}, the same order of magnitude with our result (Bruno et al., 1991). It should be noted that the concentration of OH here is not the real concentration, but it is considered as an effective average concentration for decomposition of organic compounds. **Figure 6.4** shows the concentrations of a) aqueous phenol, and b) aqueous acetaldehyde during simultaneous treatment at various inlet concentrations of gaseous acetaldehyde ranging from 0 to 200 mol-ppm for fixed initial concentration of phenol 30 mg L^{-1}. In **Figure 6.4 (a),** the experimental result shows that the aqueous concentrations of phenol rapidly decreased towards zero within around 3 h when the $C_{a\text{-}g\ inl}$ ranges from 0 – 200 mol-ppm. The acetaldehyde in this range could not obviously affect the degradation rates of phenol. In considering the concentration of aqueous acetaldehyde, **Figure 6.4 (b)** shows that the aqueous acetaldehyde initially increases at the early stage for all runs. Subsequently, aqueous acetaldehyde gradually decreases. A higher $C_{a\text{-}g\ inl}$ results in a higher residual acetaldehyde concentration. **Figure 6.5** shows the concentration of aqueous phenol during simultaneous treatment at various initial concentrations of phenol ranging from 15 – 50 mg L^{-1} for fixed inlet concentration of gaseous acetaldehyde at 30 mol-ppm. Aqueous phenol rapidly decreases towards zero for all cases while the concentration of acetaldehyde remains essentially at zero throughout the operation. The simulation results provide a good fit to the experimental ones.

Intermediate aqueous products and TOC analyses during simultaneous treatment are shown in **Figure 6.6.** Hydroquinone, Catechol, and Resorcinol are detected as primary intermediate products which are completely mineralized after about 300 min. After that, acetic acid is found as a major product. After about 7 h of treatment, acetic acid occupied approximately 75% of TOC. This indicates that more intermediate products should be included in the model in order to attain highly accurate simulation results. With the present model, the simulation results show good agreement with the experimental ones. It should be pointed out that the evaluated OH concentration would be over-estimated since the model does not include the oxidation of ozone which partially contributes to the decomposition of aqueous organic compounds. Moreover, gas corona reactions and mass transfer of gas corona species between the gas and water phases should be included in the model to determine the concentration of OH radical as well as other species in water. It should be noted that production of OH radical strongly depends on experimental conditions such as corona current, dimension of the reactor, concentration of oxygen at the inlet and water circulation rate.

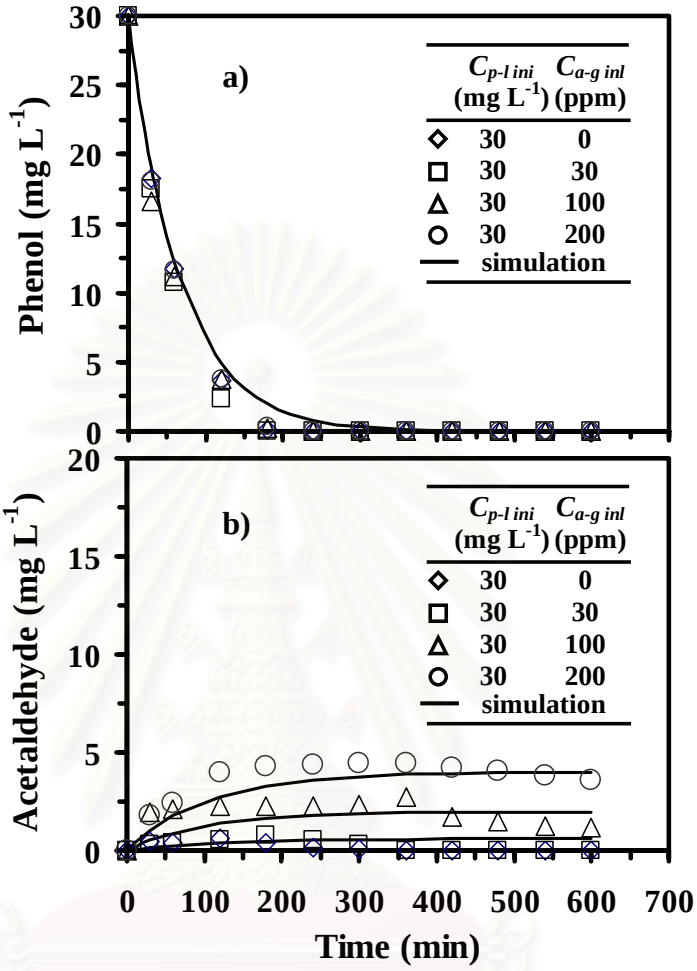

Figure 6.4 Concentration of a) aqueous phenol and b) aqueous acetaldehyde during simultaneous treatment at various inlet concentrations of gaseous acetaldehyde against fixed initial concentration of phenol. *I*=0.3 mA.

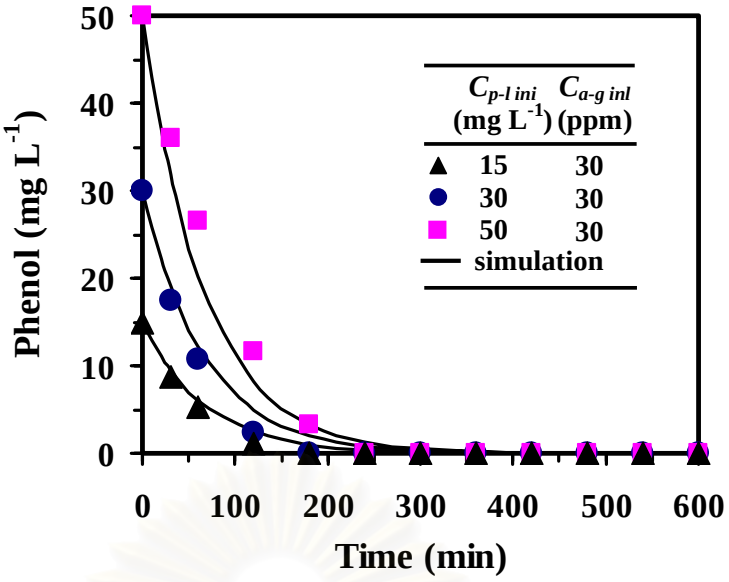

Figure 6.5 Concentration of aqueous phenol during simultaneous treatment at various initial concentrations of phenol against fixed inlet concentration of gaseous acetaldehyde. *I*=0.3 mA.

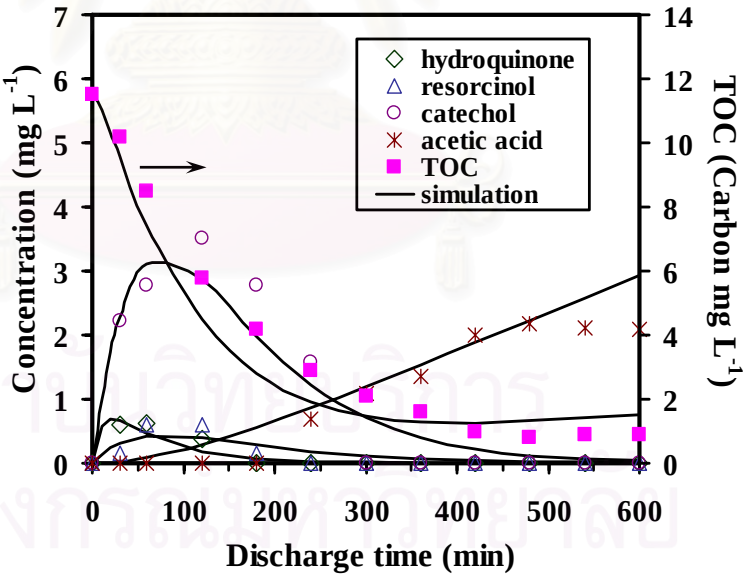

Figure 6.6 Intermediate aqueous products and TOC analysis during simultaneous treatment. $C_{a\text{-}g\ inl}$ = 30 mol-ppm, $C_{p\text{-}l\ ini}$=15 mg L^{-1}, *I*=0.3 mA.

CHAPTER 7

CONCLUSIONS AND RECOMMENDATIONS

7.1 Conclusions

7.1.1 Treatment of Gaseous Acetaldehyde

A wetted-wall corona discharge reactor was applied to purify acetaldehyde laden air. It was elucidated that acetaldehyde was readily absorbed into the circulating water before the gas stream entered the corona zone and the aqueous acetaldehyde could effectively be decomposed by this reactor. The TOC degradation was slower than the decomposition of aqueous acetaldehyde since acetic acid, converted from acetaldehyde, was more stable than aqueous acetaldehyde. It was found that there was a minimum current around at 0.1 mA and a maximum influent concentration of gaseous acetaldehyde at around 50 mol-ppm for effective decomposition of aqueous TOC. An excessive current caused a slight decrease in the removal extent because the induced gaseous turbulence broadened the residence time distribution and reduced the effectiveness of gas-phase corona reactions. As for the effect of gas flow direction, the downflow yielded a higher removal efficiency and faster TOC decomposition rate than the upflow. It was evaluated that approximately 13 molecules of acetaldehyde were removed by one electron, and $7x10^7$ J were required to remove one mole of acetaldehyde. In comparison with the deposition type, the wetted-wall type exhibited a clearly higher removal extent and less byproduct formation when the discharge current was low. The optimized discharge current was 0.1 mA for the removal of gaseous acetaldehyde and 0.5 mA for water

treatment. The recommended current lied in the range of 0.1-0.5 mA, though it depended on individual purposes.

It was found that acetaldehyde cannot be removed when oxygen does not coexist in gas stream. The sustainability of removal of acetaldehyde could be obtained in the presence of oxygen. There was an optimized O_2 concentration. When oxygen concentration was 5 %, the gaseous acetaldehyde was removed up to 98.5 %. The increase in corona current also led to an increase of its removal extent at the proper O_2 concentration. An excessive oxygen concentration brought about the lower removal extent when the current was excessively high. This could be attributed to the fact that corona-induced gaseous turbulence broadens the gas residence time distribution in the reaction region. It was also found that the increase of oxygen from 5 to 10% improved the decomposition of absorbed acetaldehyde and TOC. However, further increase of oxygen up to 21% resulted in opposite effect. Decomposition of aqueous acetaldehyde was enhanced by adding NaOH but inhibited by adding HCl although both additives could increase the absorptivity of acetaldehyde into water.

7.1.2 Treatment of Aqueous Phenol

Water purification using a wetted–wall corona discharge reactor was studied. Phenol containing water was selected as a target compound. Air was continuously fed through the reactor as oxygen source for producing shot-lived radicals and ions in the corona zone, which directly contact the interfacial water film to produce OH radical in water. The OH radical is expected to contribute to decomposition of organic compounds contaminated in water. The experimental results reveal that increase in corona current from 0 to 0.5 mA caused the increase in phenol and TOC

decompositions, but inversely when the current is higher than 0.5 mA. It was also found that increase in initial concentration of phenol from 15 to 100 mg L^{-1} caused the decrease in removal ratio rate of phenol and TOC. The corona discharge system obviously provides higher decomposition efficiency than direct ozonation method. Hydroquinone, 1,4-benzoquinone, resorcinol and catechol were detected as primary intermediate byproducts and acetic acid is found to be a final stable byproduct.

7.1.3 Simultaneous Treatment of Gaseous Acetaldehyde and Aqueous Phenol

Simultaneous purification of gas and water was experimentally investigated by using a wetted-wall corona discharge reactor. It was found that gaseous acetaldehyde can completely be removed from gas stream throughout the operation when its inlet concentration is ranging from 30 to 200 mol-ppm. Simultaneously, aqueous phenol can completely be decomposed within around 3 h when its initial concentration is at 30 mg L^{-1}. The inlet concentration of acetaldehyde ranging from 15 to 200 mol-ppm does not play a significant role on the decomposition of phenol. However, when the inlet concentration of gaseous acetaldehyde is higher than 100 mol-ppm, degradation of TOC in water is considerably retarded. This is because acetic acid is accumulated in the aqueous solution. The increase of initial concentration of phenol causes the decrease of its removal ratio. There are no significant byproducts detected in the treated gas stream. The influence of pH ranging from 2 to 13 was investigated by adding NaOH and H_3PO_4. The result shows that the decomposition of acetic acid is drastically increased when the pH is raised up to 11. Whereas, pH lower than 11 does not significantly affect the decomposition of acetic acid in water. The influence of direct ozonation is not significant in the present study.

7.1.4 Modeling and Simulation of the Simultaneous Treatment System

A dynamic model for the simultaneous treatment of acetaldehyde-laden air and phenol-containing water using corona discharge reactions in a water-film column has been developed based on the intermediate products detected during the experimental operation. Decomposition of phenol, acetaldehyde and its intermediates by hydroxyl radical is considered as main reaction pathways. Acetaldehyde is assumed to be completely absorbed into the water. Thus all acetaldehyde is considered to be decomposed in the water phase. The concentration of OH radical in water and rate constant of the reaction: $CH_3CHO + OH \rightarrow$ Acetic acid, are determined from experimental data as 2.8×10^{-10} ppm and 9.8×10^{9} $M^{-1} L^{-1}$, respectively. The influences of phenol concentration ranging from 15 – 50 mg L^{-1} and acetaldehyde ranging from 0 – 200 mol-ppm are investigated and compared with the simulation. As a result, the experimental and simulation results show good agreement in all cases in the present study.

7.2 Recommendations for Future Work

- Study on multi – component treatment system of gaseous target compounds and that of aqueous target compounds.
- Study on the contribution of gas phase reaction on the mechanism and efficiency.
- In order to understand the mechanism and characteristic of the system, more investigation on operating parameters for example gas flow rate and water flow rate is necessary.
- Scaling-up the system for practical use is indispensable.
- Improvement of the model for more accurate prediction of the system's behavior.

REFERENCES

Bielskie, B.H.J., Cabelli, D.E., Arudi, R.L., and Ross, A.B. Reactivity of HO_2/O_2^- radical in aqueous solution. J. Phys. Chem. Ref. Data. 14 (1985): 1041.

Bird, R.B., Stewart, W.E., and Lightfoot, E.N. Transport phenomena. New York: John Wiley and Sons, 1960.

Bruno, L., David, A.R., and Deborahm, R.B. Ozone in water treatment. Chelsea, Michigan: Lewis Publishers, 1991.

Butkovskaya, N. I. and. Setser, D. W. Infrared chemiluminescence study of reaction of hydroxyl radical with acetaldehyde and the secondary reactions of acetyl radical with NO_2, OH, and H. J. Phys. Chem. A. 104 (2000): 9428-9435.

Buxton, G.V., Greenstock, C.L., Helman, W.P., and Ross, A.B. Critical review of rate constants for reaction of hydrated electron, hydrogen atoms and hydroxyl radicals (OH/O^-) in aqueous solution. J. Phys. Chem. Ref. Data. 17 (1988): 693-694.

Caledonia, G. E. A survey of the gas-phase negative ion kinetics of inorganic molecules - electron attachment reactions. Chem. Rev. 75 (1975): 333-351.

Castle, G. S. P., Inculet, I. I., and Burgess, K. I. Ozone generation in positive corona electrostatic precipitators. IEEE Trans. Ind. and Gen. Appl. IGA-5 (1969): 489-496.

Castle, P. M., Kanter, I. E., Lee, P. K., and Kline, L. E. Corona glow detoxification study. Final Rep., Westinghouse Co., Contract No. DAAA 09-82-C-5396, 1984.

Chaiyo, S. Removal of dilute mixture of styrene and ammonia using corona discharge reactor at various temperatures. Master's thesis, Department of

Chemical Engineering, Faculty of Engineering, Chulalongkorn University, 2001.

Chakarbarti, A., et al. Gas cleaning with semi-wet type plasma reactor. IEEE Trans. Ind. Appl. 31 (1995): 500-506.

Chang, J. S., and Masuda S. Mechanism of pulse corona induced plasma chemical processes for removal of NO_x and SO_x from combustion gases. Conf. Rec. IEEE/IAS 1988 Meeting (1988): 1599-1635.

Chang, J. S., and Maezono, I. The electrode surface temperature profile in a corona discharge. J. Phys. D: Appl. Phys. 21 (1988): 1023-1024.

Chanin, L. M., Phelps, A. V., and Brondi, M. A. Measurement of the attachment of low-energy electrons to oxygen molecules. Physical Review. 128 (1962): 219-230.

Chen, J., and Davidson, J.H. Model of the negative DC corona plasma: comparison to the positive DC corona plasma. Plasma Chemistry and Plasma Processing. 23 (2003): 83-102.

Chen, Y.S., Zhang, X.S., Dai, Y.C., and Yaun, W.K. Pulse high-voltage discharge plasma for degradation of phenol in aqueous solution. Sep. Purif. Technol. 34 (2004): 5-12.

Colussi, A.J., Weavers, L.K., and Hoffmann, M.R. Chemical bubble dynamics and quantitative sonochemistry. J. Phys. Chem. A. 102 (1988): 6927-6934.

Davidson, J.H. and Mckinney, P.J. Chemical vapor deposition in the corona discharge of electrostatic air cleaners. Aerosol Science and Technology. 29(2) 1998.

Dorsey, J. A., and Davidson, J. H. Ozone production in electrostatic air cleaners with contaminated electrodes. IEEE Trans. Ind. Appl. 30 (1994): 370-376.

Eliasson, B., Hirth, M., and Kogelschatz, U. Ozone synthesis from oxygen in dielectric barrier discharges. J. Phys. D: Applied Phys. 20 (1987): 1421-1437.

Gottschalk, C., Libra, J. A., and Saupe, A. Ozonation of water and waste water. Weinheim, German: Wiley-VCH, 2000.

Grymonpre, D.R., Finey, W.C., and Locke B.R. Aqueous-phase pulsed streamer corona reactor using suspended activated carbon particles for phenol oxidation: model-data comparison. Chem. Eng. Sci. 54 (1999): 3095-3105.

Han, D.H.,Cha, S.Y., Yang, H.Y. Improvement of oxidative decomposition of aqueous phenol by microwave irradiation in UV/H_2O_2 process and kinetic study. Water Research 38 (2004): 2783-2790.

Hattori, H., Ito, T., Ehara, Y., and Miyata, Y. Superposition effect on ozone synthesis by two types of discharges. Trans. IEEE Japan 112A (1992): 41-46.

Higashi, M., Sugaya, M., Ueki, K., and Fujii, K. Plasma processing of exhaust gas from a diesel engine vehicle. Proc. Int. Conf. on Plasma Chem. 2 (1985): 366-371.

Hickman, W.M. and Fox, R.E. Electron attachment in sulfur hexafluoride using monoenergetic electron. J. Chem. Phys. 25 (1956):64.

Higashi, M., Uchida, S., Suzuki, N., and Fujii, K. Simultaneous reduction of soot and NO_x in a diesel engine exhaust by discharge plasma. Trans. IEEE Japan III-A (1991): 457-473.

Higashi, M. Soot elimination and NO_x and SO_x reduction in diesel engine exhaust by a combination of discharge plasma and oil dynamics. IEEE Trans. Plasma Sci. 20 (1992): 1-12.

Hoeben, W.F.L.M. Pulsed corona - induced degradation of organic materials in water. Technische Universiteit Eindhoven, Eindhoven, Netherland, 2000.

Hoigne, J. and Bader, H. Ozonation of water: selectivity and rate oxidation of solutes. Ozone Sci. Eng. 1 (1979): 357.

Horvath, M. Ozone. Amsterdam, The Netherlands: Elsevier Sci., 1980.

Ito, T., Ehara, Y., Sakai, T., and Miyata, Y. Superposition effect on ozone synthesis by discharge. J. Jpn. Res. Group Elec. Discharges. 127 (1990): 113-118.

Jacob, D.J., Gottlied, E.W., and Prather, M.J. Chemistry of a polluted boundary layer. J. Geophys. Res. 94 (1989): 12975-13002.

Joshi, A.A., Locke, B.R., Arce, P., and Finney, W.C. Formation of hydroxyl radicals, hydrogen peroxide and aqueous electrons by pulsed streamer corona discharge in aqueous solution. J. Hazard. Mater. 41 (1995): 3-30.

Kawamura, S. Integrated design of water treatment facilities. New York: John Wiley and Sons, 1991.

Khongphasarnkaln, P. Removal of trimethylamine acetaldehyde and ammonia using electron attachment reaction. Master's thesis, Department of Chemical Engineering, Faculty of Engineering, Chulalongkorn University, 1998.

Larpsuriyakul, K., Sano, N., Tamon, H., Tanthapanichakoon, W., and Okazaki, M. Influence of structure of corona-discharge reactor on removal of dilute gases using electron attachment. Proc. Himeji Conf. Soc. Chem. Engrs. Japan (1996): 270-271.

Loiseau, J.F., F. Lacassie, C. Monge, R. Peyrous, B. Held and C. Coste, J., Phys, D, 29 (1994): 63.

Masaki, K., Matsuoka, K., Takahashi, A., Shibasaki-Kitakawa, N., and Yonemoto, T. Kinetic of ultrasonic degradation of phenol in the presence of TiO_2 particles. Ultrason. Sonochem (2004) In Press

Massey, S. H. Negative Ions. Cambridge, England: Cambridge Univ. Press, 1976.

Massey, S. H. Atomic and Molecular Collisions. London: Taylor & Francis, 1979.

Masuda, S., Sato, M., and Seki, T. High efficiency ozonizer using traveling wave pulse voltage. Conf. Rec. IEEE/IAS 1984 Ann. Meet. Chicago, IL, (1984): 978-985.

Mizuno, A., Clements, J. S., and Davis, R. H. A method for the removal of sulfur dioxide from exhaust gas utilizing pulsed streamer corona for electron energization. IEEE Trans. Ind. Appl. IA-22 (1986): 516-522.

Mizuno, A., Kisanuki, Y., Noguchi, M., Katsura, S., Lee, S. H., Hong, Y. K., Shin, S. Y., and Kang, J. H. Indoor air cleaning using pulsed discharge plasma. IEEE Trans. Ind. Appl. 35 (1995): 1284-1288.

Moruzzi, J. L., and Phelps, A. V. Survey of negative-ion-molecule reactions in O_2, CO_2, H_2O, CO, and mixtures of these gases at high pressures. J. Chem. Phys. 45 (December 1966): 4617-4627.

Mukkavilli, S., Lee, C.K., Vaghese, K., Tavlarides, L.L. Modeling of the electrostatic corona discharge reactor. IEEE Trans. Plasma. Sci. 16 (1988): 652-660.

Oglesby, S., and Nichols, G. B. Electrostatic Precipitation. New York: Marcel Dekker, 1978.

Okubo, M., Kuroki, T., Kametaka, H., and Yamamoto, T. Odor control using the AC barrier-type plasma reactors. IEEE Trans. Ind. Appl. 37 (2001): 1447-1455.

Peyrous, R., Pignolet, P., Held, B. Kinetic simulation of gaseous spicies created by an electrical discharge in dry or humid oxygen J. Phys. D: Apply Phys. 22 (1989): 1658-1667.

Sano, N., Nagamoto, T., Tamon, H., and Okazaki, M. Removal of iodine and methyl iodide in gas by wetted-wall reactor based on selective electron attachment. J. Chem. Eng. Japan 29 (1996): 59-64.

Sano, N., Nagamoto, T., Tamon, H., Suzuki, T.and Okazaki, M. Removal of acetaldehyde and skatole in gas by corona-discharge. Ind. Eng. Chem. Res. 36 (1997): 3783-3791.

Sano, N, Nishimura, S., Kanki, T., Tamon, H., Tanthapanichakoon, W., Charinpanitkul, T. Influence of temperature of SO_2 removal enhanced by water vapor using a corona-discharge reactor. Chem. Eng. Technol. 24 (2001): 1295-1299.

Sano, N., Kawashima, T., Fujikawa, J., Fujimoto, T., Takaaki, K., Kanki, T., and Toyoda, A. Decomposition of organic compounds in water by direct contact of gas corona discharge: influence of discharge conditions. Ind. Eng. Chem. Res. 41 (2002): 5906- 5911.

Sano, N., Yamamoto, D., Kanki, T., and Toyoda, A. Decomposition of phenol in water by cylindrical wetted wall reactor using direct contact of gas corona discharge. Ind. Eng. Chem. Res. 42 (2003): 5423-5428.

Sano, N., Fujimoto, T., Kawashima, T., Yamamoto, D., Kanki, T., and Toyoda, A. Influence of dissolved inorganic additives on decomposition of phenol and acetic acid in water by direct contact of gas corona discharge. Sep. Purif. Technol. 37 (2004): 169-175.

Shin, W.T., Yaicoumi, S., Tsouris, C., and Dai, S. Pulseless corona discharge process for the oxidation of organic compounds in water. Ind. Eng. Chem. Res. 39 (2000): 4408-4414.

Sathiamoorthy, G., Kalyana, S., Finney, W.C., Clark, R.J., and Locke B.R. Chemical reaction kinetics and reactor modeling of NOx removal in a pulsed streamer corona discharge reactor. Ind. Eng. Chem. Res. 38 (1999): 1844-1855.

Sharma, A.K., Josephson, G.B., Camaioni, D.M., and Goheen, S.C. Environ. Sci. Technol. 34 (2000): 2267.

Tamon, H., Yano, H., and Okazaki, M. A new method of gas mixture separation based on selective electron attachment. Kagaku Kogaku Ronbunshu 15 (1989): 663-668.

Tamon, H., Mizota, H., Sano, N., Schulze, S., and Okazaki, M. New concept of gas purification by electron attachment. AIChE J. 41 (1995): 1701-1711.

Tanthapanichakoon, W., Larpsuriyakul, K., Charinpanitkul, T., Sano, N., Tamon, H., and Okazaki, M. Effect of structure of corona-discharge reactor on removal of dilute gaseous pollutant using selective electron attachment. J. Chem. Eng. Japan. 31 (1998): 7-13.

Tanthapanichakoon, W., Dhattavorn, N., Chaiyo, S., Tamon, H., and Sano, N. Development of odor control technology for crematory furnace using corona discharge reaction. J. Multidisciplinary Res. 14(2001): 34-41.

Tanthapanichakoon, W., Sano, N. Charinpanitkul, T., Dhattavorn, N., Chaiyo, S., and Tamon, H. Influence of electric field strength in a high-temperature corona discharge reactor on removal of toluene from nitrogen and air. J. Chem. Eng. Japan 36 (2003): 946-952.

Tanthapanichakoon, W., Charinpanitkul, T., Chaiyo, S., Dhattavorn, N., Chaichanawong, J., Sano, N., and Tamon, H. Effect of oxygen and water vapor on the removal of styrene and ammonia from nitrogen by non-pulse corona discharge at elevated temperatures. Chem. Eng. J. 97 (2004): 213-223.

Tomas, A., Villenave, E., and Lesclaux, R. Reaction of the HO_2 radical with CH_3CHO and $CH_3C(O)O_2$ in the gas phase. J. Phys. Chem. A. 105 (2001): 3505-3514.

Uhm, H.S. Influence of chamber temperature on properties of the corona discharge system. Physics of Plasmas 6(2) 1999: 623-626.

Ushijima, S., Nishioka, M., and Sadakata, M. Selective generation of O^- under atmospheric pressure. J. Chem. Eng. Japan 37 (2004): 758-763.

Walling, C. and Goosen, A.J. Mechanism of ferric ion catalyzed decomposition of hydrogen-peroxide-effect of organic substrates. J. Am. Chem. Soc. 95 (1973): 2987.

Weiss, H. R. Plasma induced dissociation of carbon dioxide. Proc. Int. Conf. on Plasma Chem. 2 (1985): 383-388.

Yabe, A., Mori, Y., and Hijikata, K. EHD study of the corona wind between wire and plate electrodes. AIAA J. 16 (1978): 340-345.

Yamamoto, T., et al. Catalysis-assisted plasma technology for carbon tetrachloride destruction. IEEE Trans. Ind. Appl. 32 (1996): 100-105.

Zhang, R., Yamamoto, T., and Bundy, D. S. Control of ammonia and odors in animal house by a ferroelectric plasma reactor. IEEE Trans. Ind. Appl. 32 (1996): 113-117.

APPENDICES

APPENDIX A

Publications Resulting from This Research Work

PUBLICATIONS

International Research Paper

1. **K. Faungnawakij**, N. Sano, D. Yamamoto, T. Kanki, T. Charinpanitkul, W. Tanthapanichakoon, "Removal of Acetaldehyde in Air Using a Wetted-Wall Corona Discharge Reactor," *Chemical Engineering Journal*, Vol. 103, **2004**, Pages 105-122.
2. **K. Faungnawakij**, N. Sano, D. Yamamoto, T. Kanki, T. Charinpanitkul, W. Tanthapanichakoon, "Influence of Oxygen and Dissolved Inorganic Additives on Removal of Gaseous Acetaldehyde by Use of Wetted-Wall Corona Discharge Reactor," *Chemical Engineering and Technology*, Vol. 27, Issue 10, **2004**, Pages 1115-1121.
3. **K. Faungnawakij**, N. Sano, D. Yamamoto, T. Kanki, T. Charinpanitkul, W. Tanthapanichakoon, "Simultaneous Gas-Water Purification by a Wetted-Wall Corona Discharge Reactor: Decomposition of Aqueous Phenol and Gaseous Acetaldehyde," *Journal of Chemical Engineering of Japan*, Vol. 37, No. 11, **2004**, Pages 1373-1378.

International Proceedings

1. **K. Faungnawakij**, N. Sano, T. Kanki, W. Tanthapanichakoon, "Removal of Acetaldehyde in Oxygen-Nitrogen Mixture by a Wetted-Wall Corona Discharge Reactor," *Proceedings of the International COE Forum on Plasma Science and Technology*, pp. 259-260, April 5-7, **2004**, Nagoya, Japan.

2. **K. Faungnawakij**, W. Tanthapanichakoon, T. Charinpanitkul, N. Sano, T. Kanki, D. Yamamoto, "Removal of Acetaldehyde from Gas Stream by a Wetted-Wall Corona Discharge Reactor," *Proceedings of the 10th Asian-Pacific Confederation of Chemical Engineering Congress (APCChE 2004)*, October 17 -21, **2004**, Kitakyushu, Japan.
3. **K. Faungnawakij**, N. Sano, T. Charinpanitkul, W. Tanthapanichakoon, "Dynamic Simulation of Simultaneous Treatment of Gaseous Acetaldehyde and Aqueous Phenol Using Corona Discharge Reactions in a Water-Film Column," *Proceedings of Regional Symposium on Chemical Engineering (RSCE 2004)*, December 1-3, **2004**, Bangkok, Thailand.
4. **K. Faungnawakij**, N. Sano, D. Yamamoto, T. Kanki, T. Charinpanitkul, W. Tanthapanichakoon, "Simultaneous Treatment of Acetaldehyde-Laden Air and Phenol-Containing Wastewater Using Corona Discharge Reactions in a Water-Film Reactor," *accepted for Proceedings of the 5th Asia Pacific Conference on Sustainable Energy and Environmental Technologies (APCSEET 2005)*, May 9-11, **2005**, Wellington, New Zealand.

APPENDIX B

Experimental Results

Subject: Decomposition of aqueous phenol by wetted-wall corona discharge reactor

I	0.30	mA	***V***	11.7	kV(negative)
$C_{a\text{-}g\ inl}$	0	mole-ppm	**[O_2]**	21	%
$C_{p\text{-}l\ ini}$	30	ppm			

	Gas phase		Water phase								
Discharge Time (min)	$C_{a\text{-}g}$ (mole-ppm)	[O_3] (ppm)	[PH] (ppm)	[HQ] (ppm)	[BQ] (ppm)	[RC] (ppm)	[CC] (ppm)	[AA] (ppm)	[AD] (ppm)	TOC (ppm)	pH
0	0	0	30.0	0.0	0.0	0.0	0.0	0.0	0	23.00	5.91
30	0.00	943	18.3	1.1	2.3	0.8	4.0	0.0	0.49	21.57	4.24
60	0.00	1451	11.7	1.3	2.8	2.3	4.3	0.0	0.36	20.91	4.02
120	0.00	1004	3.6	1.0	0.6	2.0	0.5	0.0	0.62	19.37	3.74
180	0.00	1104	0.1	0.3	0.0	0.7	0.0	0.0	0.42	15.60	3.68
240	0.00	1164	0.0	0.3	0.0	0.0	0.0	0.6	0.19	11.76	3.78
300	0.00	1541	0.0	0.0	0.0	0.0	0.0	0.6	0.06	7.44	4.00
360	0.00	1175	0.0	0.0	0.0	0.0	0.0	0.8	0.00	4.02	4.17
420	0.00	1138	0.0	0.0	0.0	0.0	0.0	0.7	0.00	2.19	4.29
480	0.00	1509	0.0	0.0	0.0	0.0	0.0	0.7	0.00	1.89	4.31
540	0.00	1647	0.0	0.0	0.0	0.0	0.0	0.7	0.00	0.86	4.33
600	0.00	1751	0.0	0.0	0.0	0.0	0.0	0.6	0.00	0.36	4.35

Subject: Simulteneous treatment by wetted-wall corona discharge reactor

I	0.30	mA	***V***	11.7	kV(negative)
$C_{a\text{-}g\ inl}$	30	mole-ppm	**[O_2]**	21	%
$C_{p\text{-}l\ ini}$	30	ppm			

	Gas phase		Water phase								
Discharge Time (min)	$C_{a\text{-}g}$ (mole-ppm)	[O_3] (ppm)	[PH] (ppm)	[HQ] (ppm)	[BQ] (ppm)	[RC] (ppm)	[CC] (ppm)	[AA] (ppm)	[AD] (ppm)	TOC (ppm)	pH
0	0	0	30.0	0.0	0.0	0.0	0.0	0.0	0	23.00	6.05
30	0.00	1503	17.5	0.6	3.3	1.3	4.4	0.0	0.35	21.30	3.99
60	0.00	1583	10.7	1.3	3.4	2.9	2.9	0.0	0.35	20.97	3.96
120	0.00	1058	2.4	1.0	0.0	3.0	0.3	0.0	0.58	18.96	3.86
180	0.00	1212	0.0	0.2	0.0	0.8	0.0	0.0	0.81	15.80	3.71
240	0.00	1413	0.0	0.0	0.0	0.0	0.0	0.0	0.53	11.29	3.82
300	0.00	1760	0.0	0.0	0.0	0.0	0.0	1.4	0.32	7.56	4.03
360	0.00	2027	0.0	0.0	0.0	0.0	0.0	2.7	0.00	4.41	4.10
420	0.00	2054	0.0	0.0	0.0	0.0	0.0	4.0	0.00	3.47	4.19
480	0.00	2142	0.0	0.0	0.0	0.0	0.0	4.9	0.00	3.07	4.17
540	0.00	2054	0.0	0.0	0.0	0.0	0.0	4.6	0.00	3.02	4.16
600	0.00	2142	0.0	0.0	0.0	0.0	0.0	4.4	0.00	3.05	4.18

Subject: Simulteneous treatment by wetted-wall corona discharge reactor

I	0.30	mA	***V***	11.8	kV(negative)
$C_{a\text{-}g\ inl}$	100	mole-ppm	**[O_2]**	21	%
$C_{p\text{-}l\ ini}$	30	ppm			

	Gas phase		Water phase								
Discharge Time (min)	$C_{a\text{-}g}$ (mole-ppm)	[O_3] (ppm)	[PH] (ppm)	[HQ] (ppm)	[BQ] (ppm)	[RC] (ppm)	[CC] (ppm)	[AA] (ppm)	[AD] (ppm)	TOC (ppm)	pH
0	0	0	30.0	0.0	0.0	0.0	0.0	0.0	0	23.00	5.82
30	0.00	1690	16.6	1.0	1.5	1.4	4.5	0.1	1.94	23.00	4.68
60	0.00	1718	11.2	1.4	1.7	2.1	2.8	0.3	2.13	22.82	4.11
120	0.00	1068	3.8	0.9	1.4	3.0	0.4	0.9	2.27	22.42	4.01
180	0.00	1268	0.2	0.2	0.0	1.5	0.0	1.4	2.26	19.70	3.92
240	0.00	1413	0.0	0.0	0.0	0.3	0.0	5.4	2.28	16.88	3.86
300	0.00	1187	0.0	0.0	0.0	0.0	0.0	7.6	2.33	13.10	4.12
360	0.00	1727	0.0	0.0	0.0	0.0	0.0	8.2	2.72	11.21	4.60
420	0.00	2054	0.0	0.0	0.0	0.0	0.0	9.6	1.71	10.28	4.59
480	0.00	2260	0.0	0.0	0.0	0.0	0.0	10.7	1.52	9.91	4.60
540	0.00	2283	0.0	0.0	0.0	0.0	0.0	10.3	1.27	9.96	4.59
600	0.00	2250	0.0	0.0	0.0	0.0	0.0	10.3	1.21	9.96	4.56

Subject: Simulteneous treatment by wetted-wall corona discharge reactor

I	0.30	mA	***V***	11.8	kV(negative)
$C_{a\text{-}g\ inl}$	200	mole-ppm	**[O_2]**	21	%
$C_{p\text{-}l\ ini}$	30	ppm			

	Gas phase		Water phase								
Discharge Time (min)	$C_{a\text{-}g}$ (mole-ppm)	[O_3] (ppm)	[PH] (ppm)	[HQ] (ppm)	[BQ] (ppm)	[RC] (ppm)	[CC] (ppm)	[AA] (ppm)	[AD] (ppm)	TOC (ppm)	pH
0	0	0	30.0	0.0	0.0	0.0	0.0	0.0	0	23.00	5.63
30	0.00	1690	18.0	0.8	1.7	1.2	4.4	0.0	1.81	23.00	4.30
60	0.00	1718	11.6	1.0	1.9	2.0	3.4	0.9	2.42	22.98	4.10
120	0.00	1068	3.8	0.7	1.7	2.4	0.4	1.7	3.97	22.88	3.98
180	0.00	1268	0.4	0.4	0.0	1.6	0.0	5.4	4.31	22.08	3.78
240	0.00	1413	0.0	0.0	0.0	0.4	0.0	7.6	4.38	20.67	3.88
300	0.00	1187	0.0	0.0	0.0	0.0	0.0	10.2	4.44	17.49	4.01
360	0.00	1727	0.0	0.0	0.0	0.0	0.0	14.9	4.45	15.72	4.25
420	0.00	2054	0.0	0.0	0.0	0.0	0.0	19.2	4.22	15.95	4.41
480	0.00	2260	0.0	0.0	0.0	0.0	0.0	20.3	4.03	16.02	4.39
540	0.00	2283	0.0	0.0	0.0	0.0	0.0	26.1	3.84	16.26	4.50
600	0.00	2250	0.0	0.0	0.0	0.0	0.0	28.0	3.59	16.35	4.52

Subject: Decomposition of gaseous acetaldehyde by wetted-wall corona discharge reactor

I	0.30	mA	***V***	11.8	kV(negative)
$C_{a\text{-}g\ inl}$	30	mole-ppm	$[O_2]$	21	%
$C_{p\text{-}l\ ini}$	0	ppm			

	Gas phase		Water phase								
Discharge Time (min)	$C_{a\text{-}g}$ (mole-ppm)	$[O_3]$ (ppm)	[PH] (ppm)	[HQ] (ppm)	[BQ] (ppm)	[RC] (ppm)	[CC] (ppm)	[AA] (ppm)	[AD] (ppm)	TOC (ppm)	pH
0	0	0	0.0	0.0	0.0	0.0	0.0	0.0	0	0.00	6.05
30	0.00	1503	0.0	0.0	0.0	0.0	0.0	0.0	0.00	0.39	4.48
60	0.00	1583	0.0	0.0	0.0	0.0	0.0	0.0	0.00	0.73	4.35
120	0.00	1058	0.0	0.0	0.0	0.0	0.0	1.2	0.00	1.12	4.14
180	0.00	1212	0.0	0.0	0.0	0.0	0.0	1.3	0.00	1.47	4.25
240	0.00	1413	0.0	0.0	0.0	0.0	0.0	1.5	0.00	1.02	4.01
300	0.00	1760	0.0	0.0	0.0	0.0	0.0	3.1	0.00	1.31	4.03
360	0.00	2027	0.0	0.0	0.0	0.0	0.0	3.2	0.00	1.33	4.10
420	0.00	2054	0.0	0.0	0.0	0.0	0.0	2.9	0.00	1.45	4.12
480	0.00	2142	0.0	0.0	0.0	0.0	0.0	3.1	0.00	1.44	4.17
540	0.00	2054	0.0	0.0	0.0	0.0	0.0	3.7	0.00	1.58	4.16
600	0.00	2142	0.0	0.0	0.0	0.0	0.0	3.4	0.00	1.46	4.12

Subject: Simulteneous treatment by wetted-wall corona discharge reactor

I	0.30	mA	***V***	11.8	kV(negative)
$C_{a\text{-}g\ inl}$	30	mole-ppm	$[O_2]$	21	%
$C_{p\text{-}l\ ini}$	15	ppm			

	Gas phase		Water phase								
Discharge Time (min)	$C_{a\text{-}g}$ (mole-ppm)	$[O_3]$ (ppm)	[PH] (ppm)	[HQ] (ppm)	[BQ] (ppm)	[RC] (ppm)	[CC] (ppm)	[AA] (ppm)	[AD] (ppm)	TOC (ppm)	pH
0	0	0	15.0	0.0	0.0	0.0	0.0	0.0	0	11.50	5.98
30	0.00	1503	8.7	0.6	1.7	0.2	2.2	0.0	0.22	10.20	3.90
60	0.00	1583	5.3	0.6	1.7	0.6	2.8	0.0	0.29	8.50	3.91
120	0.00	1058	1.2	0.4	0.0	0.6	3.5	0.0	0.51	5.80	3.84
180	0.00	1212	0.0	0.0	0.0	0.2	2.8	0.0	0.36	4.20	3.81
240	0.00	1413	0.0	0.0	0.0	0.0	1.6	0.7	0.23	2.90	3.80
300	0.00	1760	0.0	0.0	0.0	0.0	0.0	1.1	0.00	2.10	4.00
360	0.00	2027	0.0	0.0	0.0	0.0	0.0	1.3	0.00	1.60	4.20
420	0.00	2054	0.0	0.0	0.0	0.0	0.0	2.0	0.00	1.00	4.15
480	0.00	2142	0.0	0.0	0.0	0.0	0.0	2.2	0.00	0.80	4.18
540	0.00	2054	0.0	0.0	0.0	0.0	0.0	2.1	0.00	0.90	4.16
600	0.00	2142	0.0	0.0	0.0	0.0	0.0	2.1	0.00	0.90	4.18

Subject: Simulteneous treatment by wetted-wall corona discharge reactor

I	0.30	mA	***V***	11.8	kV(negative)
$C_{a\text{-}g\ inl}$	30	mole-ppm	**[O_2]**	21	%
$C_{p\text{-}l\ ini}$	50	ppm			

	Gas phase		Water phase								
Discharge Time (min)	$C_{a\text{-}g}$ (mole-ppm)	[O_3] (ppm)	[PH] (ppm)	[HQ] (ppm)	[BQ] (ppm)	[RC] (ppm)	[CC] (ppm)	[AA] (ppm)	[AD] (ppm)	TOC (ppm)	pH
0	0.0	0	50.0	0.0	0.0	0.0	0.0	0.0	0.0	38.30	5.88
30	0.0	943	36.0	2.0	1.1	1.0	4.6	0.0	0.68	36.62	4.20
60	0.0	1451	26.5	2.7	0.9	2.1	6.3	0.0	0.63	34.90	3.90
120	0.0	1004	11.7	2.9	0.6	2.9	1.5	0.0	0.30	33.20	3.66
180	0.0	1104	3.3	1.7	0.0	2.3	0.3	1.7	0.47	30.12	3.45
240	0.0	1164	0.0	0.1	0.0	0.7	0.0	3.5	0.39	26.02	3.46
300	0.0	1541	0.0	0.0	0.0	0.0	0.0	4.0	0.27	19.56	3.53
360	0.0	1175	0.0	0.0	0.0	0.0	0.0	4.0	0.14	14.35	3.68
420	0.0	1138	0.0	0.0	0.0	0.0	0.0	4.2	0.06	9.56	3.98
480	0.0	1509	0.0	0.0	0.0	0.0	0.0	4.4	0.00	5.51	4.21
540	0.0	1647	0.0	0.0	0.0	0.0	0.0	4.4	0.00	3.56	4.44
600	0.0	1751	0.0	0.0	0.0	0.0	0.0	4.8	0.00	2.13	4.63

Subject: Simulteneous treatment by wetted-wall corona discharge reactor

I	0.30	mA	***V***	11.9	kV(negative)
$C_{a\text{-}g\ inl}$	30	mole-ppm	**[O_2]**	21	%
$C_{p\text{-}l\ ini}$	100	ppm			

	Gas phase		Water phase								
Discharge Time (min)	$C_{a\text{-}g}$ (mole-ppm)	[O_3] (ppm)	[PH] (ppm)	[HQ] (ppm)	[BQ] (ppm)	[RC] (ppm)	[CC] (ppm)	[AA] (ppm)	[AD] (ppm)	TOC (ppm)	pH
0	0.0	0	100.0	0.0	0.0	0.0	0.0	0.0	0.0	76.60	5.78
30	0.0	943	85.2	1.5	3.2	2.0	7.0	0.0	0.73	73.56	4.09
60	0.0	1451	69.3	1.9	4.5	4.2	11.5	0.0	0.88	72.32	4.02
120	0.0	1004	58.0	2.0	6.2	7.5	11.5	0.2	1.05	69.36	3.75
180	0.0	1104	42.1	1.8	6.4	9.3	8.0	2.7	0.98	67.25	3.54
240	0.0	1164	31.4	1.8	6.1	10.1	4.9	3.5	1.05	63.23	3.45
300	0.0	1541	16.6	1.7	5.6	9.7	2.3	3.7	0.97	61.25	3.37
360	0.0	1175	10.1	1.5	4.4	8.1	0.9	3.8	1.03	58.36	3.35
420	0.0	1138	3.9	1.1	0.6	6.0	0.3	4.8	0.98	54.23	3.31
480	0.0	1509	0.5	0.4	0.0	3.0	0.1	4.9	0.98	50.12	3.34
540	0.0	1647	0.0	0.0	0.0	0.0	0.0	5.0	0.92	43.55	3.35
600	0.0	1751	0.0	0.0	0.0	0.0	0.0	5.2	0.97	37.56	3.37

VITA

Mr. Kajornsak Faungnawakij, the third son of Mr. Somsak and Mrs. Warunee Faungnawakij, was born on 3rd July 1978 in Nakhon Si Thammarat, Thailand. He spent 6 years studying in primary and secondary educations at Benjamarachuthit School, Nakhon Si Thammarat. In June 1997, he entered Prince of Songkla University to study in Bachelor of Engineering. He was awarded the GOLD MEDAL for outstanding engineering student from the Engineering Institute of Thailand under H.M. the King's Patronage in 2000. In March 2001, he received a Bachelor of Engineering, majoring in Chemical Engineering with 1st class honor. Subsequently, he continued to study in Doctor of Philosophy under the Royal Golden Jubilee Ph.D. program in Chulalongkorn University. During April 2003 to April 2004, he lived in Japan to carry out a part of his dissertation. He was awarded a Ph.D. degree in Chemical Engineering in April 2005.